UPPSALA UNIVERSITET

"Multiscale modelling and computational spectroscopy"

Kersti Hermansson (*kersti @ kemi.uu.se*)
Dept. of Chemistry, The Ångström Laboratory, Uppsala University, Uppsala, Sweden

Barcelona

Uppsala

IWCN BARCELONA 2023

International Workshop on Computational Nanotechnology
12-16 June 2023

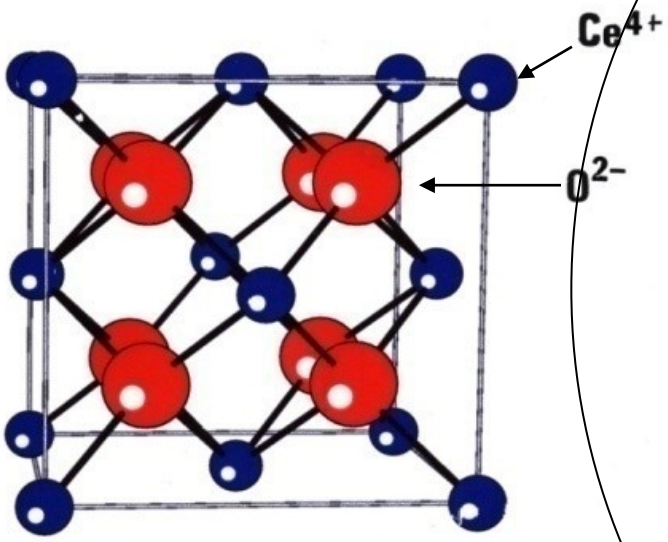

$CeO_2(s)$

CeO_2 surface

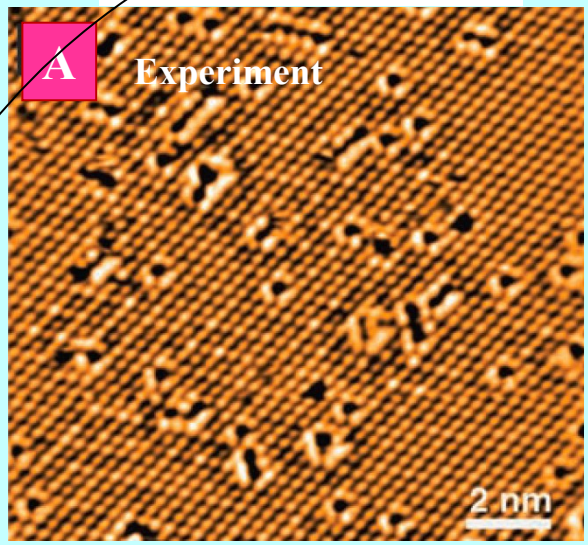

CeO_2 nanoparticles

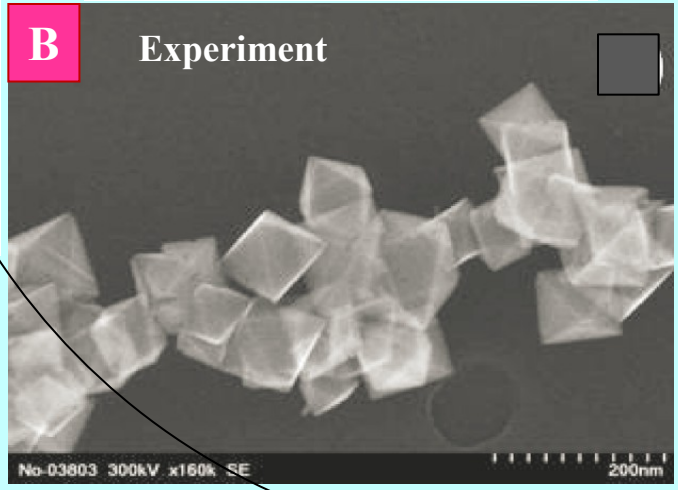

Molecules on a CeO_2 surface

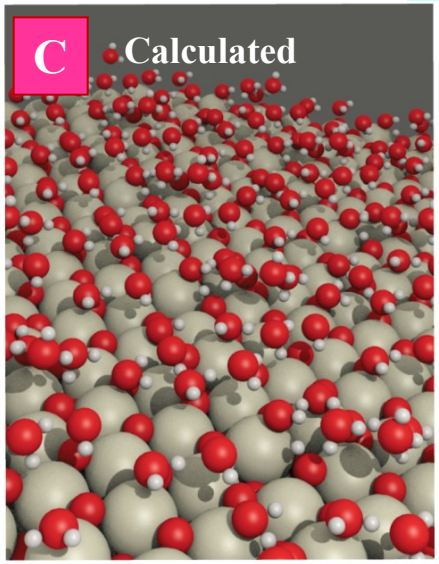

Ceria oxygen vacancies, or ...?

Example: Ceria (CeO_2)

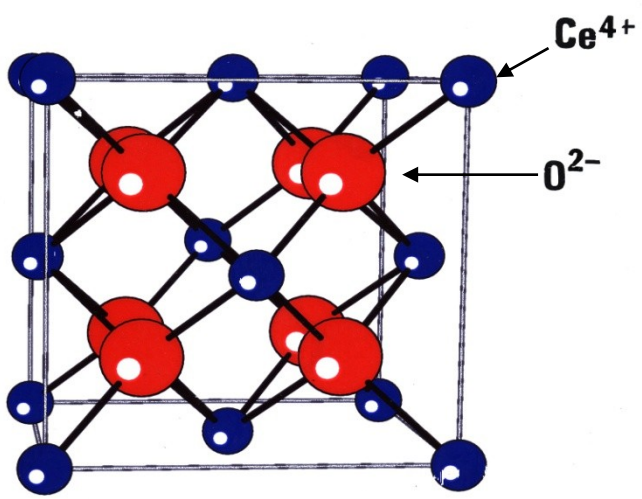

Bulk CeO_2 (s)

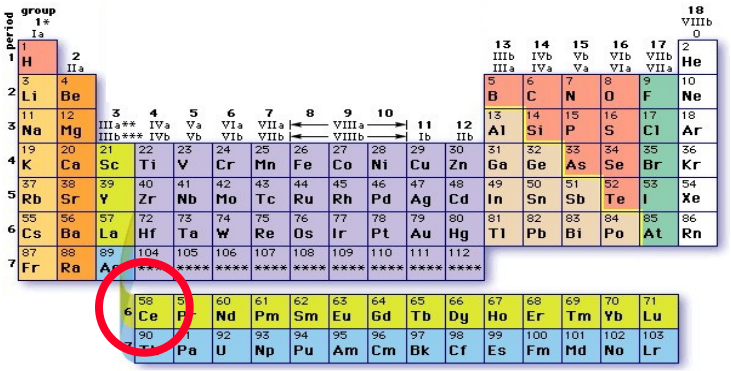

Ce: [Xe] $4f^1\ 5d^1\ 6s^2$

Ce^{4+} : [Xe]

Ce^{3+} : [Xe] $4f^1$

$$O_{latt}^{2-} + 2\ Ce^{4+} \rightarrow \text{'O vacancy'} + 1/2\ O_2\ (g) + 2\ Ce^{3+}$$

Applications

1. Fuel cells: ceria electrolyte
2. Heterogeneous catalysis
3. Oxygen storage
4. Molecular sensors and SOx trapping
5. Medical applications

Electronic structure of CeO_{2-x}

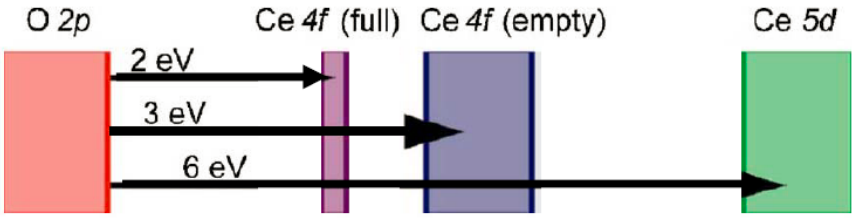

The (111) surface of CeO_2 from STM experiments at 600 K

Esch et al. Science 309, 752-755 (2005)

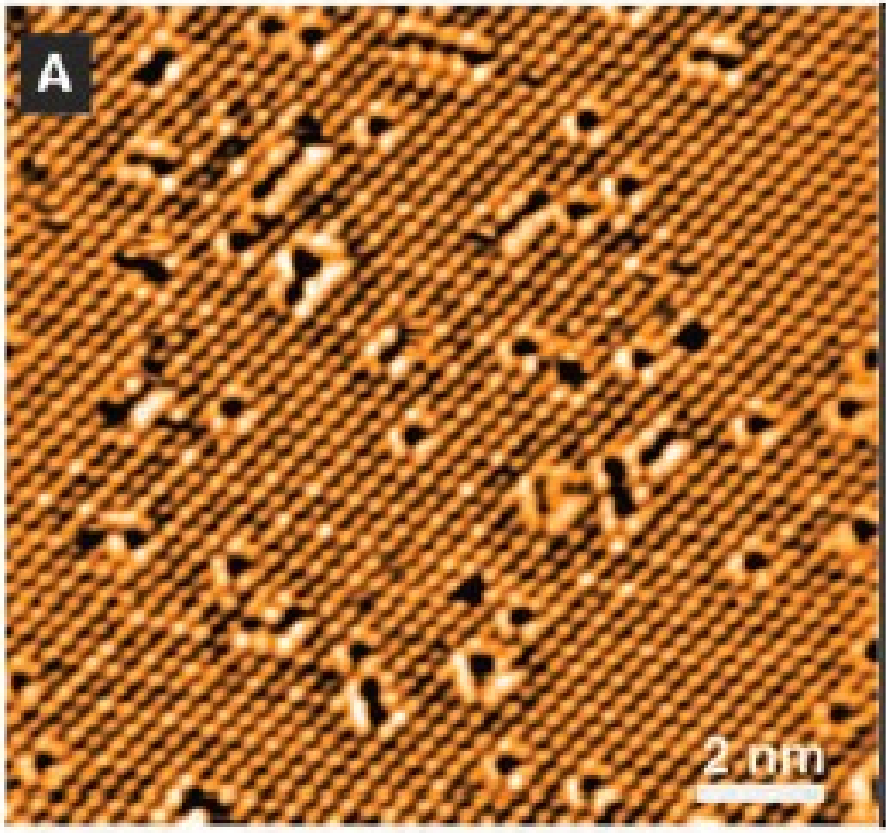

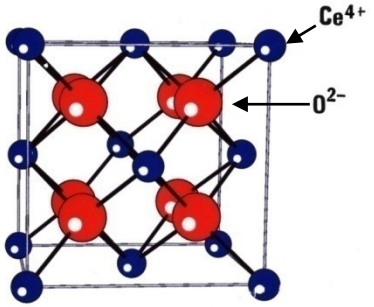

Bulk CeO_2 (s)

What are the black dots? =>

Projected densities of states

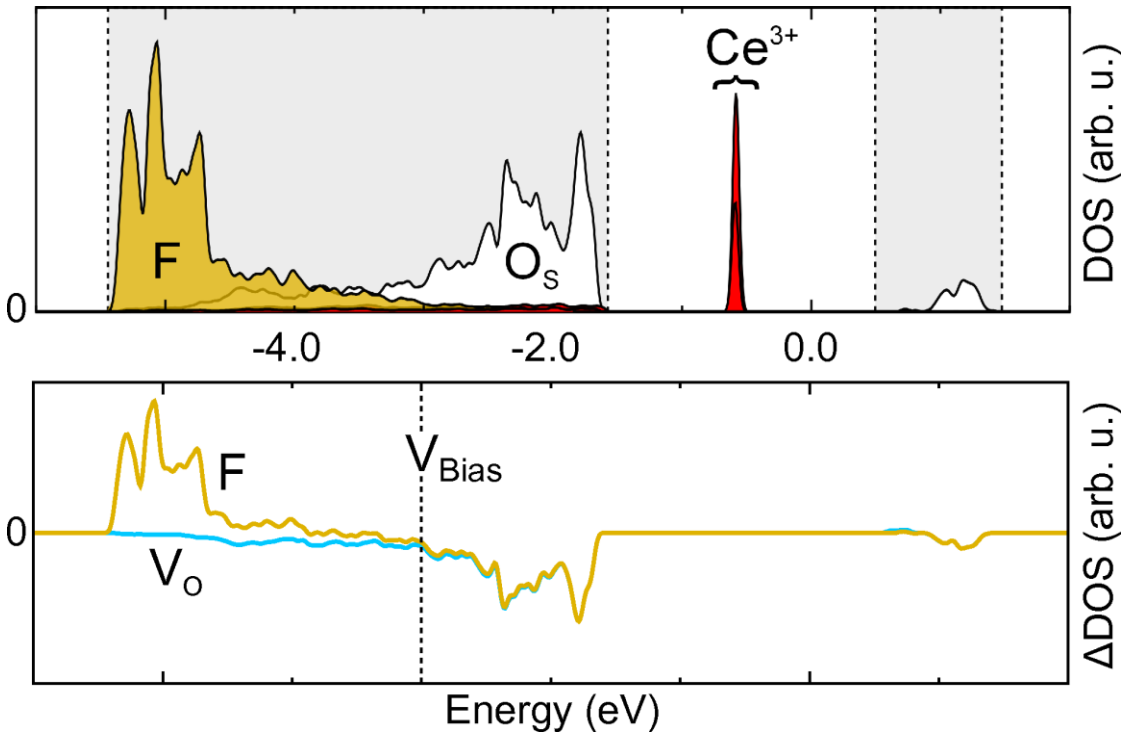

- Due to larger nuclear charge, occupied fluorine 2*p* states are at lower energy than those of oxygen
- Invisible to STM probing upper portion of local valence band

Method: DFT (PBE+U)

We simulated filled-state STM images:

J. Kullgren, M. Wolf, P. Broqvist, K. Hermansson, PRB 2014

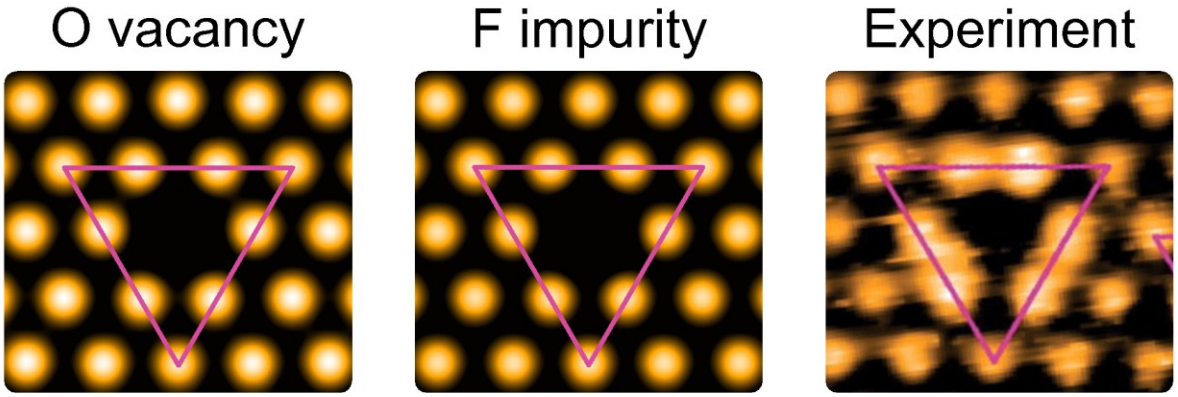

Experiments found for the black dots:	*Our calculations found:*	
1. Black spots in filled-state STM image	O vacancy ✓	Fluorine ✓
2. The defects are most stable at the surface	O vacancy ✗	Fluorine ✓
3. The defects are immobile on a time-scale of minutes	O vacancy ✗	Fluorine ✓
4. The defects form clusters and chains	O vacancy ✗	Fluorine ✓

Our conclusions: F is in quite good agreement with experiments on single ceria(111) surface !
(N.B. We are *not* claiming that O vacancies do not exist in ceria)

A very simple interaction model

- Pair-wise interaction fitted on 78 DFT F-clusters.
- Only Coulomb energy for intermediate to long distances, charge is used as a parameter (fitted).
- For short distances (NN) we allow for contributions from “relaxation overlap”, additional NN parameter (also fitted).

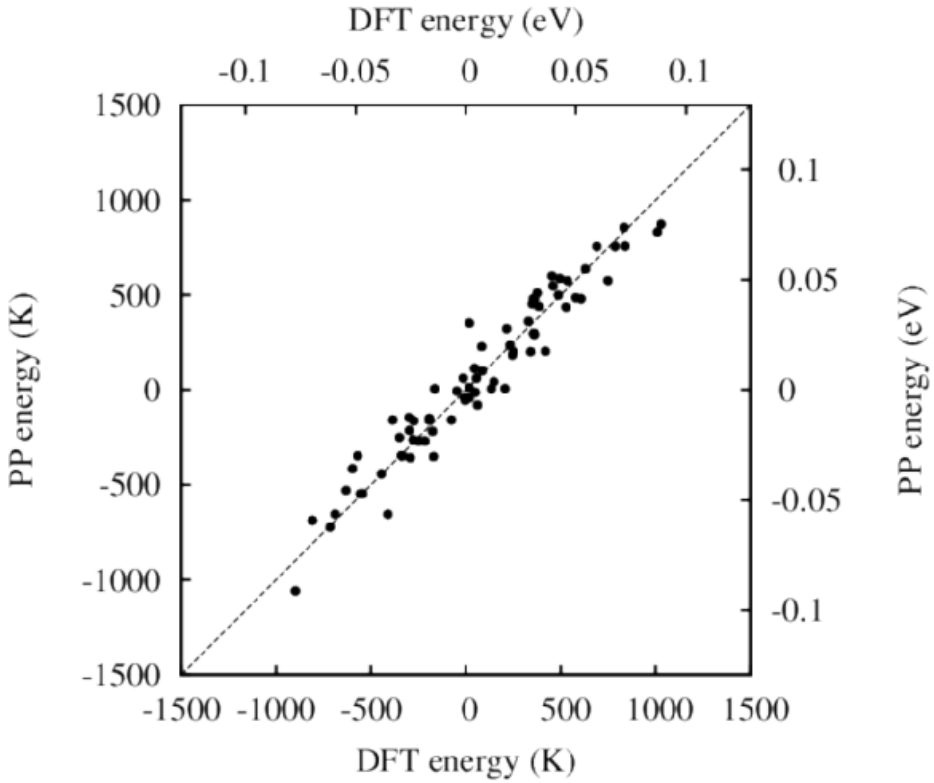

C_{NN}(F-F) = 0.299 eV C_{NN}(Ce^{3+}-Ce^{3+}) = 0.220 eV
C_{NN}(F-Ce^{3+}) = -0.370 eV q=0.276 e

q corresponds to a static dielectric constant of 13.

J. Kullgren, M. J. Wolf, P. D. Mitev, K. Hermansson and W. J. Briels, *J. Phys. Chem. C 28*, 121 (2017)

Clustering of defects
-larger clusters

Metropolis Monte-Carlo (MC) procedure:

* 4800 lattice sites (40x40 supercell)
* Defect conc.: 5%, 10% and 15%
* Temperatures: 200, 400 and 600 K
* MC move: swap ions on the lattice
* For each conc. and T: 1000 snap-shots analyzed
  → histograms and representative snapshots

The chemical/physical problem =>

Results: 15% defect conc.
The random distribution

Statistics over 1000 snapshots

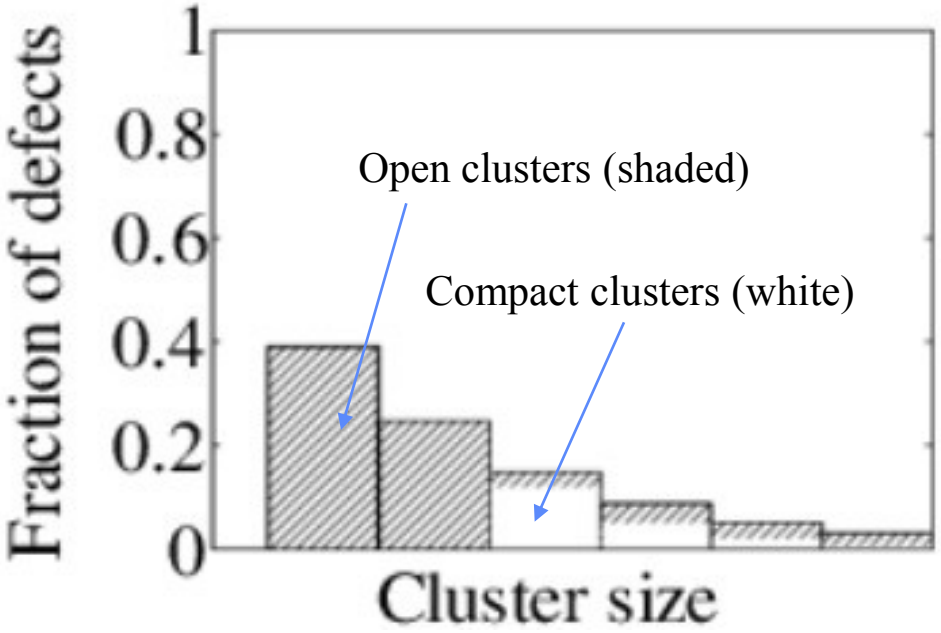

One represenatative snapshot

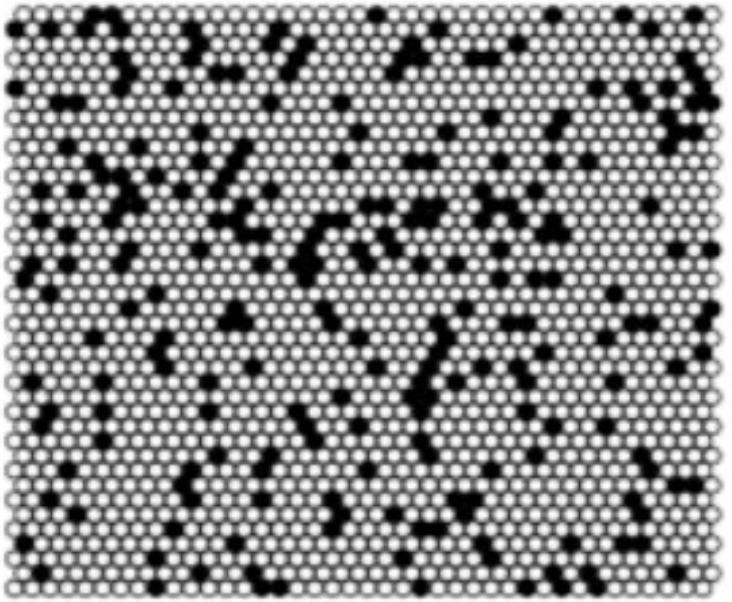

Conclusion: Even a random distribution has many clusters.

Result: 15% F defect conc. MC at 300 K

Statistics over 1000 snapshots

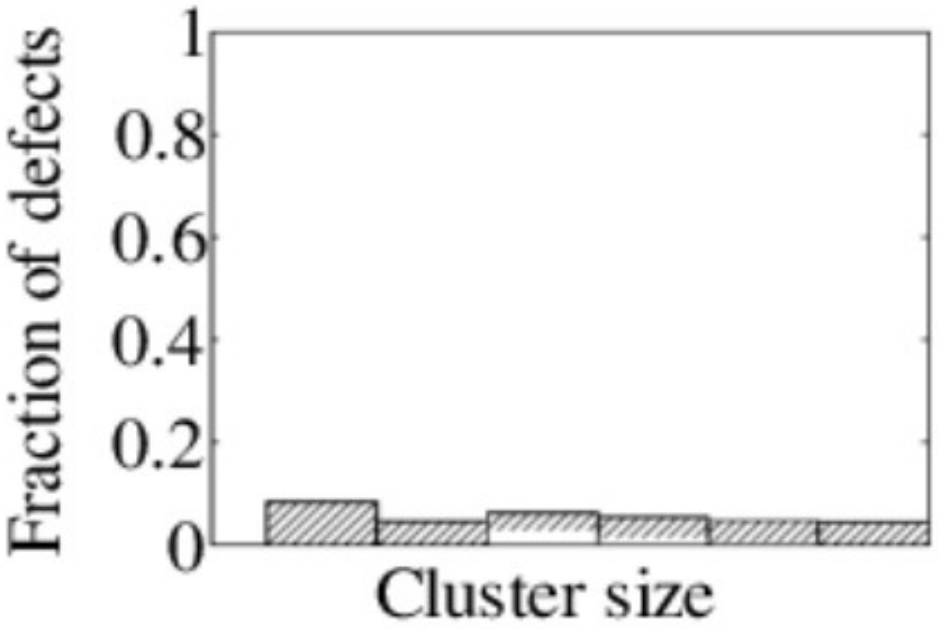

One represenatative snapshot

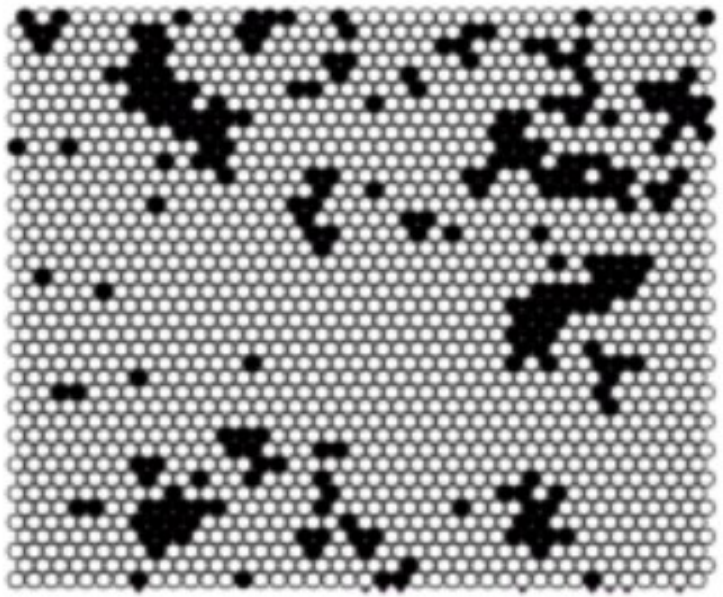

* All cluster sizes represented. Clusters are typically compact.

Result: 15% F defect conc. MC at 600 K

Statistics over 1000 snapshots

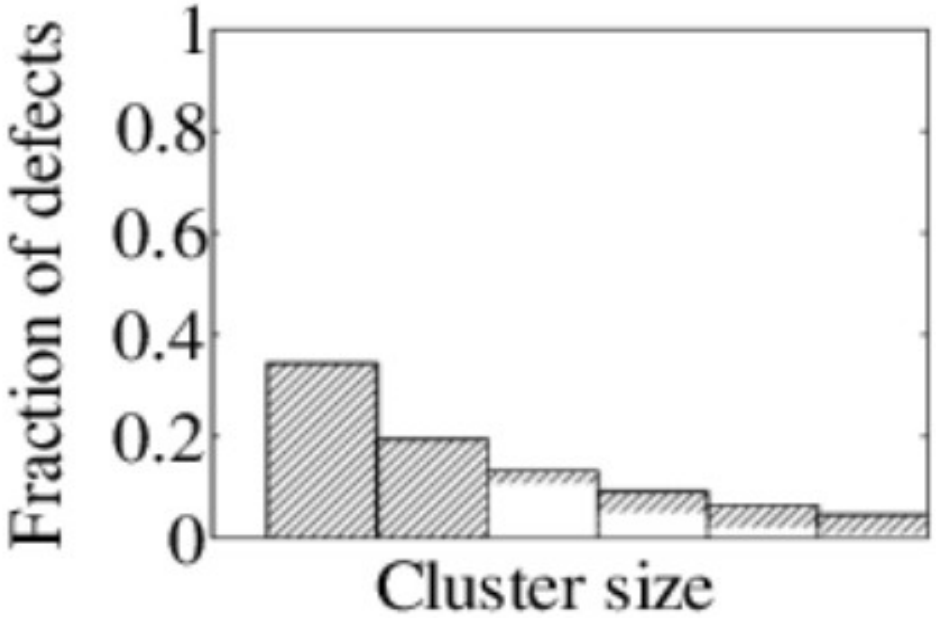

One representative snapshot

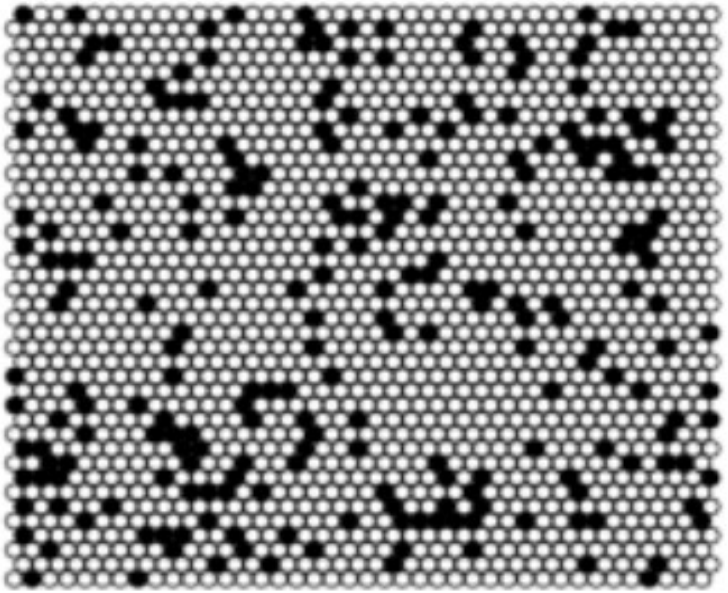

* Small clusters and monomers becomes dominant.
* Clusters are more open (few compact clusters)

Result: 15% F defect conc. MC at 900 K

Statistics over 1000 snapshots

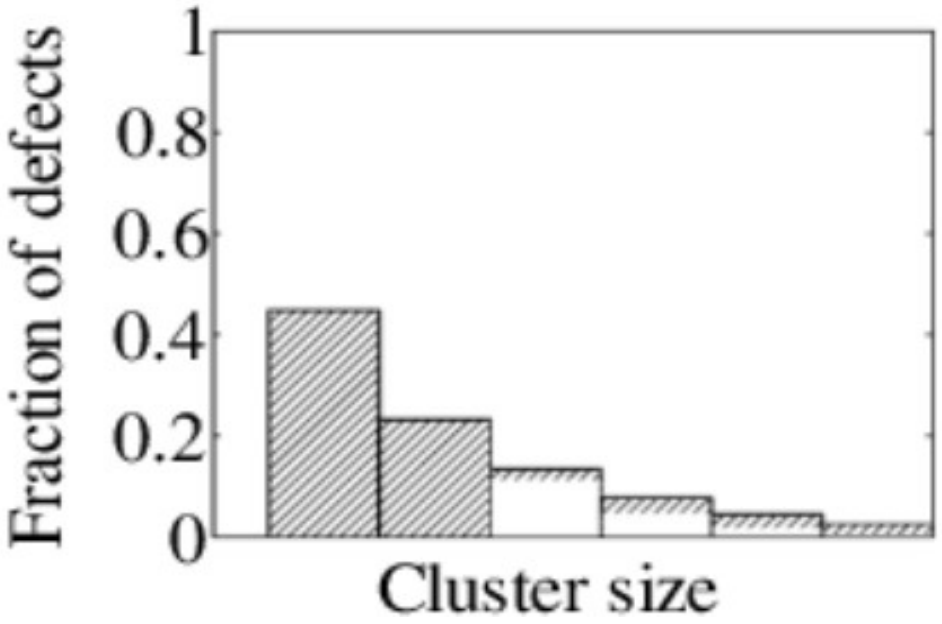

One represenatative snapshot

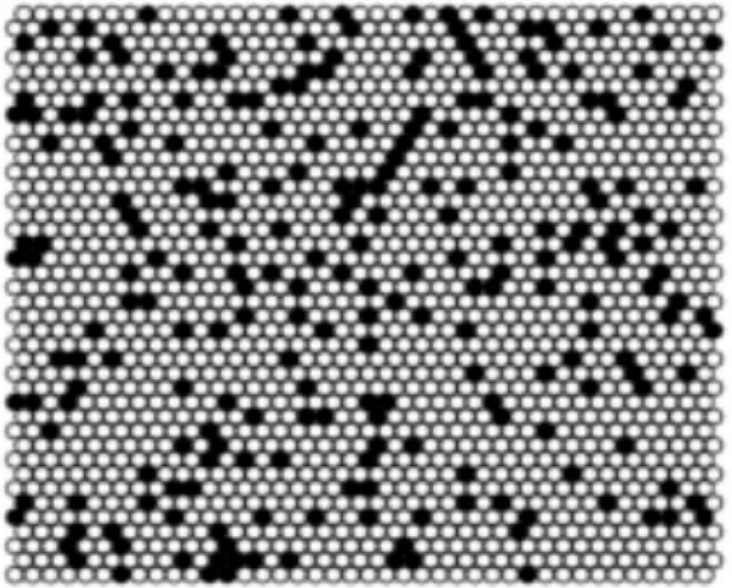

* Small clusters and monomers becomes even more dominating.
* More “linear clusters” appear.
* Number of isolated F is larger than in the random distribution!
* Good agreement with experimental image.

J.Phys.Chem.C2017, 121, 15127−15134

DFT-based Monte Carlo Simulations of Impurity Clustering at CeO_2(111)

Jolla Kullgren,*[,†] Matthew J. Wolf,[†] Pavlin D. Mitev,[†] Kersti Hermansson,[†] and Wim J. Briels[‡,§]

ABSTRACT: The interplay between energetics and entropy in determining defect distributions at ceria(111) is studied using a combination of DFT+*U* and lattice Monte Carlo simulations. Our main example is fluorine impurities, although we also present preliminary results for surface hydroxyl groups. A simple classical force-field model was constructed from a training set of DFT+*U* data for all symmetrically inequivalent $(F^-)_n(Ce^{3+})_n$ nearest-neighbor clusters with $n = 2$ or 3. Our fitted model reproduces the DFT energies well. We find that for an impurity concentration of 15% at 600 K, straight and hooked linear fluorine clusters are surprisingly abundant, with similarities to experimental STM images from the literature. We also find that with increasing temperature the fluorine cluster sizes show a transition from being governed by an attractive potential to being governed by a repulsive potential as a consequence of the increasing importance of the entropy of the Ce^{3+} ions. The distributions of surface hydroxyl groups are noticeably different.

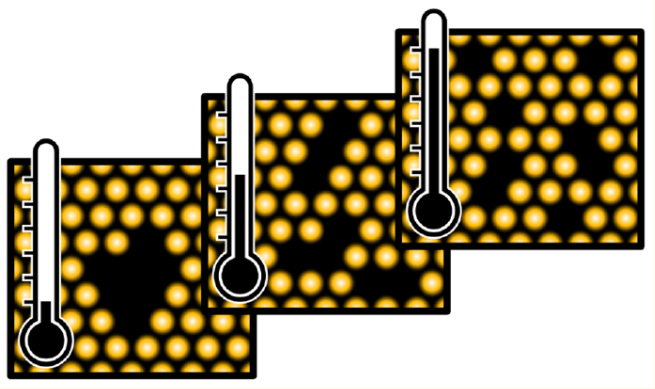

Experiment

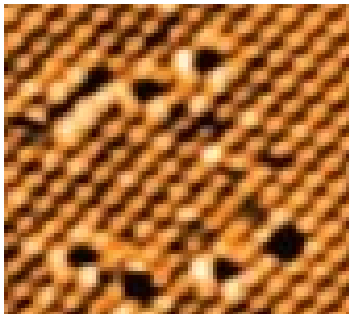

Frontiers in Chemistry, June 2019, doi: 10.3389/fchem.2019.00212

"Atlas" over STM Images of Anionic Defects at ceria surfaces

M.J.Wolf, CWM Castleton, K Hermansson, J.Kullgren*

Ceria NPs

Our multi-scale modelling strategy for chemistry in and on materials:

Broqvist, Kullgren, Hermansson, *ongoing work*.

in collaborations with the main developers of ReaxFF (van Duin) and DFTB+ (Frauenheim)

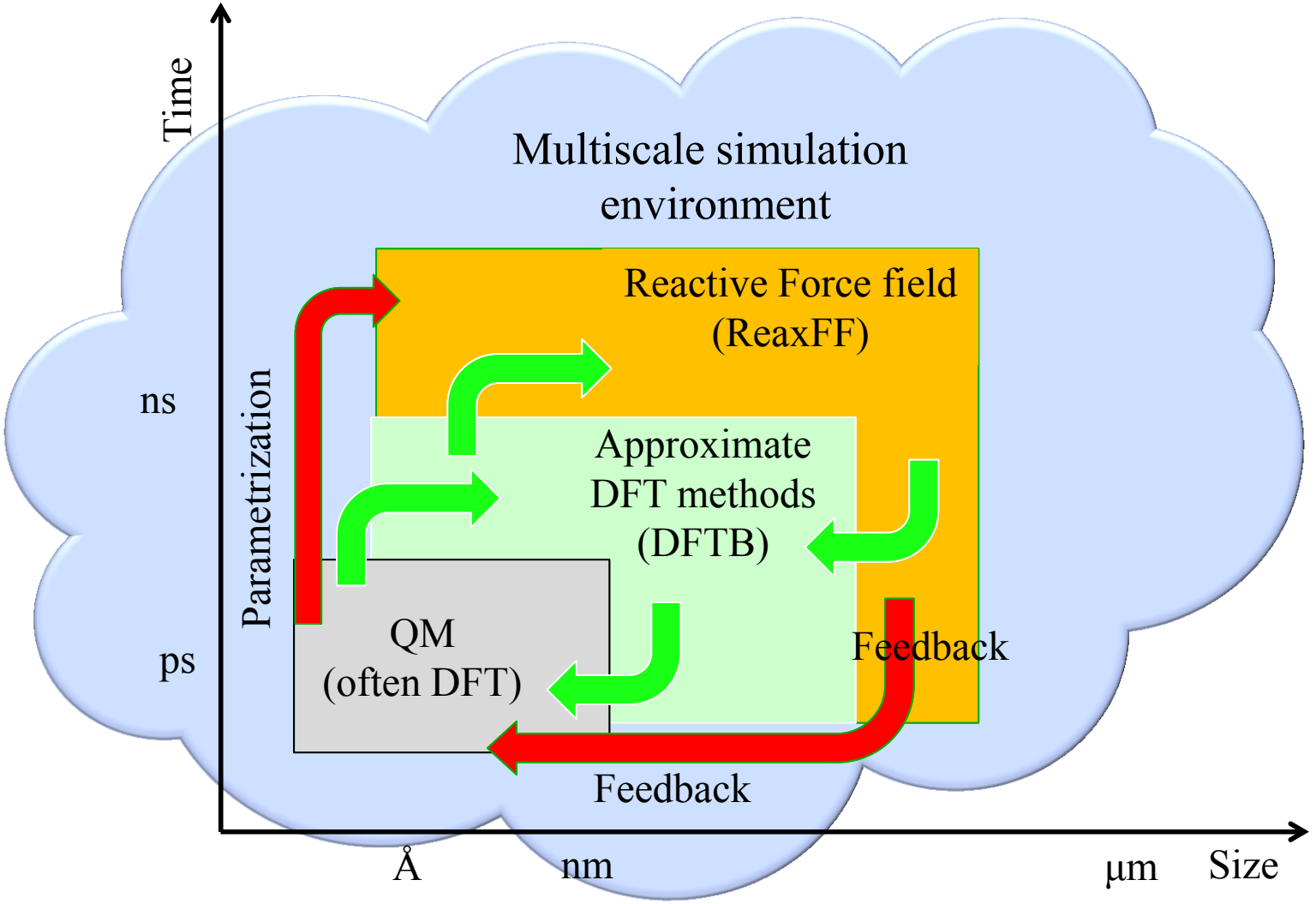

Some details about our approach

Peter Broqvist et al.

DFTB+

We make parameter sets in collaboration with the main developers of the code in Bremen, Prof. Thomas Frauenheim.

Hubbard +U correction for d/f electrons

- Reactive Force Fields (50'000*)
  - Many parameters
- Approximate DFT (300*)
  - Density functional tight binding
  - Few parameters
- QM (1*)
  - e.g Density functional theory
  - No parameters

Explicit treatment of electrons

ReaxFF

Sometimes in collaboration with Prof. Adri van Duin Penn State U

*Speed-up relative to DFT

THE JOURNAL OF PHYSICAL CHEMISTRY C
Article
pubs.acs.org/JPCC
J. Phys. Chem. C, **121**, pp 4593–4607 (2017)

Self-Consistent-Charge Density-Functional Tight-Binding (SCC-DFTB) Parameters for Ceria in 0D to 3D

Jolla Kullgren,*[,†] Matthew J. Wolf,[†] Kersti Hermansson,[†] Christof Köhler,[‡] Bálint Aradi,[‡] Thomas Frauenheim,[‡] and Peter Broqvist*[,†]

[†]Department of Chemistry—Ångström Laboratory, Uppsala University, Box 538, S-751 21 Uppsala, Sweden
[‡]Bremen Center for Computational Materials Science, Universität Bremen, P.O.B. 330440, D-28334 Bremen, Germany

Supporting Information

ABSTRACT: Reducible oxides such as CeO_2 are challenging to describe with standard density-functional theory (DFT) due to the mixed valence states of the cations; they often require the use of non-standard correction schemes, and/or more computationally expensive methods. This adds a new layer of complexity when it comes to the generation of Slater–Koster tables and the corresponding repulsive potentials for self-consistent density-functional based tight-binding (SCC-DFTB) calculations of such materials. In this work, we provide guidelines for how to set up a parametrization scheme for mixed valence oxides within the SCC-DFTB framework, with a focus on reproducing structural and electronic properties as well as redox reaction energies calculated using a

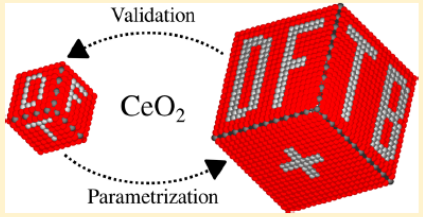

How well does our DFTB model perform for ceria ?

THE JOURNAL OF PHYSICAL CHEMISTRY C
Article
pubs.acs.org/JPCC
J. Phys. Chem. C, **119**, pp 13598–13609 (2015)

ReaxFF Force-Field for Ceria Bulk, Surfaces, and Nanoparticles

Peter Broqvist,[†] Jolla Kullgren,[†] Matthew J. Wolf,[†] Adri C. T. van Duin,[‡] and Kersti Hermansson*[,†]

[†]Department of Chemistry—Ångström, Uppsala University, Box 538, S-751 21, Uppsala, Sweden
[‡]Department of Mechanical and Nuclear Engineering, The Pennsylvania State University, University Park, Pennsylvania 16802, United States

ABSTRACT: We have developed a reactive force-field of the ReaxFF type for stoichiometric ceria (CeO_2) and partially reduced ceria (CeO_{2-x}). We describe the parametrization procedure and provide results validating the parameters in terms of their ability to accurately describe the oxygen chemistry of the bulk, extended surfaces, surface steps, and nanoparticles of the material. By comparison with our reference electronic structure method (PBE+U), we find that the stoichiometric bulk and surface systems are well reproduced in terms of bulk modulus, lattice parameters, and surface energies. For the surfaces, step energies on the (111) surface are also well described. Upon reduction, the force-field is able to capture the bulk and surface vacancy formation energies (E_{vac}), and in particular, it reproduces the E_{vac} variation with depth from the (110) and (111) surfaces. The force-field is also able to capture the energy hierarchy of differently shaped stoichiometric nanoparticles (tetrahedra, octahedra, and cubes), and of partially reduced octahedra. For these reasons, we believe that this force-field provides a significant addition to the method repertoire available for simulating redox properties at ceria surfaces.

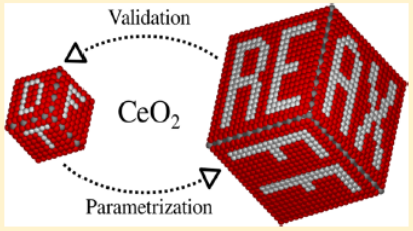

How well does ReaxFF perform for ceria ?

DFTB performance for bulk band structure

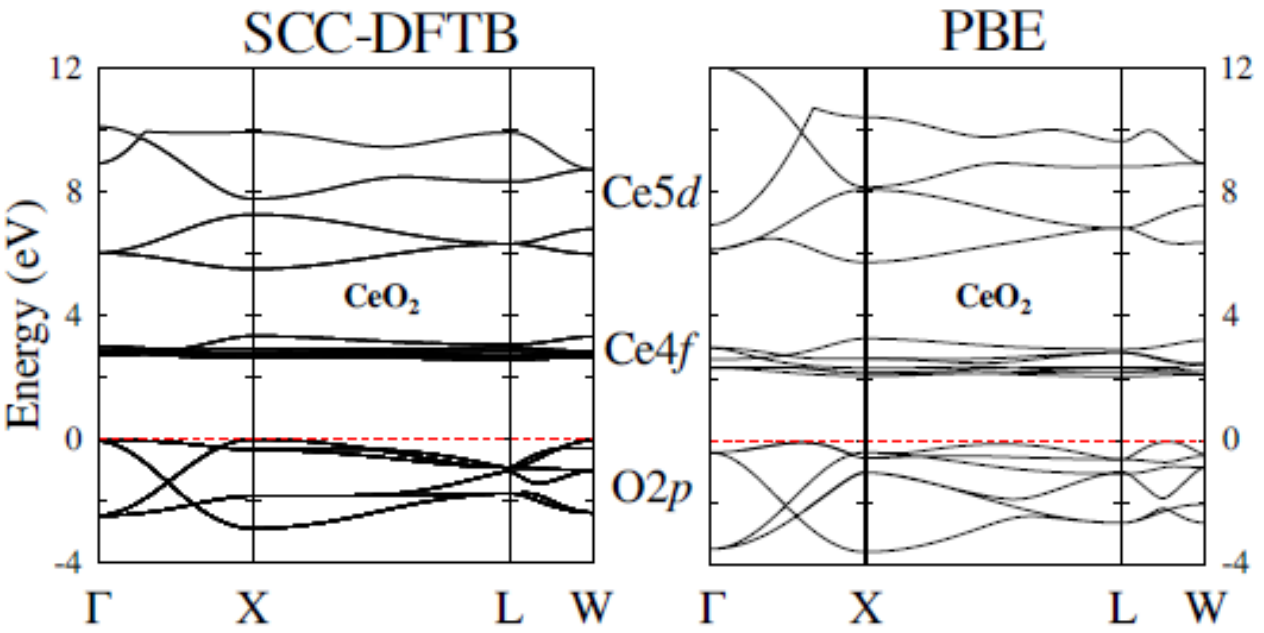

J. Phys. Chem. C, **121**, pp 4593–4607 (2017)

SCC-DFTB performance -Some key features

The electronic structure is in good agreement with the DFT reference.

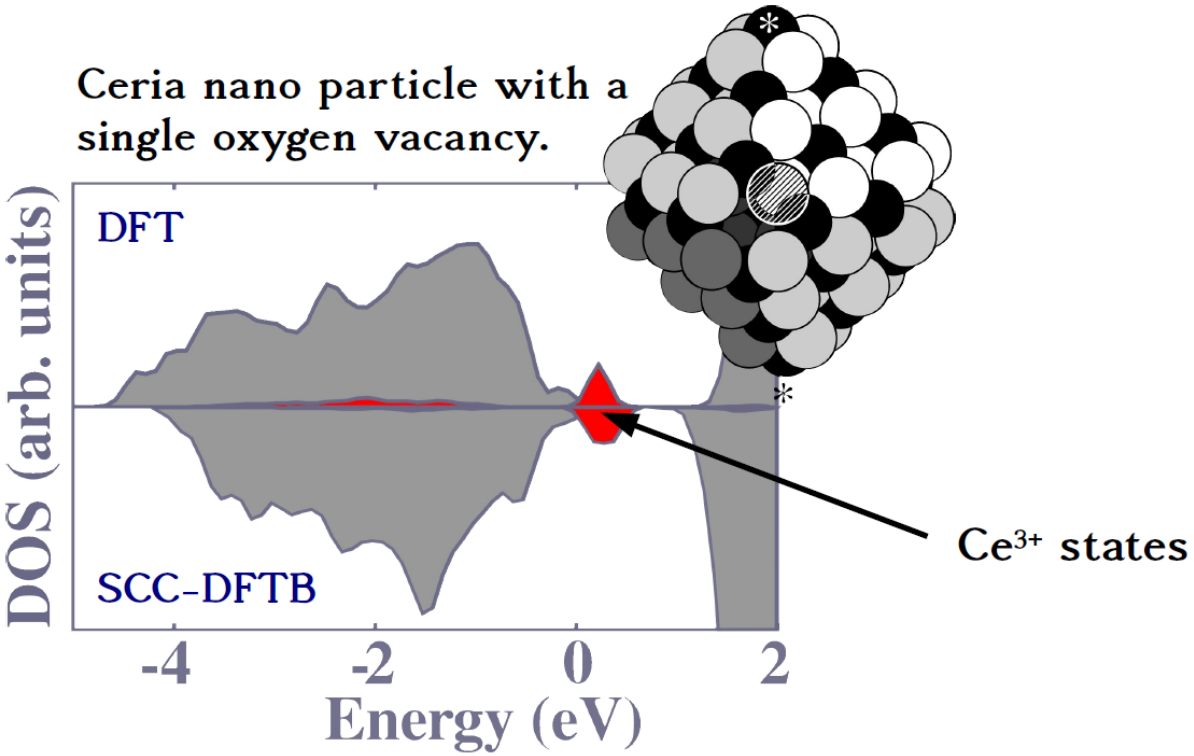

J. Phys. Chem. C, **121**, pp 4593–4607 (2017)

DFTB performance for nanoparticles

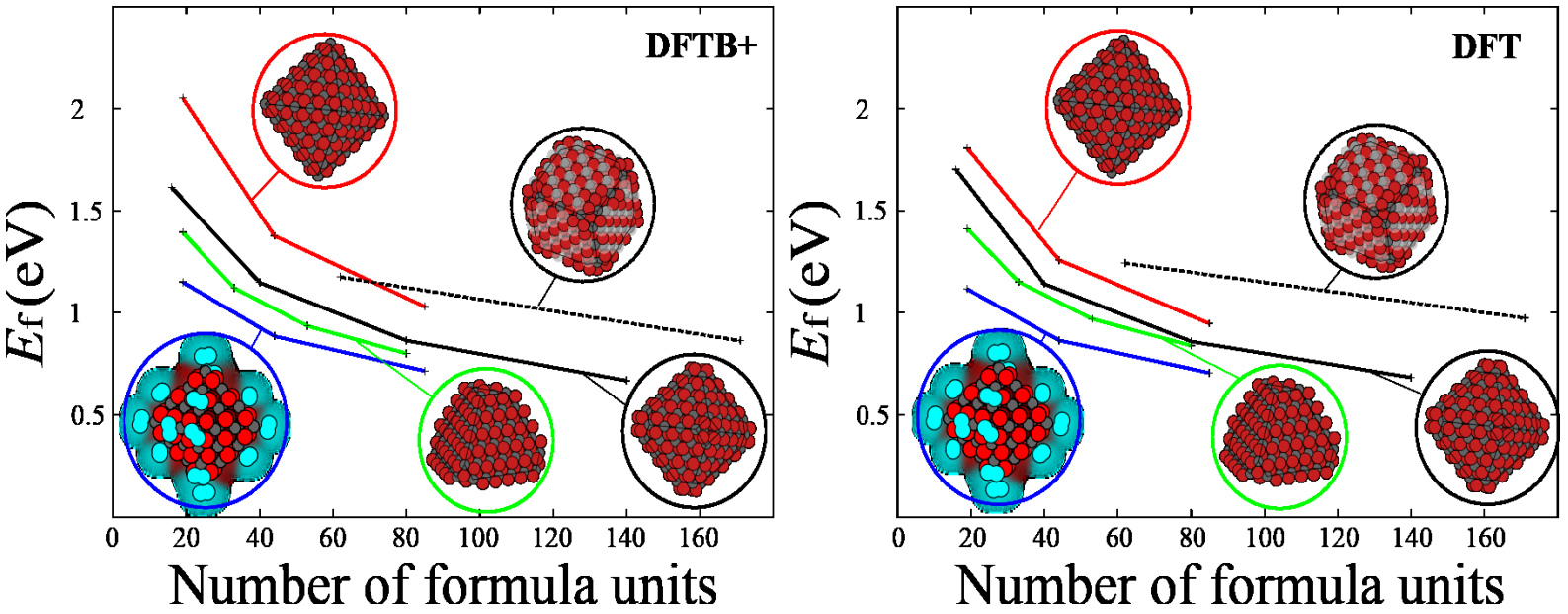

Peter Broqvist, M. Wolf, K. Hermansson, Jolla Kullgren. To be published.

See the turqoise NPs.... That's O_2 molecules which become O_2^- (superoxide ions)...

Huber surfaces =>

SURFACE RECONSTRUCTIONS USING DFTB

[Stefan Huber et al.]

Zn terminated surface

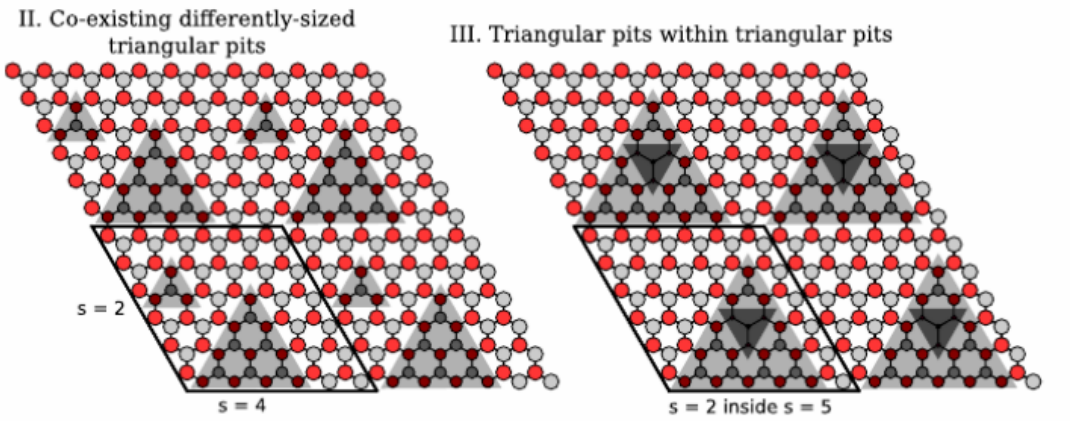

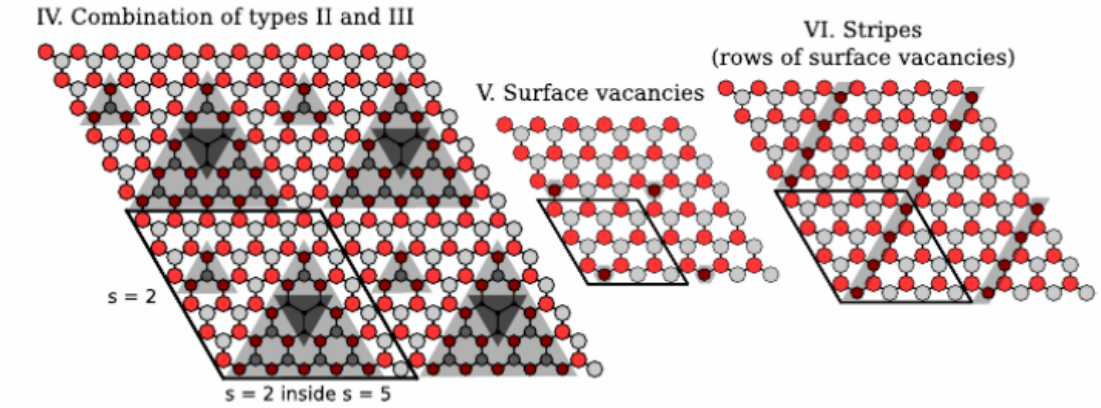

O terminated surface

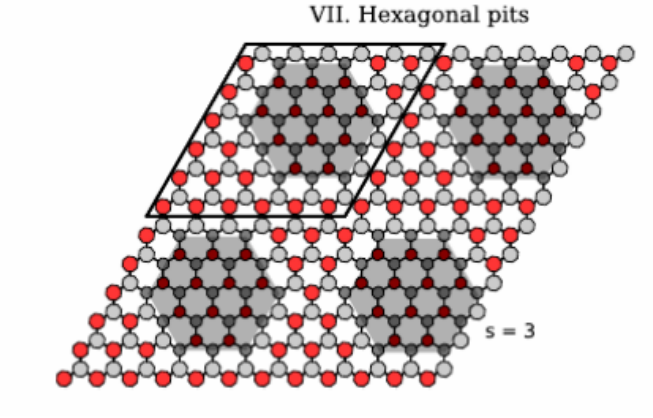

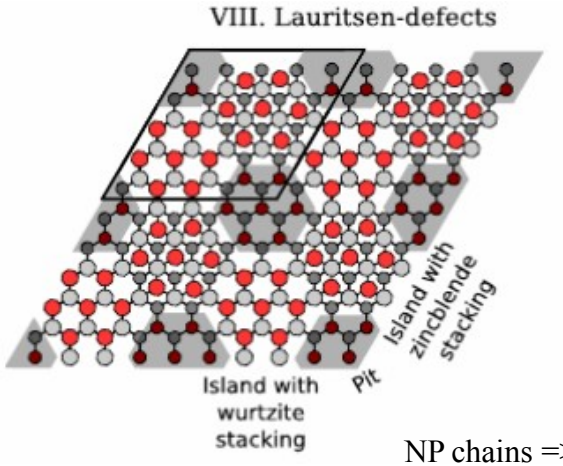

NP chains =>

Ceria Nanochain Growth - with the reactive force-field ReaxFF

ReaxFF force-field: P. Broqvist, J. Kullgren, A van Duin, K. Hermansson, *J. Phys. Chem. C 119* (2015), 13598
MD: B-H Kim, J. Kullgren, M. J. Wolf, K. Hermansson and P. Broqvist, *Frontiers in Chemistry* **7** (2019), 203.

$$E_{System} = E_{bond} + E_{over} + E_{under} + E_{lp} + E_{val} + E_{pen} + E_{tors} + E_{conj} + E_{vdWaals} + E_{Coulomb}$$

Formalism developed by Dr. Adri van Duin (Caltech and Penn State)

Experiment

Wu et al., Langmuir 26, 16595 (2010). TEM images of nano-octahedra.

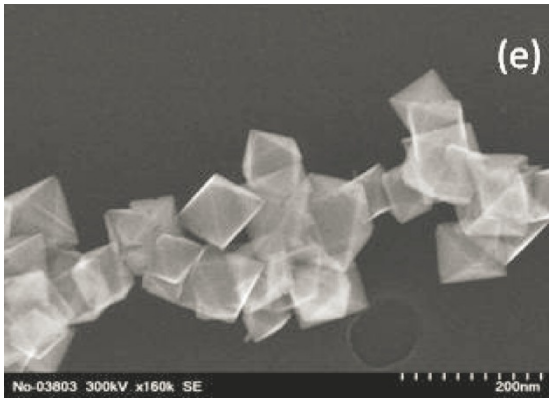

MD simulation

ReaxFF / Canonical ensemble w/ 400 K (Nosé-Hoover thermostat) / Timestep 1 fs / Total 2 ns / 10 NPs of $Ce_{140}O_{280}$ (4200 atoms)

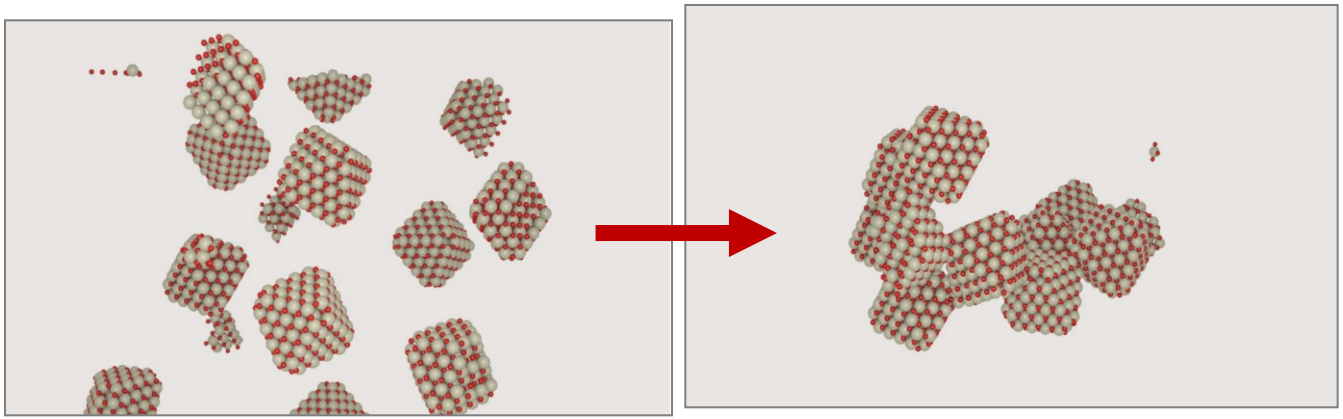

“Reactive Hot Spots”?

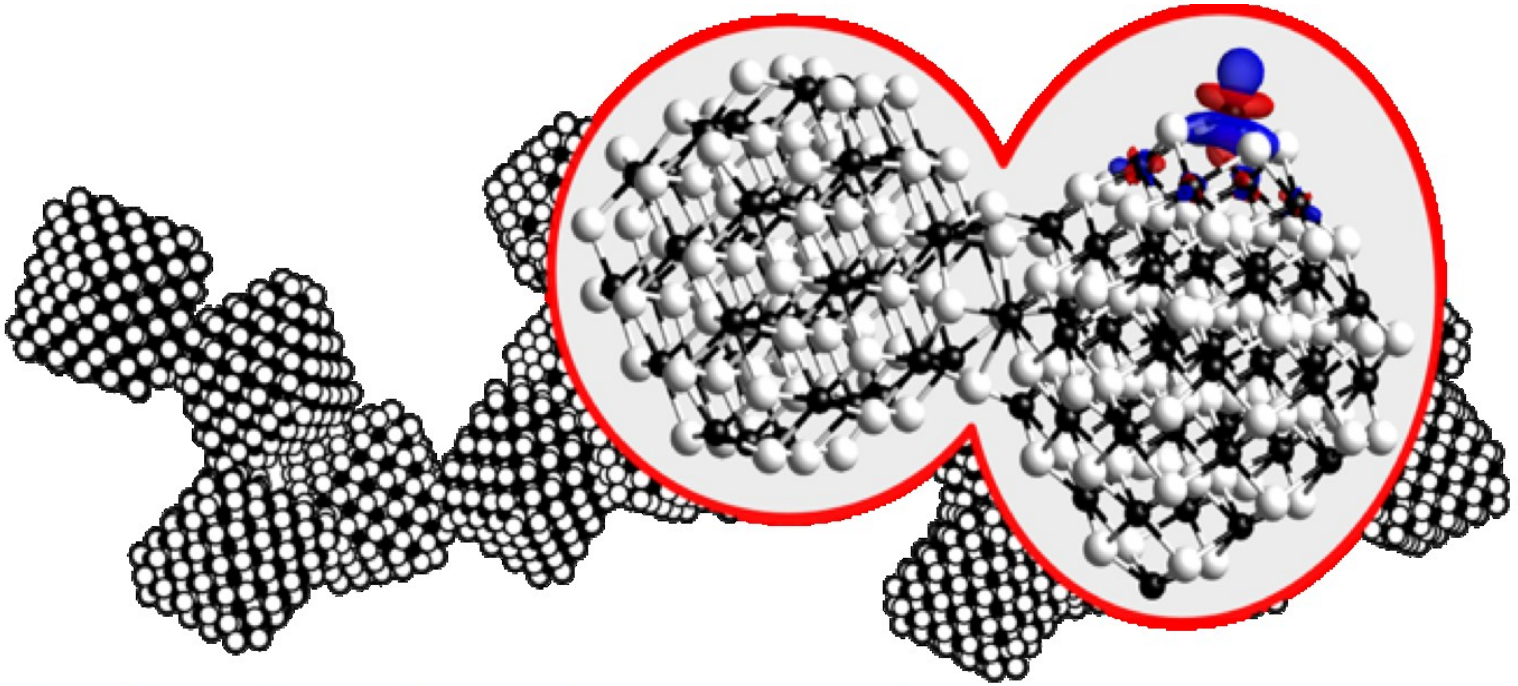

Multiscale simulations [Front. Chem. 7:203, 2019]

Water molecules on ceria =>

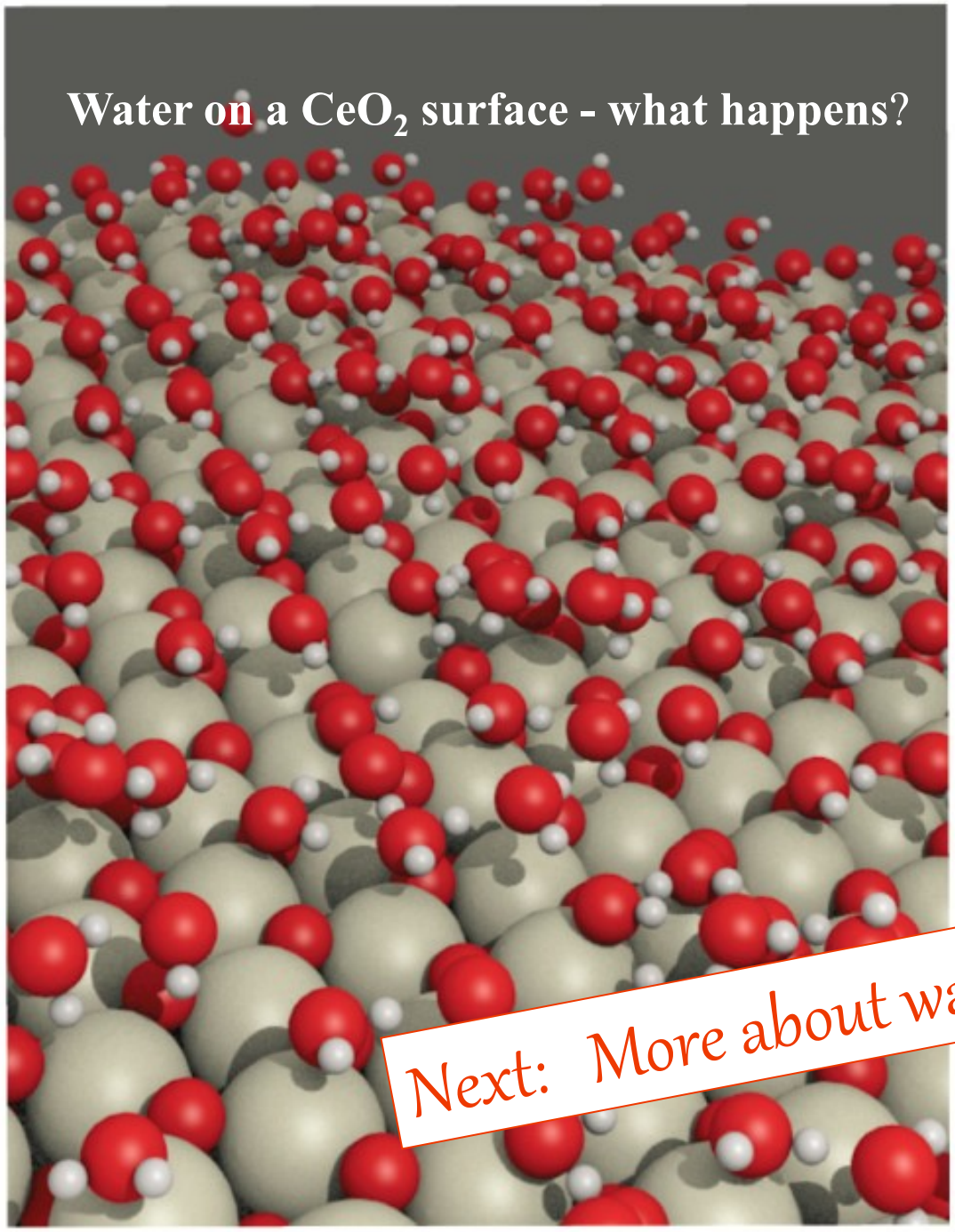
Water on a CeO_2 surface - what happens?
Next: More about water systems!

Water in and on crystals...

Ice II

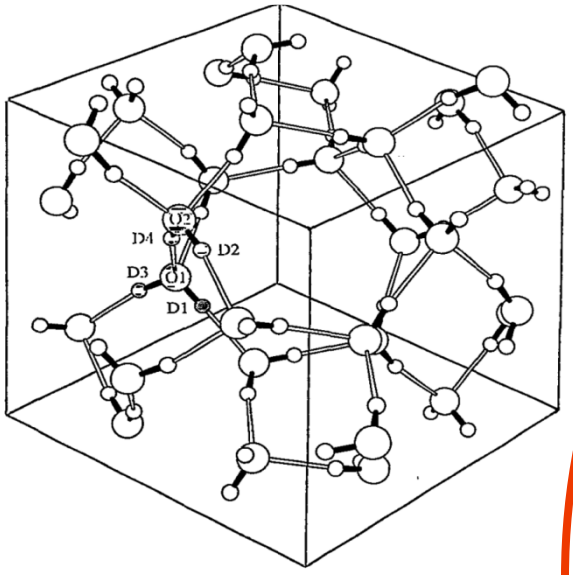

LiOH crystal

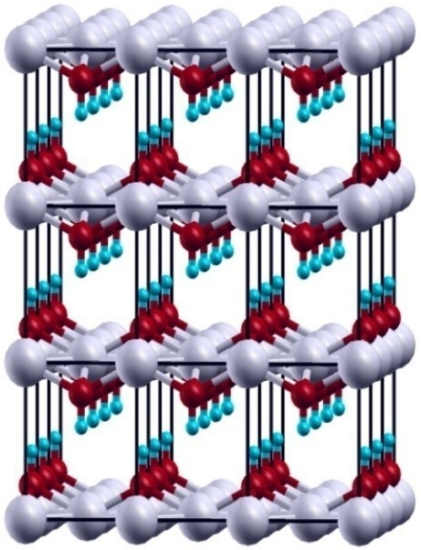

$NaCO_3.10H_2O$

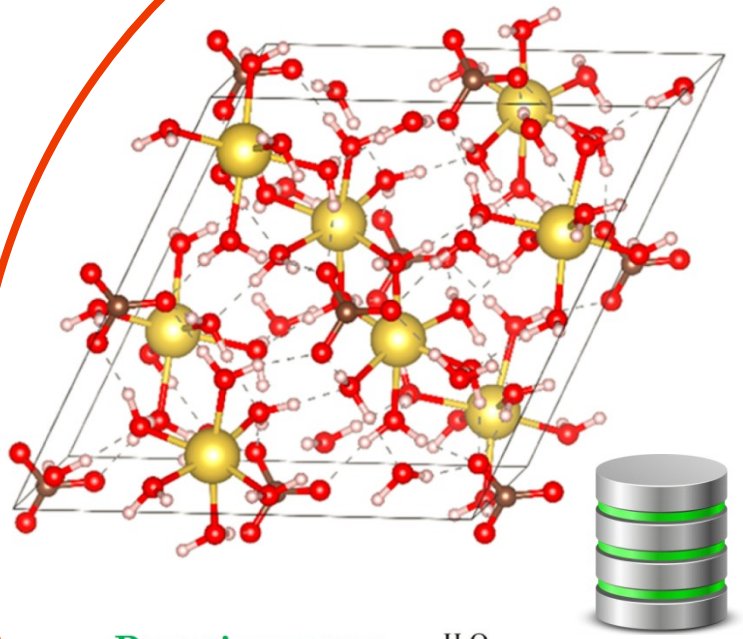

Reactive water

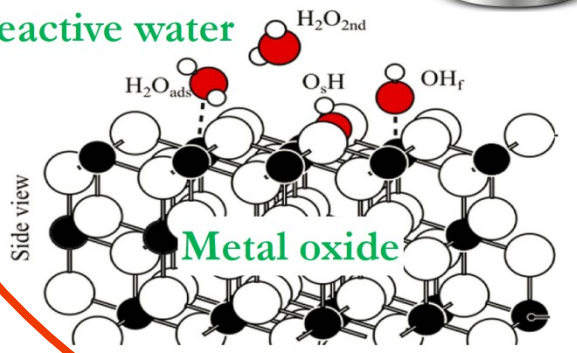

A water film on CeO_2

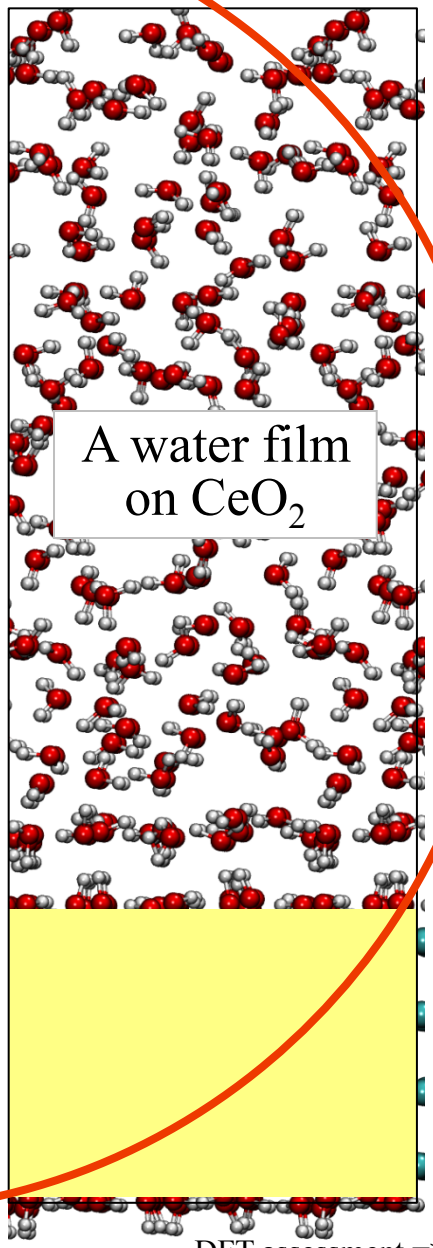

DFT assessment =>

Validation of functional: Calculated vs. experimental neutron diffraction R(O···O) distances

G. Kebede, P. Mitev, P. Broqvist, K. Hermansson, J. Chem. Theory Comput. 15, 584−594 (2019)

MRE, MARE

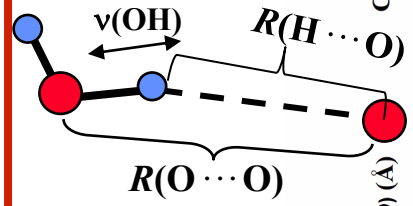

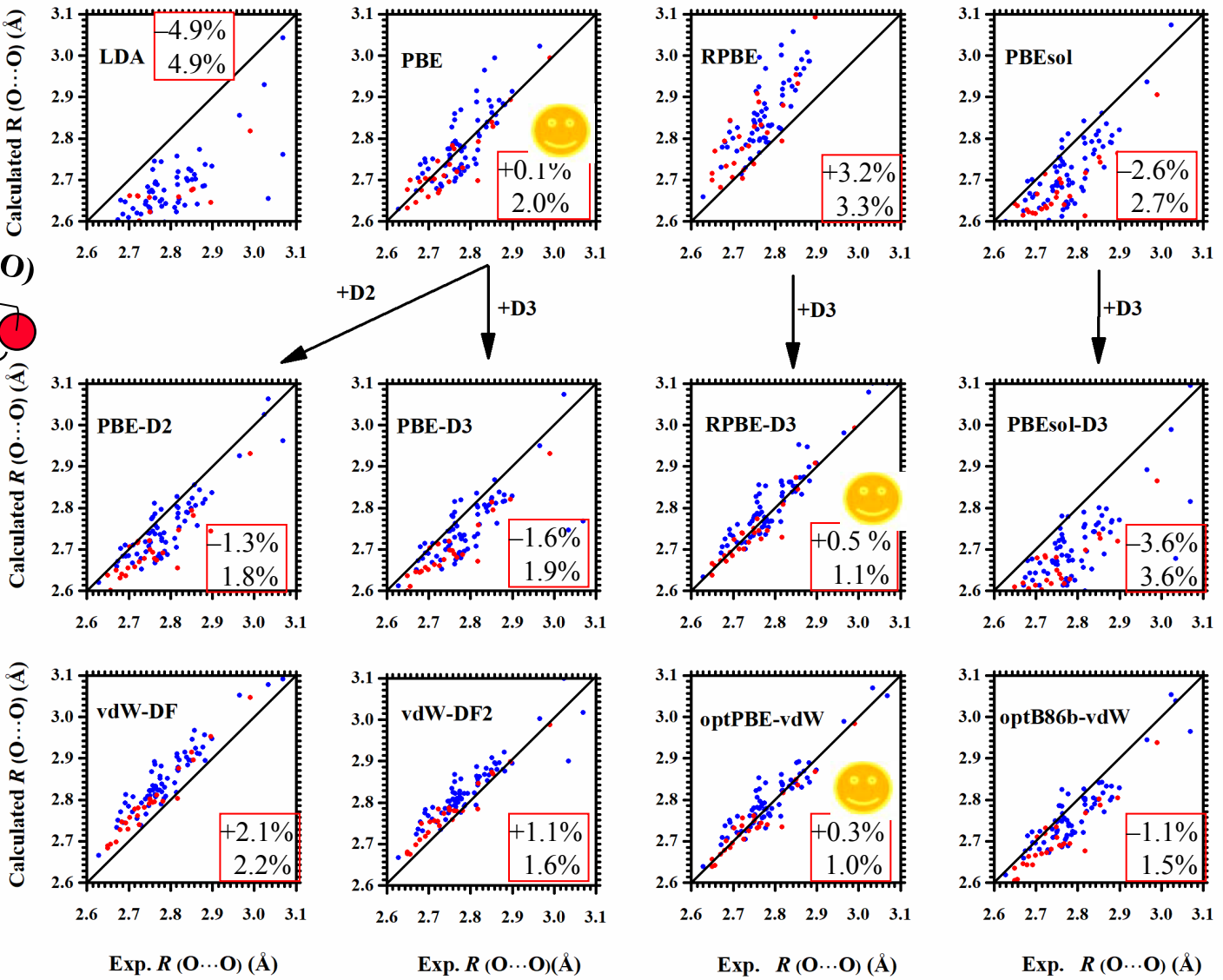

Goal of ML modelling =>

Objective: Predict property XXX for water and OH groups on and in crystals.
Goal: good predictive model + insight (= physics/chemistry). Choice of descriptor.
Here and now Property XXX = IR spectra

Experiment.
There are at least 25 (!) FTIR studies of OH groups on CeO_2. Here from Badri et al. (1996).

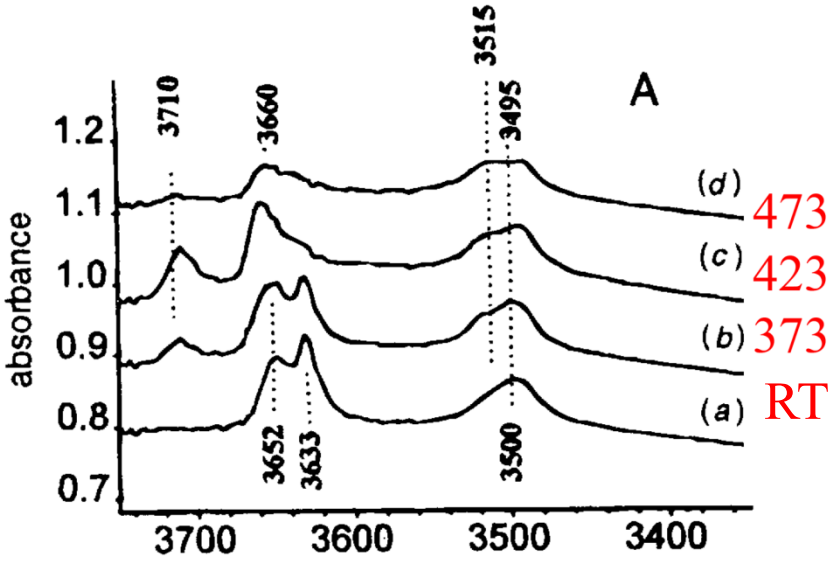

Why are there so many frequencies? =>

... Water OH frquencies are always redshifted by the environment

(gas)

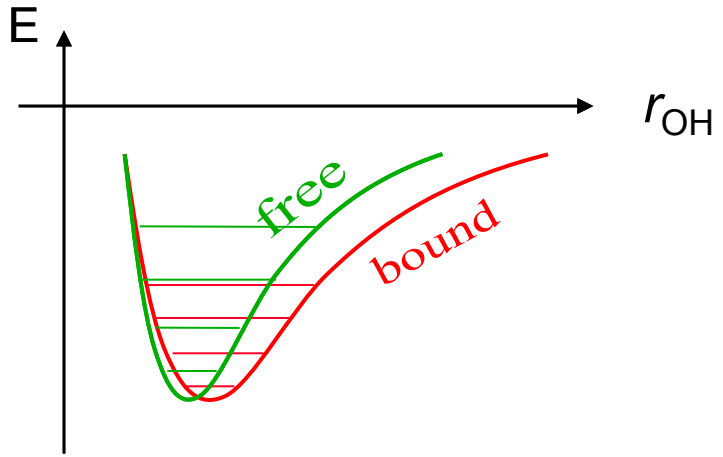

(bound)

Stronger intermol interaction
$\Rightarrow$ weaker intramol bond
$\Rightarrow$ Flatter pot.en curve
$\Rightarrow$ ν(OH) downshifted ("red-shifted")

Regression philosopy =>

Regression philosophy: To make the comparison between descriptors as unified as possible, . . .

- We use the same data points in the regression.
- We use the same regression method (Gaussian process regression)
- We use the same measures of quality for all descriptors.

Kullgren, Röckert, Hermansson (2023). In press.

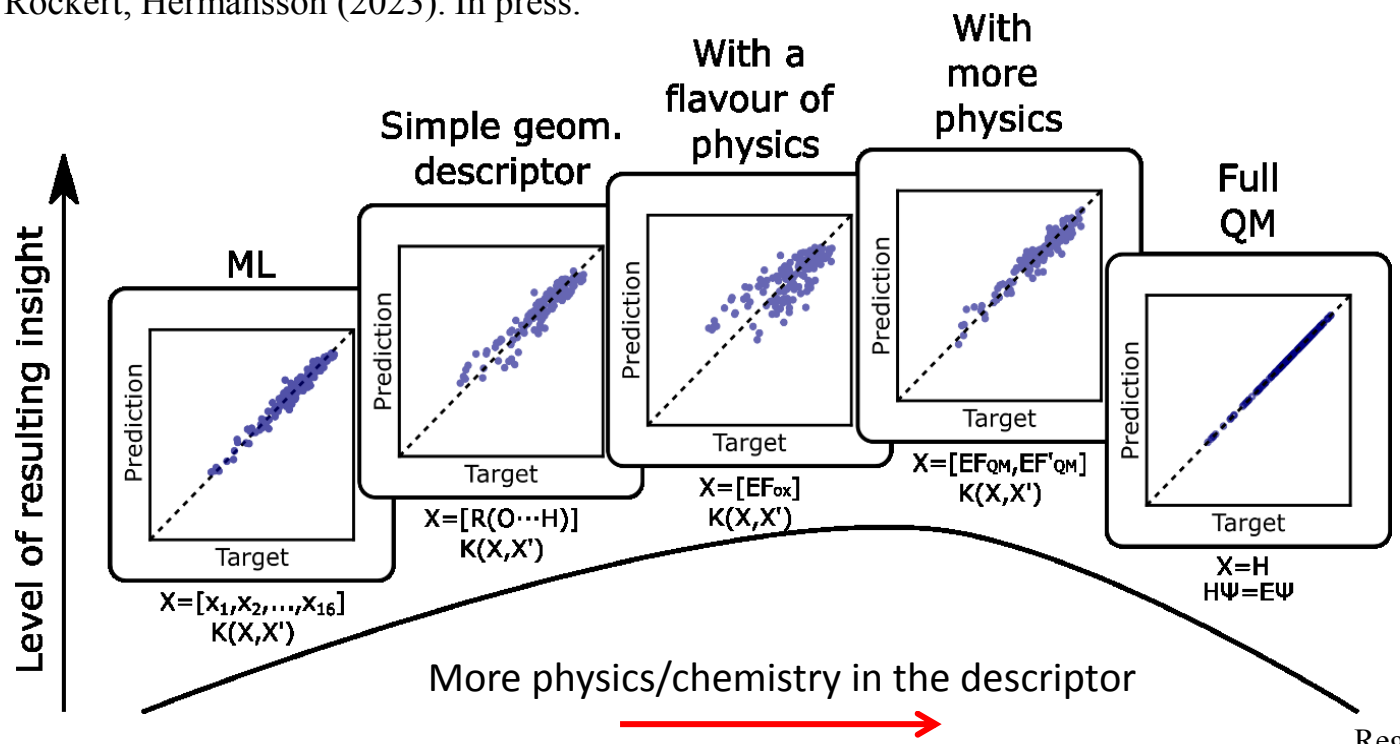

Regression results =>

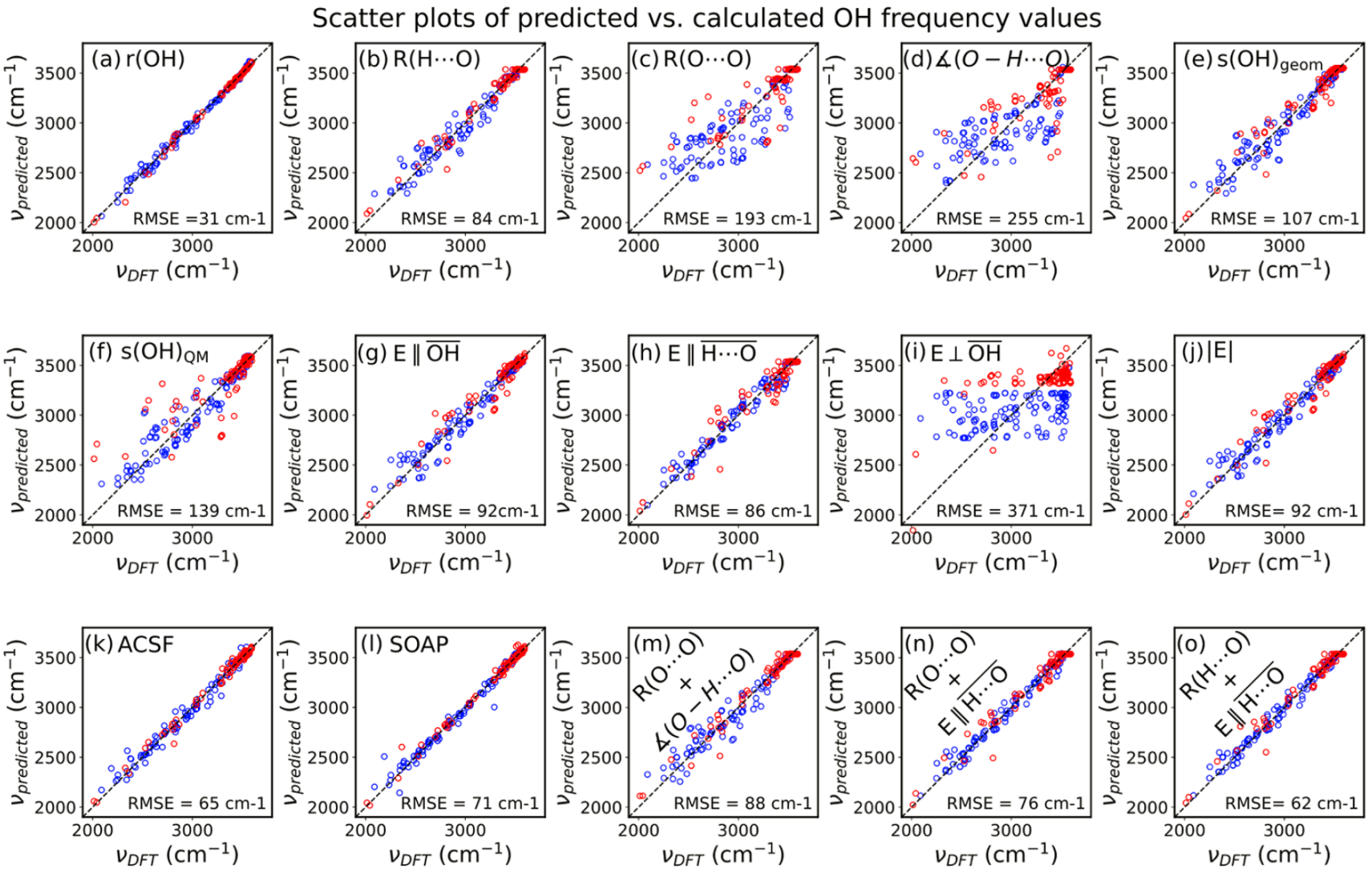
Scatter plots of predicted vs. calculated OH frequency values
(a) r(OH)
RMSE =31 cm-1
(b) R(H···O)
RMSE = 84 cm-1
(c) R(O···O)
RMSE = 193 cm-1
(d) ∢(O − H···O)
RMSE = 255 cm-1
(e) s(OH)geom
RMSE = 107 cm-1
(f) s(OH)QM
RMSE = 139 cm-1
(g) E ∥ OH
RMSE = 92cm-1
(h) E ∥ H···O
RMSE = 86 cm-1
(i) E ⊥ OH
RMSE = 371 cm-1
(j) |E|
RMSE= 92 cm-1
(k) ACSF
RMSE = 65 cm-1
(l) SOAP
RMSE = 71 cm-1
(m) R(O···O) + ∢(O − H···O)
RMSE = 88 cm-1
(n) R(O···O) + E ∥ H···O
RMSE = 76 cm-1
(o) R(H···O) + E ∥ H···O
RMSE= 62 cm-1
νpredicted (cm−1)
νDFT (cm−1)
2000
2500
3000
3500

RMSEs =>

Results for H-bonded water molecules.

Extrapolation to non-H bonded territory.

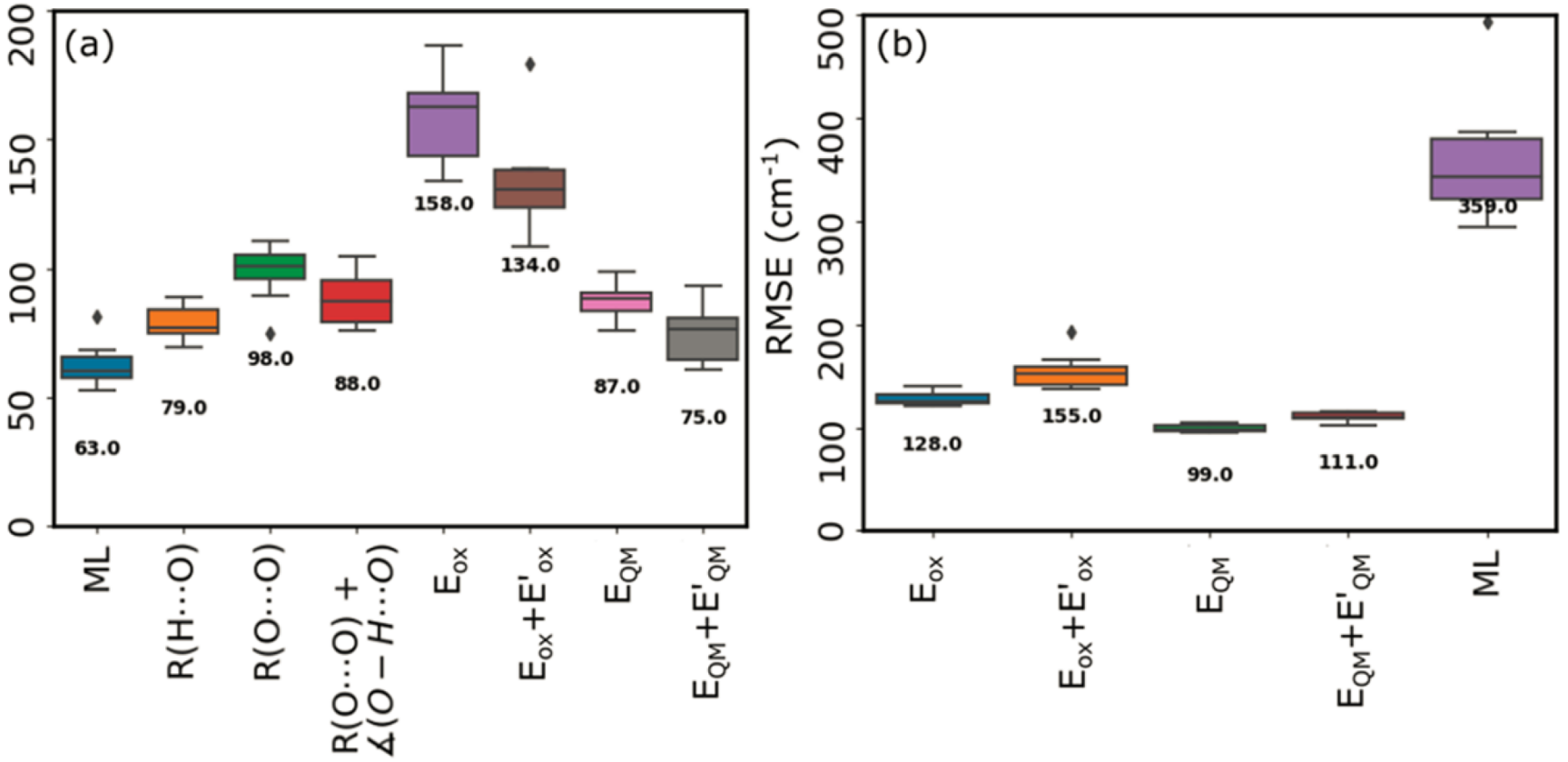

Boxplots summarizing the RMSE values from regression using the various descriptors examined in this study. (a) Regression using the DS_{H2O}^{HB} dataset. (b) Extrapolation to the set of non-hydrogen-bonded data (DS_{H2O}^{NHB}) but using the water models from (a). Each descriptor was fitted 8 times with different splits of training/test data. In each case the value written below the box is the average RMSE over these eight splits, calculated for the test-sets (see text for more details). Scatter plots corresponding to the regressions with the ML, R(H···O), E_{ox} and E_{QM}+E'$_{QM}$ descriptors, respectively, for the DS_{H2O}^{HB} dataset in (a) are shown in the separate panels in Fig. 1. Note that the scales on the y-axes are different in (a) an (b).

Vibrational protocol =>

Our protocol to calculate anharmonic OH stretching vibrational frequency [1]

The structural and vibrational data were collected from the optimized geometries obtained from periodic DFT calculations (optPBE-vdW functional!) usingVASP. To mimic experiments we then calculated 1-D & uncoupled & anharmonic OH vibrational frequencies .

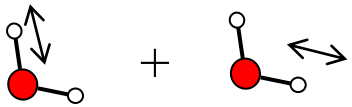

Select the structure (optimized or snapshots from AIMD simulations)

↓

Construct 1D pot. energy curve (PES) with energy points above and below r_e

↓

Solve 1D nuclear Schrödinger equation for the PES using the DVR method =>energy levels; see picture

↓

Calculate the uncoupled , anharmonic OH frequency ν(OH) from $E_1 - E_0$

We use NO scaling!

[1] P.D. Mitev, A.Eriksson, J-F Boily, K. Hermansson, *PCCP 17, 10520--10531 (2015)*

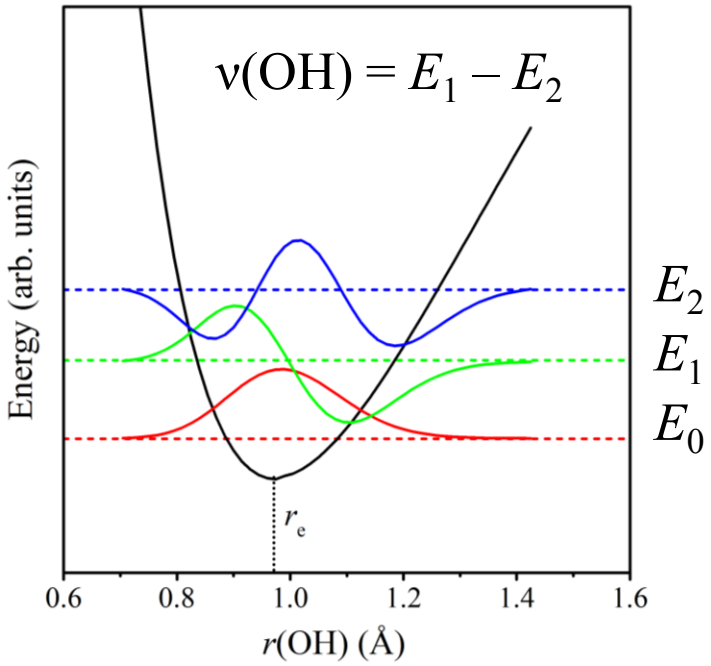

A few correlation curves =>

A closer look at some of the descriptors (here only for ceria)

H_2O and OH^- groups on ceria surfaces

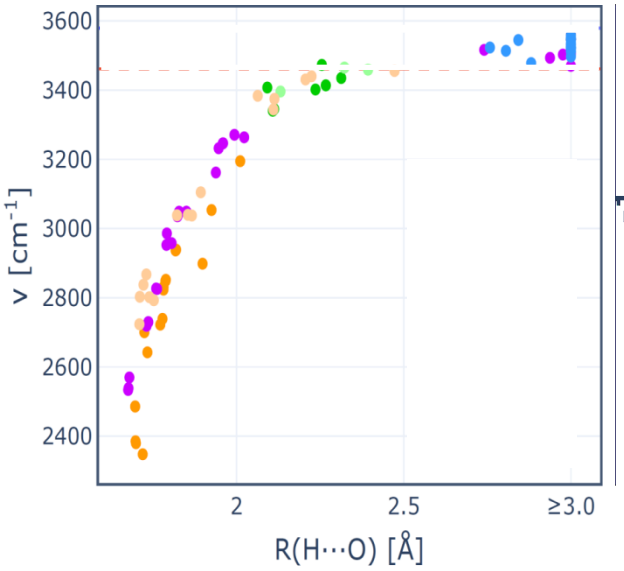

H_2O on ceria surfaces

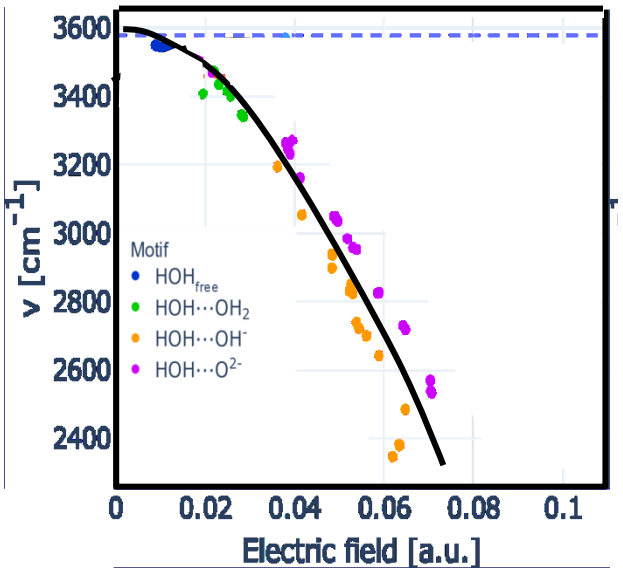

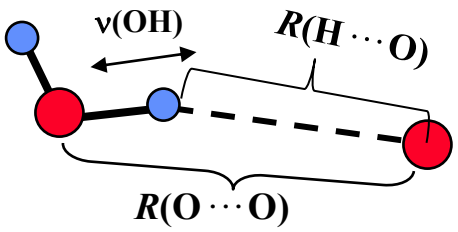

There is **no external** electric field. This is the ***in situ*** electric field, evaluated at the vibrating H atom from the rest of the system outside the H_2O or OH^- .

A closer look at some of the descriptors (here only for ceria)

H_2O and OH^- groups on ceria surfaces

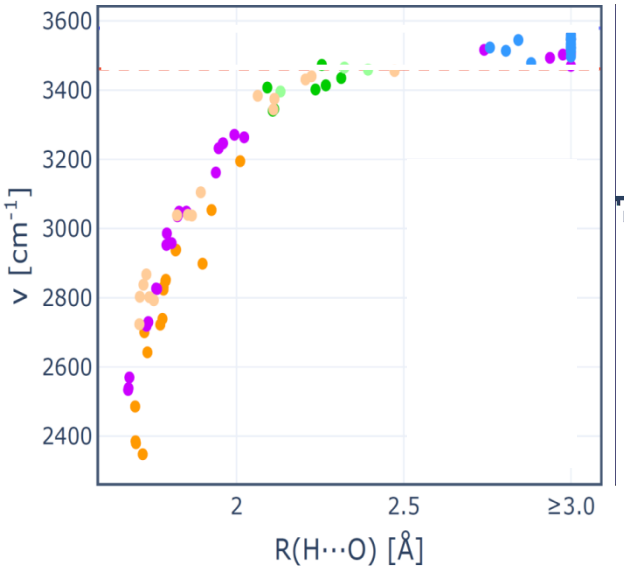

H_2O on ceria surfaces

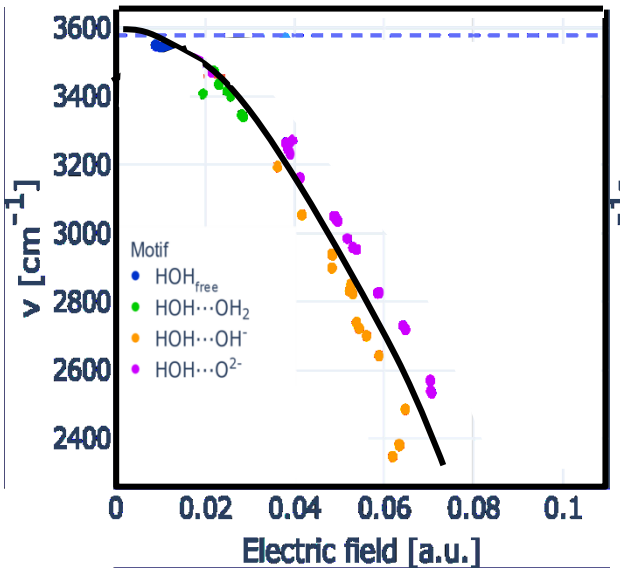

H_2O and OH^- groups on ceria surfaces

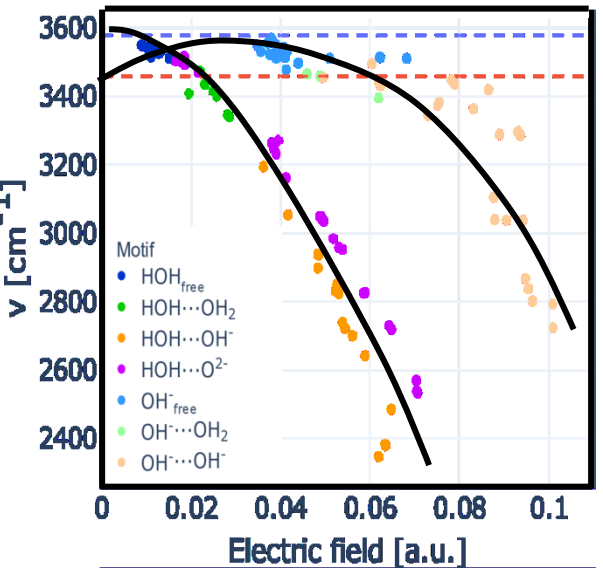

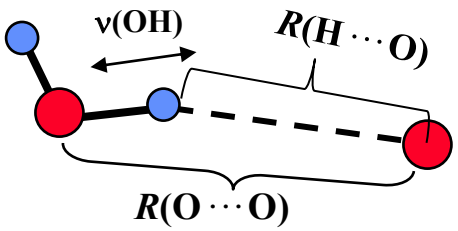

There is **no external** electric field.
This is the ***in situ*** electric field, evaluated at the vibrating H atom from the rest of the system outside the H_2O or OH^- .

Water on ZnO, NN =>

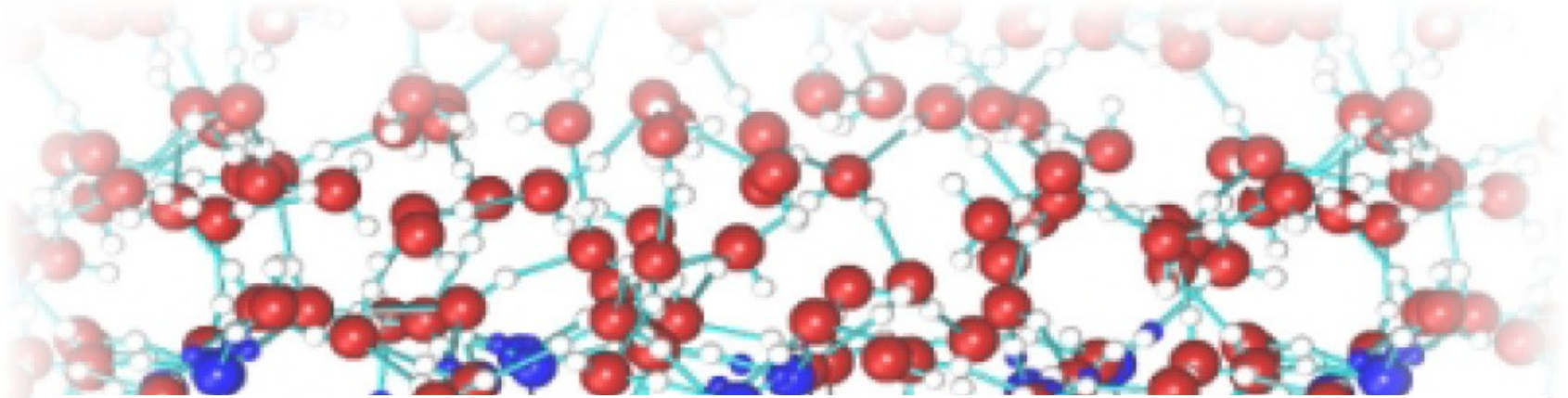

A thick water film on ZnO(1 0 -1 0).
Altogether 35440 oscillators were examined and their v(OH) values calculated

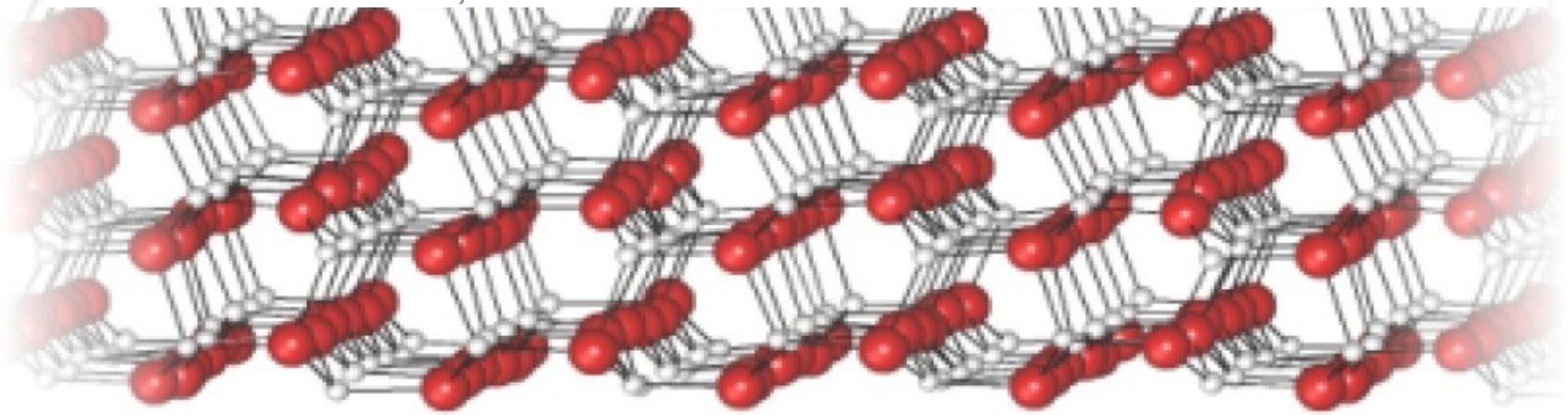

Method: protocol

Generate stuctures from MD starting from 50000 DFT calculations

[V. Quaranta, et al. JPCLett. 8, 1476 (2017)]

#1. Generated a large *training set* of DFT-energies (RPBE-D3) for Zn-water clusters

#2. Generated a force-field from DFT.
This *NN-based force-field is fast and accurate*.

#3 Performed a long ab initio-MD simulation with this energy function, (LAMMPS with NNP extension).

Generate spectra (for 35000 MD structures)

[V. Quaranta, et al. J Chem Phys 148, 241720 (2019)]

#4. Select snapshots, make Energy scans along OH stretching coordinate, periodic calculations.

#5. Solve vibrational Schrödinger eqn using a DVR approach (discrete-variable basis set representation)

#6. Calculate anharmonic vibrational OH spectra. **[P.D. Mitev, et al., PCCP 17 (2015)]**

The MD simulation system

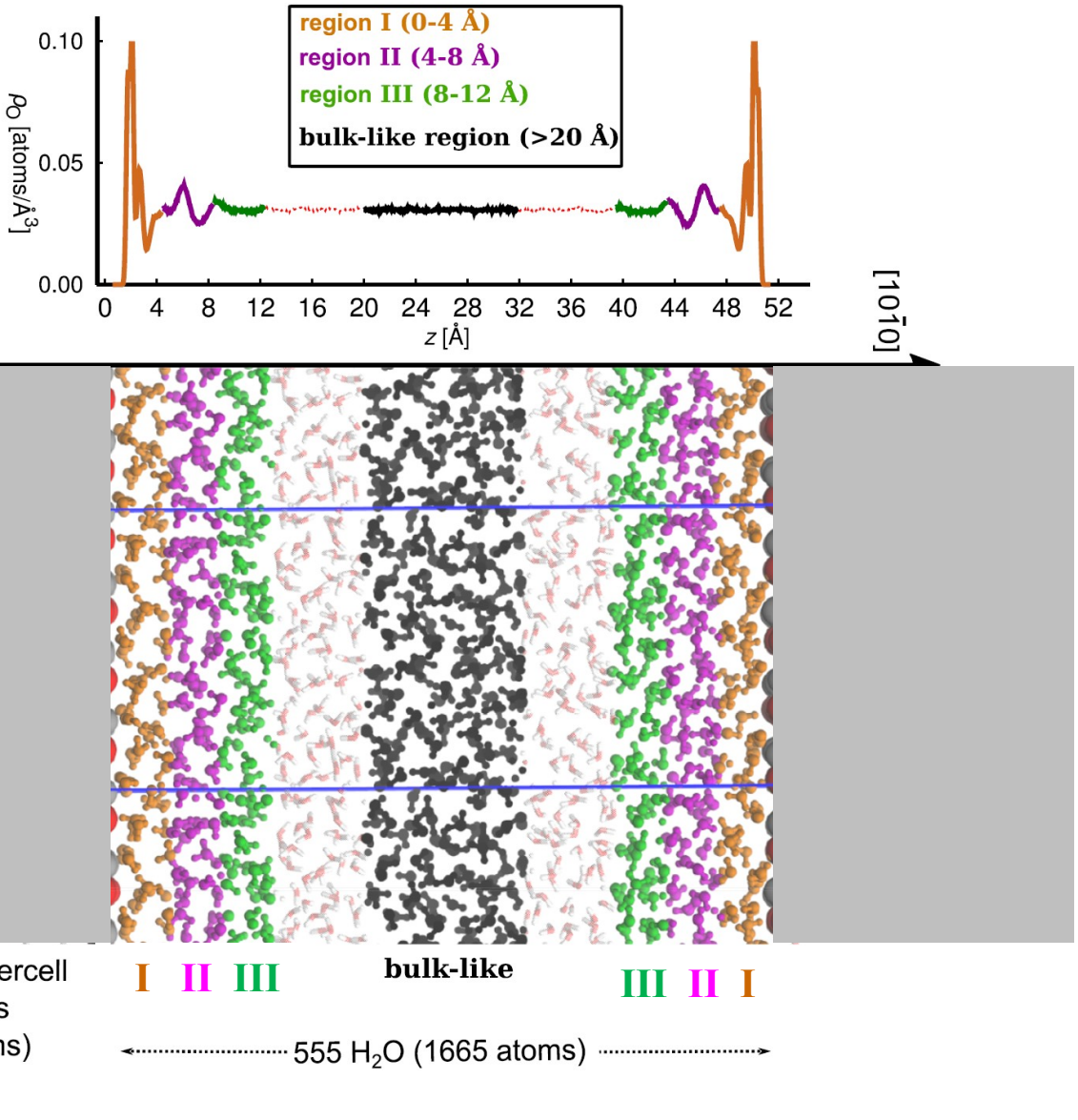

Result

OH vibrational spectra at the interface

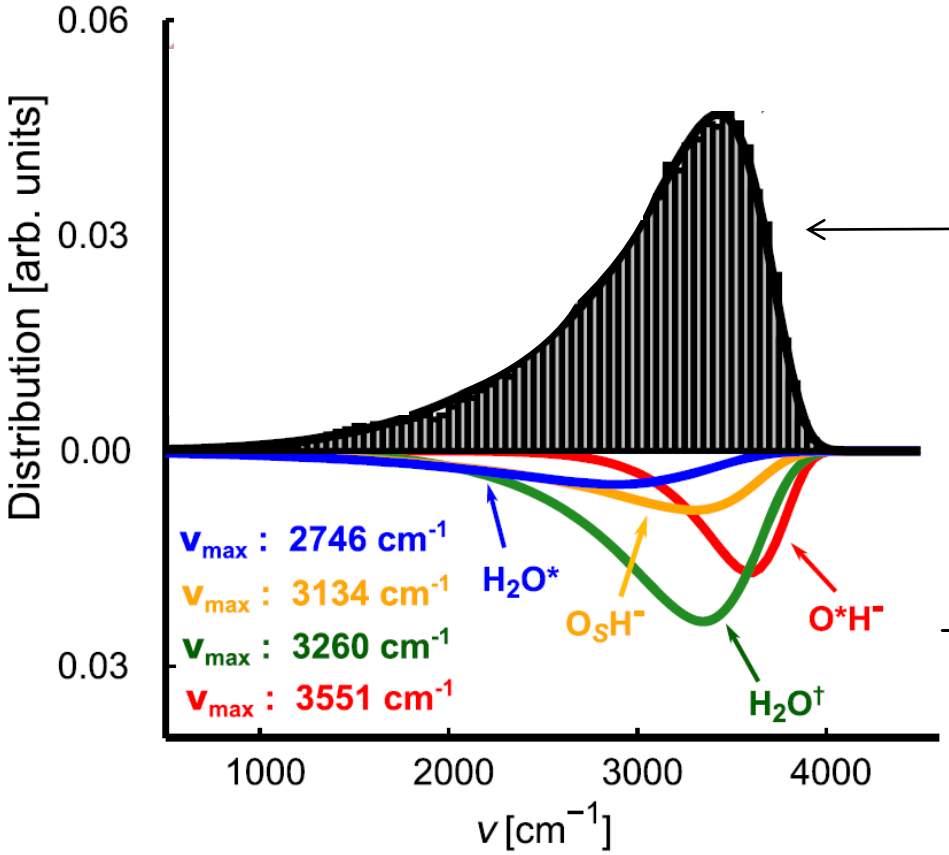

Total spectrum
i.e. all OH

"Title: Maximally resolved OH spectrum.

This is possible because we have such very good statistics.

Good statistics is possible because we use the NNP potentials."

Result, cont.:

The structural motifs behind the spectral peaks (in region closest to slab)

from surface (Å)	No. of frequencies
0–4	29 531
4–8	1 931
8–12	1 914
>20	2 064

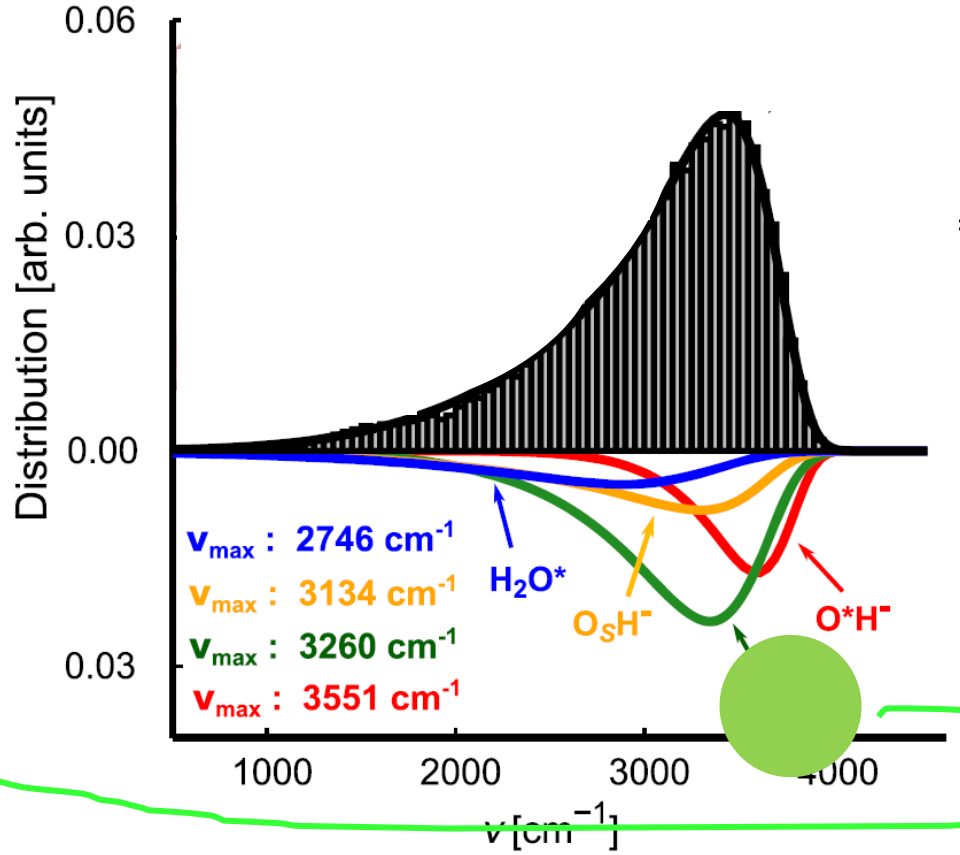

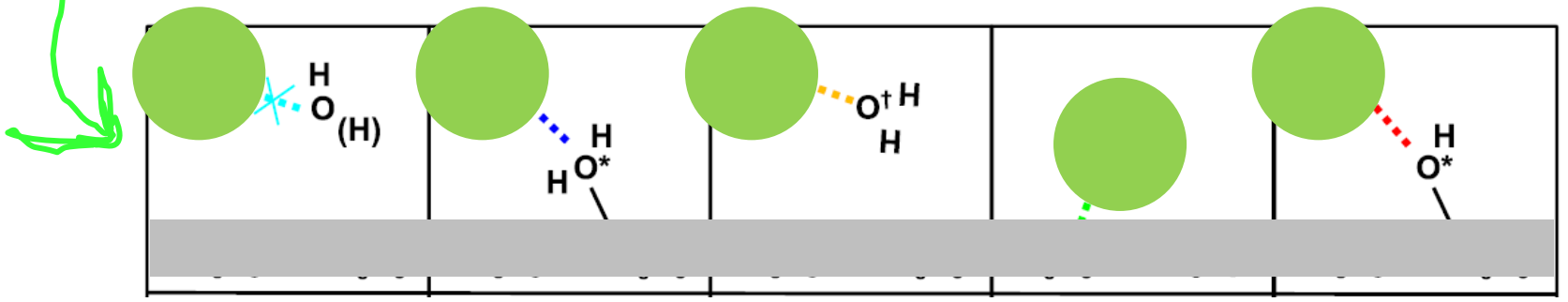

Result: ν(OH) vs R(H•••O) correlation

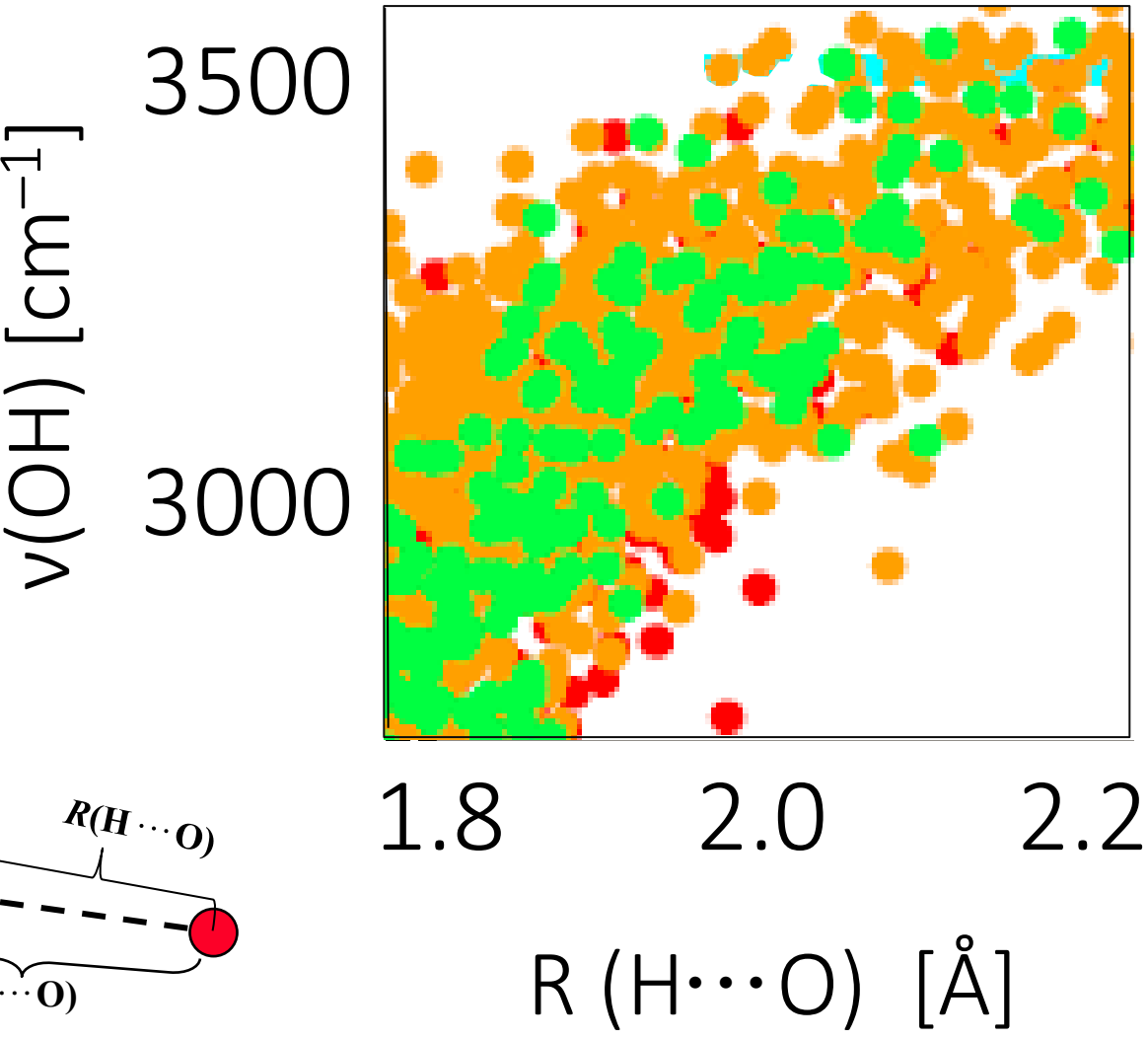

Hydrophobicity

Water on ceria

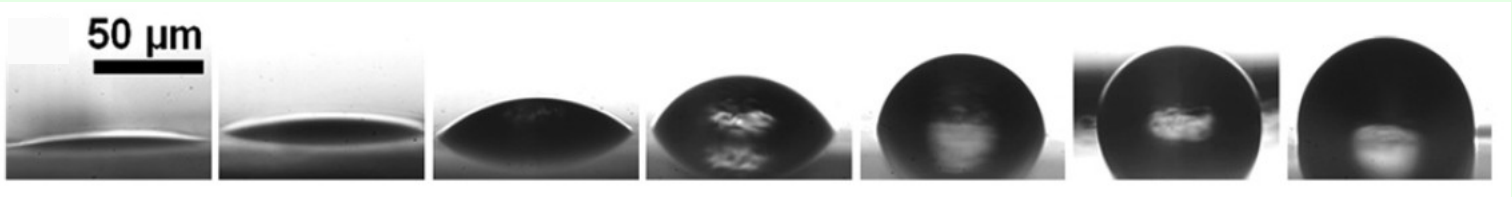

Preston et al., Appl Phys Lett. 105, 011601 (2014)

Agosta, Dzugutov, Hermansson, Angewandte Chemie Comm. (2023) In press.

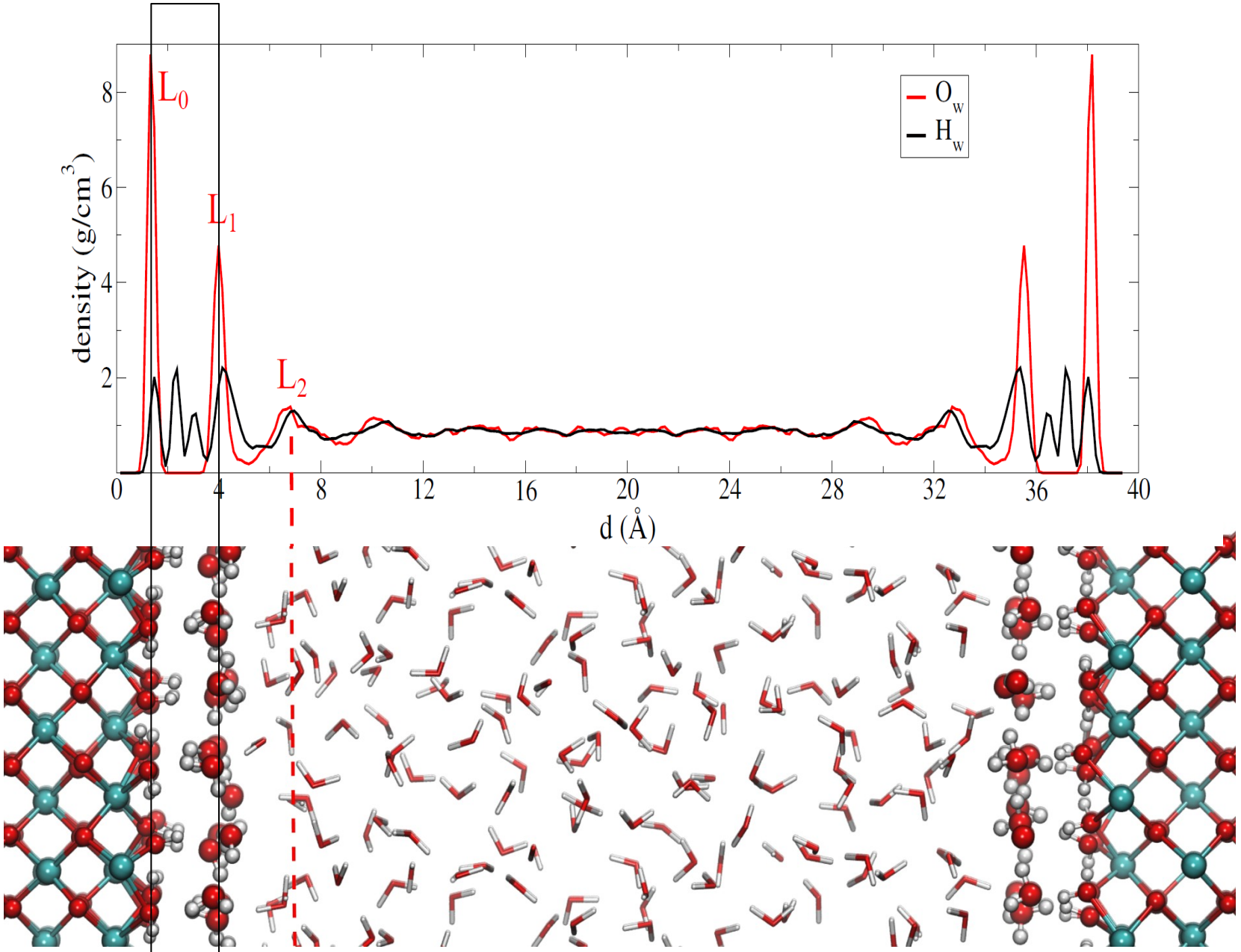
L0
L1
L2
O_w
H_w
density (g/cm^3)
d (Å)
0
4
8
12
16
20
24
28
32
36
40
2
4
6
8

We find the hydrophobicity to manifest itself in several ways, namely by **...**

... A considerable **diffusion enhancement** of the confined liquid water compared to bulk water at the same thermodynamic condition.

... **Weak adhesion** energy of the water film on the hydroxylated ceria surface.

Interaction type	Energy (eV)
L_0-L_1	0.53
L_1-L_2	0.28
bulk water	0.45

... The small number of **H-bonds formed between** the hydrophobic water layer and the rest of the water film.

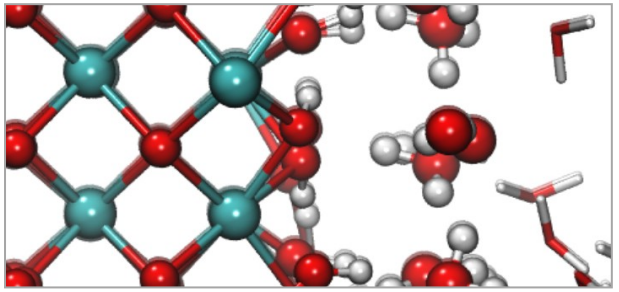

... The fact that the (100) surface appears to sustain a **water droplet** (additional simulations)

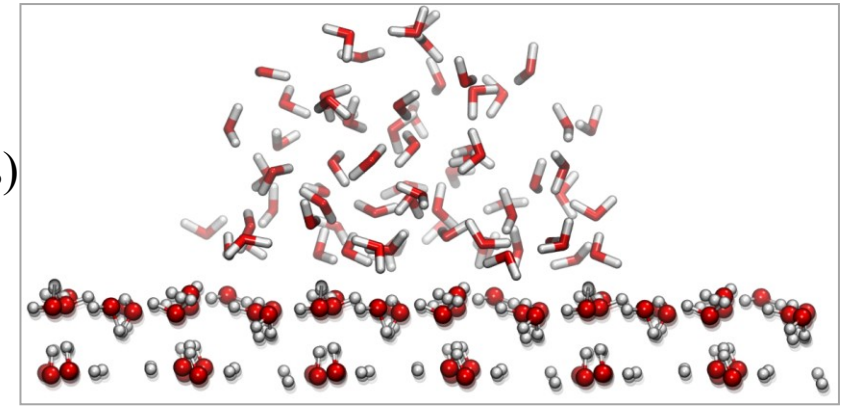

Conclusions

* Ceria F-defects? A multiscalar journey
* Ceria NPs: DFTB ≈ DFT
* Two data-bases: Crystalline hydrates and Water/OH on metal oxide surfaces
  - assessment of descriptors with the goal of balance
  - a closer look at the some of *the simpler descriptors*
* Vibrational frequencies were chosen as a sample property because...
* Two examples of solid-liquid interface simulations.


Thank you!
and thanks to
Drs. Peter Broqvist, Jolla Kullgren, Pavlin Mitev, Matthew Wolf, Lorenzo Agosta
and PhD student work by Getachew Kebede, Dou Du and Andreas Röckert

3. DFTB

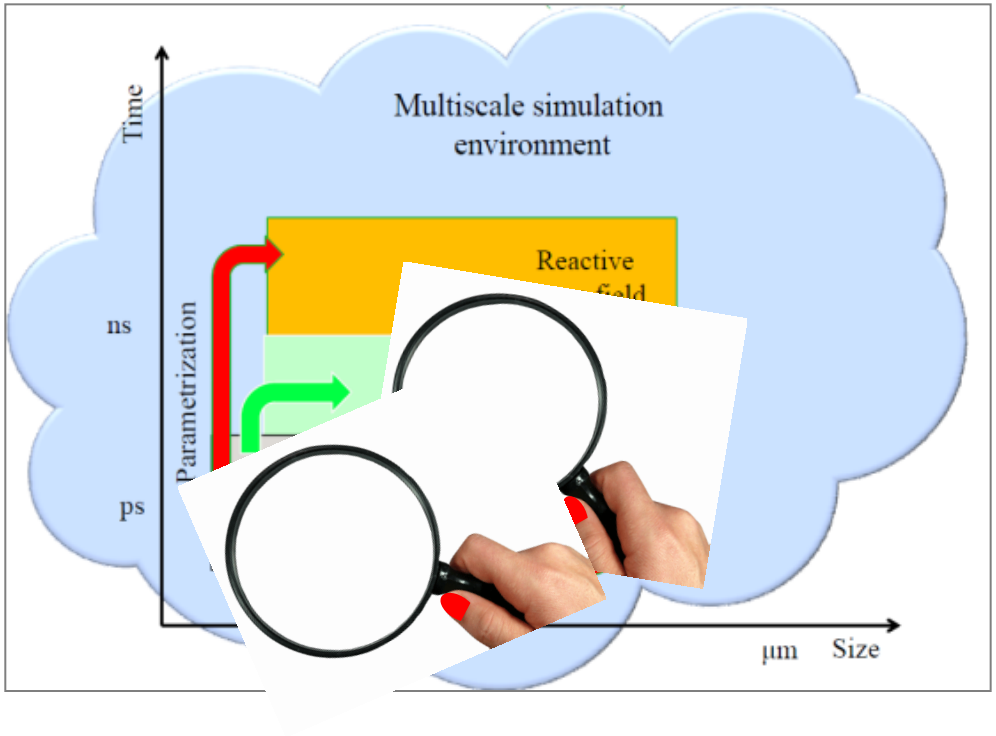

Collaboration with Prof. Thomas Frauenheim, Dr. Balint Aradi, Dr. Christof Köhler, *Bremen Center for Computational Materials Science*

Uppsala: Jolla Kullgren, Peter Broqvist, Matthew J. Wolf, KH

SCC-DFTB

Self-Consistent-Charge Density-Functional Tight-Binding (SCC-DFTB) parameters for Ceria – from 0 D to 3D

Second order expansion of the DFT Kohn-Sham energy w.r.t. density fluctuations

Total Energy

Second order expansion of exchange-correlation functional w.r.t the charge density fluctuations

$$E_{\text{tot}}^{\text{DFTB}} = \sum_{i}^{\text{occ}} n_i \langle \Psi_i | \hat{H}_0 | \Psi_i \rangle + \frac{1}{2} \sum_{\alpha\beta}^{N} \gamma_{\alpha\beta} \Delta q_\alpha \Delta q_\beta + E_{\text{rep}}$$

Zero-order term: summation over all occupied electronic states

Accounts for the double-counting terms and the ion-ion interaction

$$E_{\text{rep}} = \sum_{I<J} V_{\text{rep}}^{IJ}(r_{IJ})$$

Porezag, Frauenheim, Köhler, Seifert, Kaschner, Phys. Rev. B. 51, 12947 (1995)
Seifert, Porezag, Frauenheim, Int. J. Quantum. Chem. 58, 185 (1996)

”Second order expansion of the DFT Kohn-Sham energy w.r.t. density fluctuations”

$$E = \sum_{i}^{occ} \langle \Psi_i | \hat{H}^0 | \Psi_i \rangle + \frac{1}{2} \iint' \left(\frac{1}{|\vec{r} - \vec{r}'|} + \left. \frac{\delta^2 E_{xc}}{\delta\rho\, \delta\rho'} \right|_{n_0} \right) \Delta\rho\, \Delta\rho'.$$

$$- \frac{1}{2} \iint' \frac{\rho_0' \rho_0}{|\vec{r} - \vec{r}'|} + E_{xc}[\rho_0] - \int V_{xc}[\rho_0] n_0 + E_{cc}$$

2-center only, tabulated

Depends only on reference density

$$E^{SCC} = \sum_{i\mu\nu} c_\mu^i c_\nu^i H_{\mu\nu}^0 + \frac{1}{2} \sum_{\alpha\beta} \gamma_{\alpha\beta} \Delta q_\alpha \Delta q_\beta + \frac{1}{2} \sum_{\alpha\beta} U[\rho_0^\alpha, \rho_0^\beta]$$

Porezag, Frauenheim, Köhler, Seifert, Kaschner, Phys. Rev. B. 51, 12947 (1995)
Seifert, Porezag, Frauenheim, Int. J. Quantum. Chem. 58, 185 (1996)

Why SCC-DFTB?

- SCC-DFTB combines reliability of DFT with computational efficiency of ReaxFF
  - Parameters based on atoms and pairs of atoms
  - The parameters can be made transferable
  - Flexible w.r.t parameterization

Getting the DFTB parameters

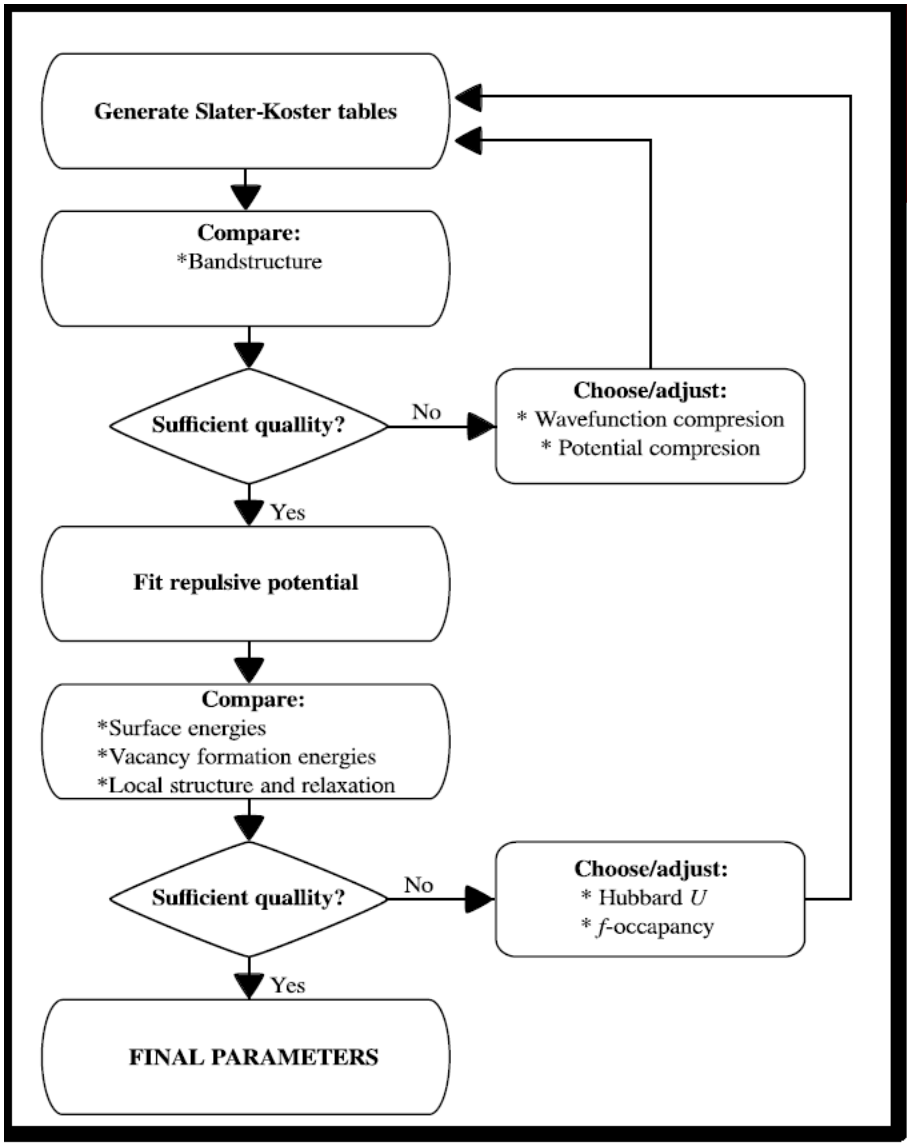

* No strict fitting
* Qualitative assessment
* f-occupancy important!
  - similar to pseudo potentials
* Special focus on:
  - 3D → 0D transferability (bulk to nano)
  - Vacancy formation energies

Getting the DFTB parameters

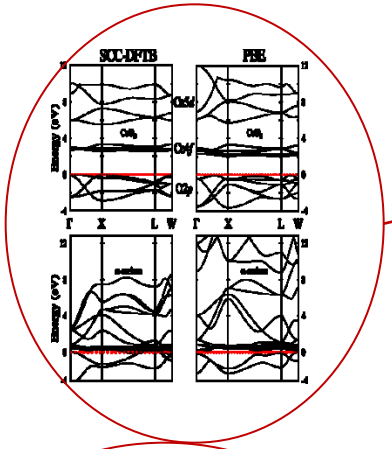

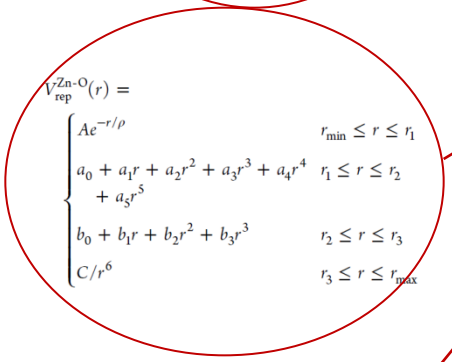

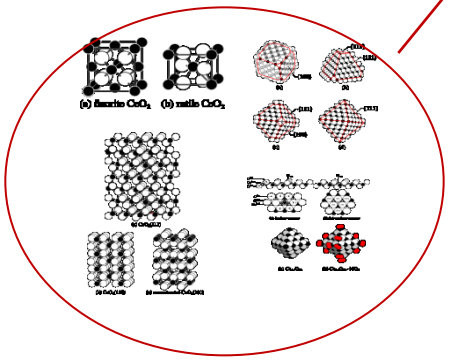

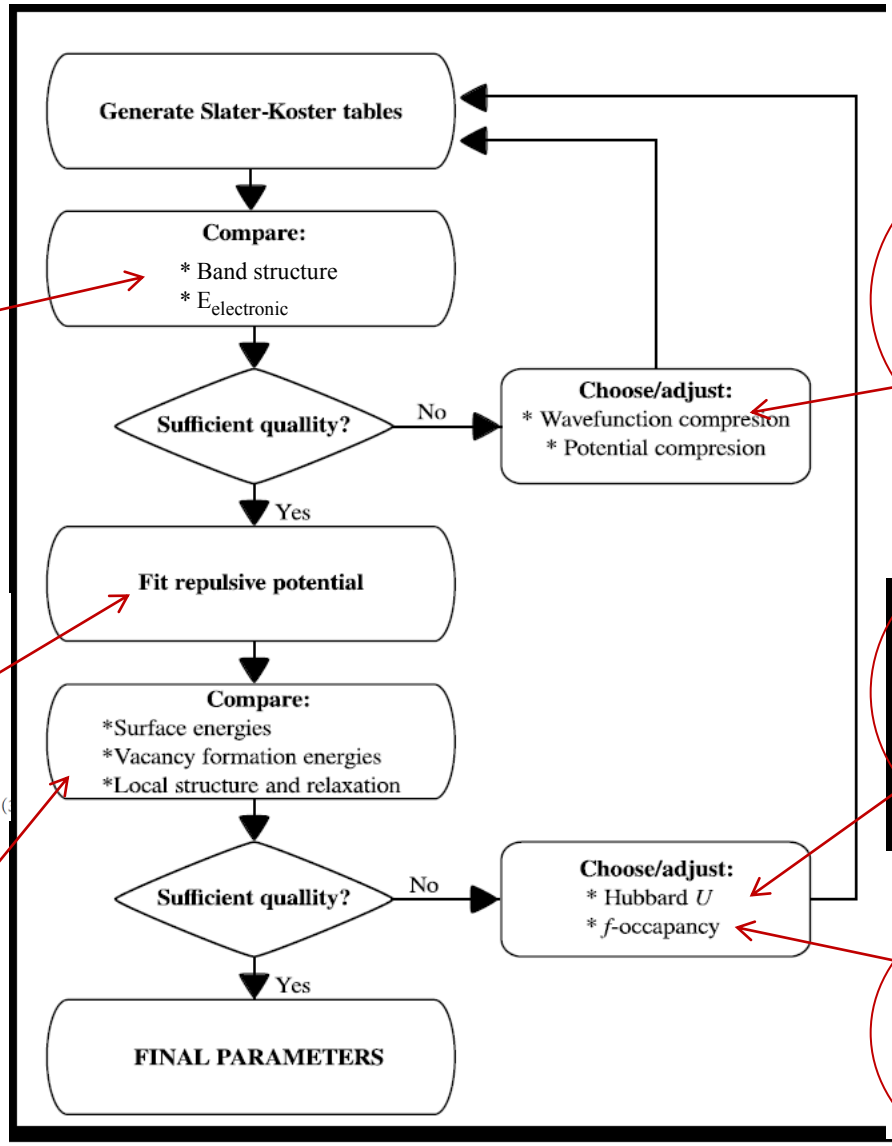

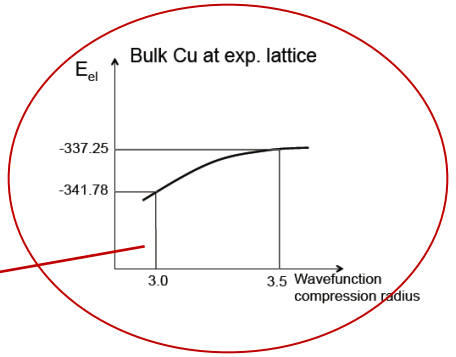

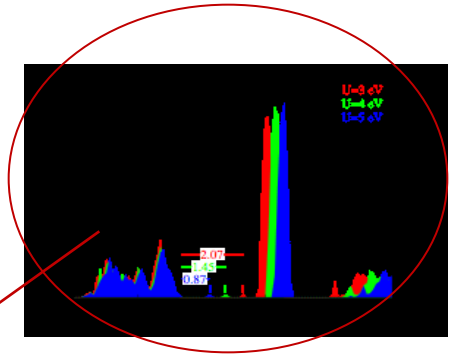

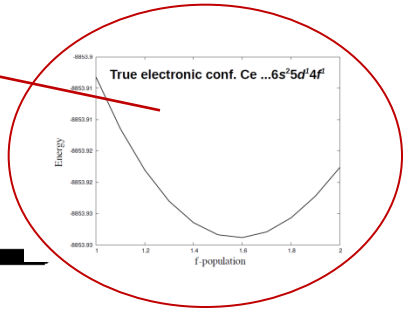

Method

First: Global optimization of particles (e.g. the perfect octahedra $Ce_{19}O_{32}$, $Ce_{44}O_{80}$, $Ce_{85}O_{160}$) using a shell-model force field

Input: No. of atoms **Output:** Most stable structure

Then: Local optimization with DFT

Then: O_2 adsorption calculations with DFT with optimization.

DFT calculations:

- Vienna Ab-initio Simulation Package (VASP)
- The GGA+U functional is used to "correctly" describe localized Ce*4f* electrons
- Plane-wave basis / PAW potentials
- Periodic calculations

SEM image of ceria (CeO_2) nanocrystals

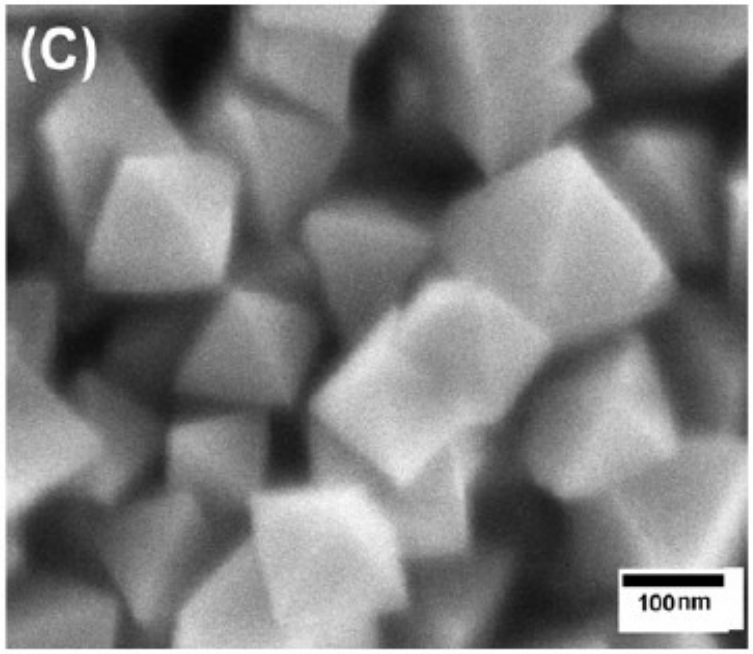

{111}-terminated octahedra

"SEM image of ceria (CeO_2) octahedra"
[Z. Wu et al., Journal of Catalysis 285, 61 (2012)].

It has been found experimentally that the oxygen storage capacity of very small CeO_2 nanoparticles increases drastically.
EPR spectroscopy has detected O_2^- ions (superoxo ions).

No mechanism was proposed. We made DFT calc. and proposed a mechanism.
Broqvist, Kullgren, Hermansson, J. Phys. Chem. Letters (2014)

We constructed regular octahedral nanoparticles
(understoichiometric w r t oxygen)

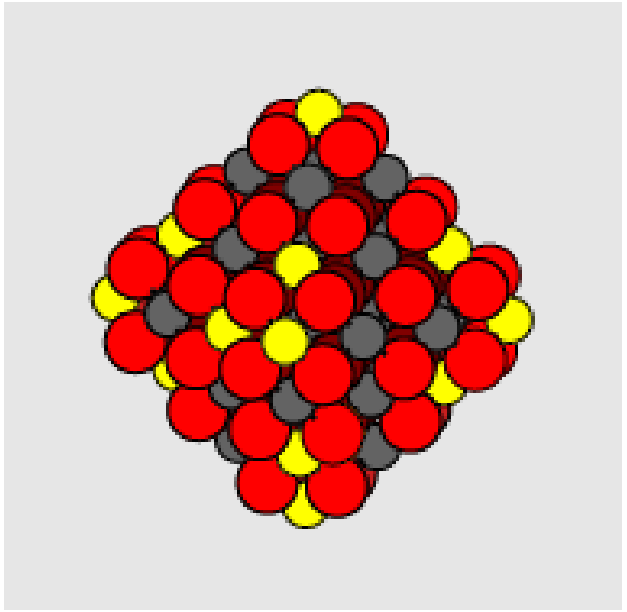

$Ce_{44}O_{80}$

O^{2-}

Ce^{3+}

Ce^{4+}

Superoxide (

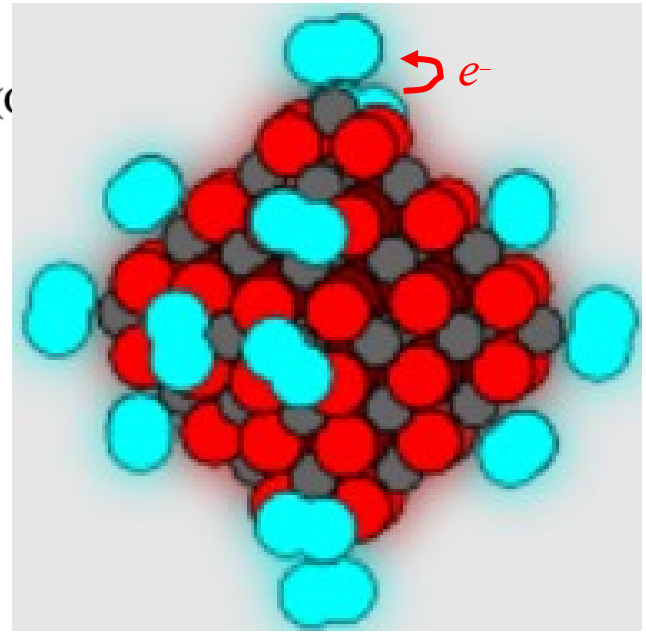

$Ce^{3+} \rightarrow Ce^{4+}$

$O_2 \rightarrow O_2^-$

We then added O_2 molecules to the regular octahedron, .and found ...

$Ce_{44}O_{80}*16O_2$

We proposed that the large OSC originates from ”supercharged" ceria NPs

Small ceria nanoparticles

Xu et al. Chem. Commun, 46, 1887 (2010)

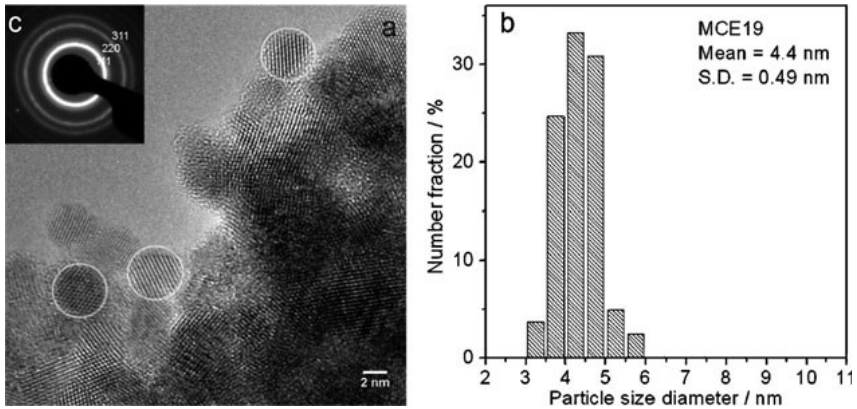

Well defined ceria nano- particles with sharp size distributions [Xu et al, (2010)]

Experiments find large enhancement of Oxygen storage for nanocrystals compared to extended surfaces.

* OSC boosted for d < 5 nm

* The phenomenon was linked to the presence of superoxide species (O_2^-) **but no mechanism was given.**

Temperature programed reduction of CeO_2 sampes with H_2

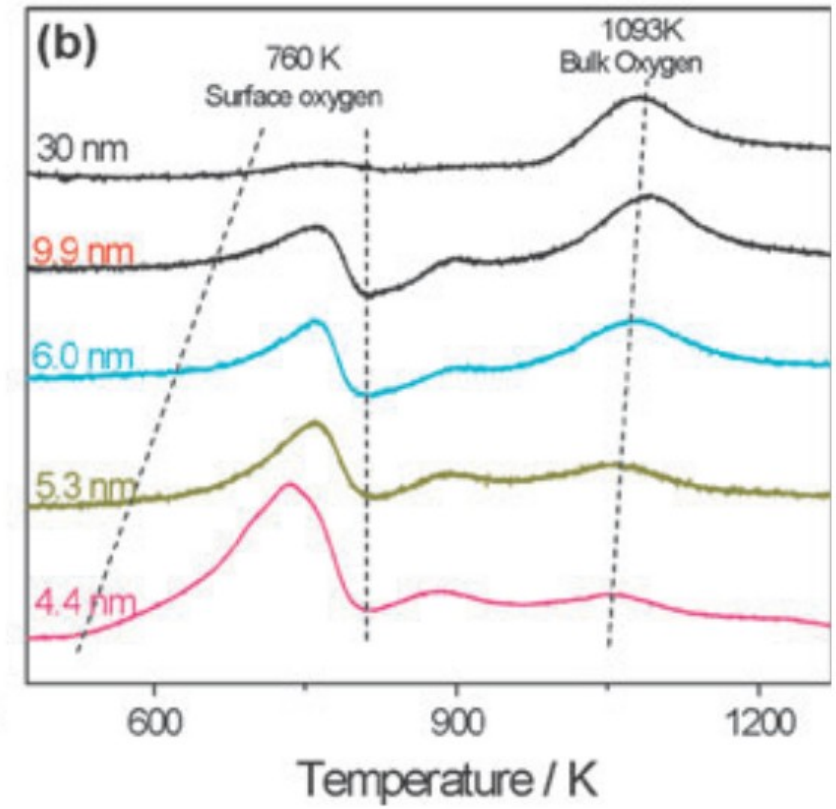

Broqvist, Kullgren, Hermansson, J. Phys. Chem. Letters (2013)

We constructed regular octahedral nanoparticles (understoichiometric w r t oxygen)

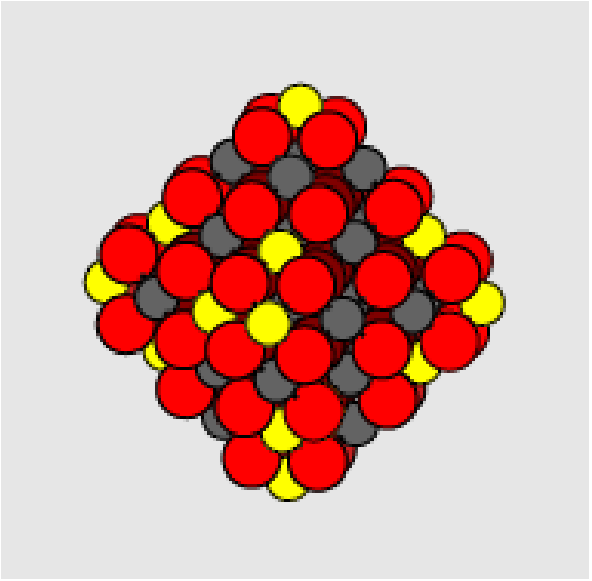

$Ce_{44}O_{80}$

We then added O_2 molecules to the regular octahedron

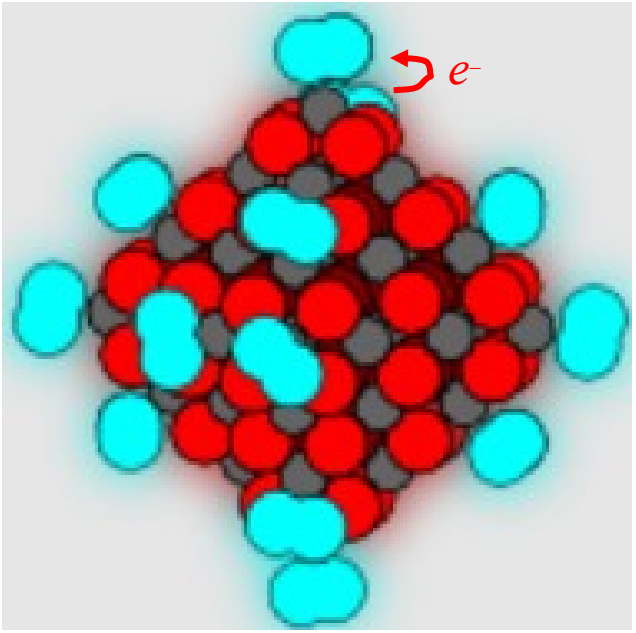

$Ce^{3+} \rightarrow Ce^{4+}$

$O_2 \rightarrow O_2^-$

$Ce_{44}O_{80}*16O_2$

O^{2-}

Ce^{3+}

Ce^{4+}

Superoxide (O_2^-)

Broqvist, Kullgren, Hermansson, J. Phys. Chem. Letters (2013)

We constructed regular octahedral nanoparticles (understoichiometric w r t oxygen)

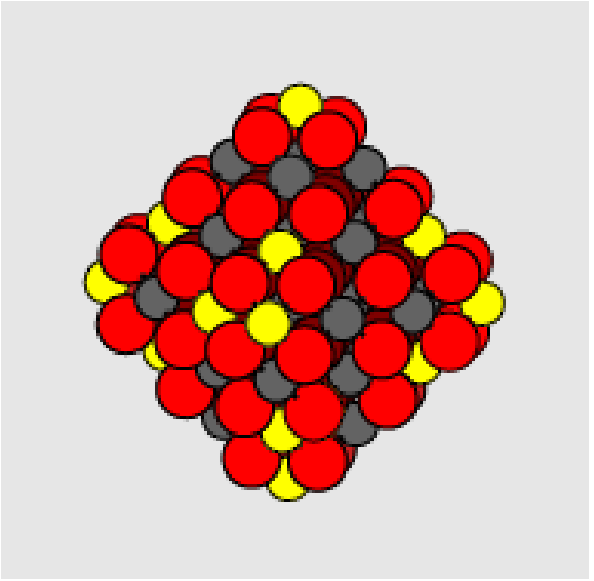

$Ce_{44}O_{80}$

We then added O_2 molecules to the regular octahedron

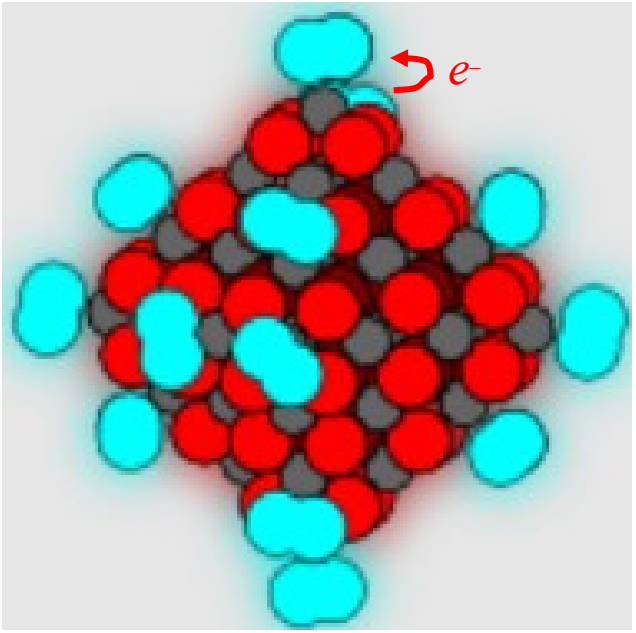

$Ce^{3+} \rightarrow Ce^{4+}$

$O_2 \rightarrow O_2^-$

$Ce_{44}O_{80}*16O_2$

O^{2-}

Ce^{3+}

Ce^{4+}

Superoxide (O_2^-)

We proposed that the large OSC observed experimentally originates from ”supercharged" ceria NPs

Another example of the useful use of modelling: 1.5 monolager CO on $TiO_2(110)$ – studied by IRRAS*

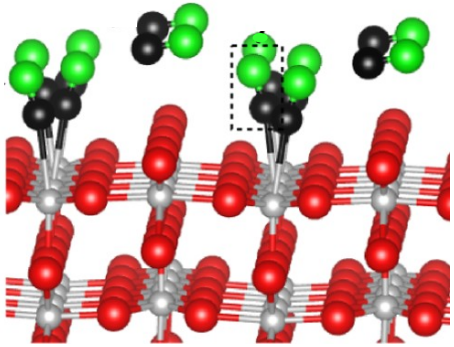

Experimental IRRAS spectra
USA 2012

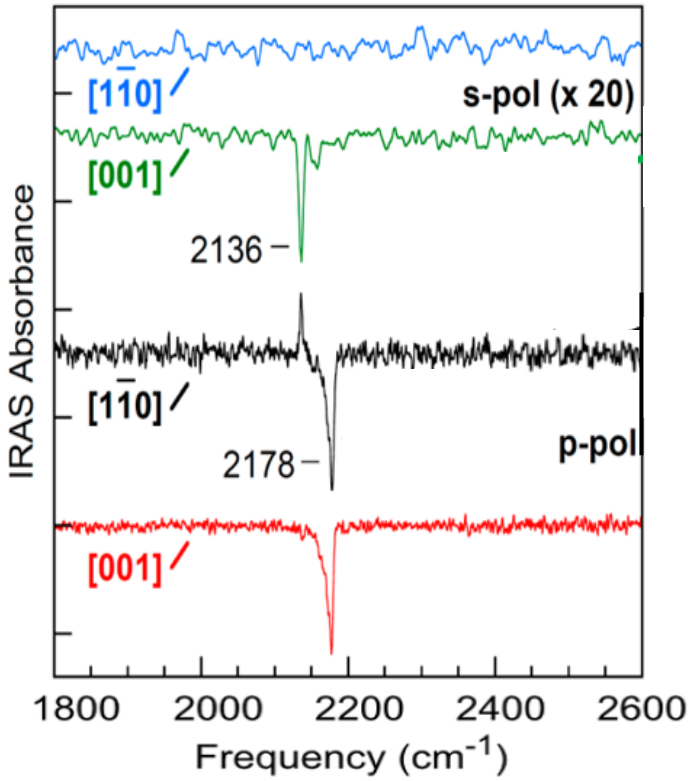

Nikolay G. Petrik and Greg A. Kimmel
J. Phys. Chem. Lett. **2012**, 3, 3425.

*IRRAS = infrared reflection-adsorption spectroscopy

Now how do we calculate this?

1.5 monolager CO on TiO_2(110) – studied by IRRAS*

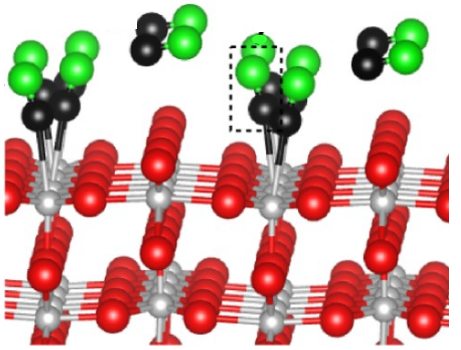

Experimental IRRAS spectra
USA 2012

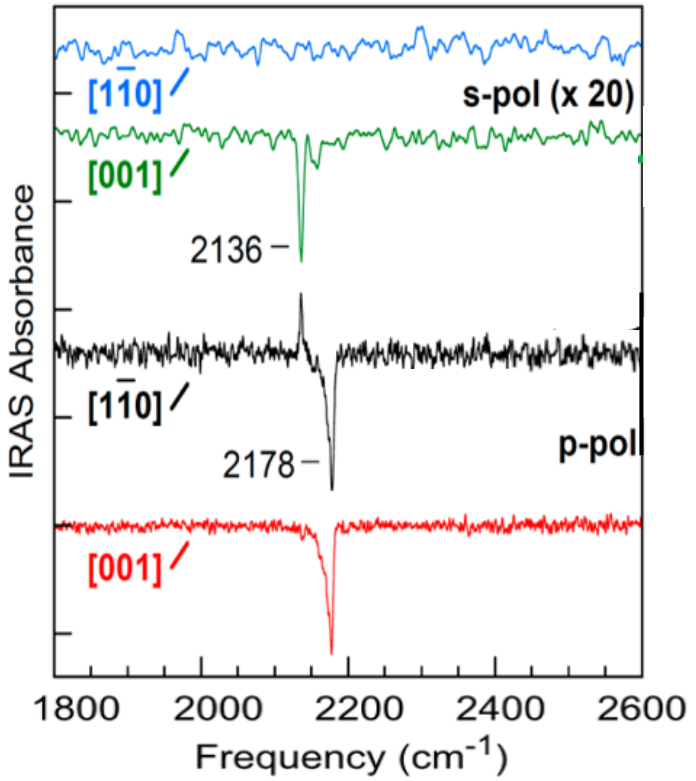

Nikolay G. Petrik and Greg A. Kimmel
J. Phys. Chem. Lett. **2012**, 3, 3425.

Simulated IRRAS spectra
Sweden 2015

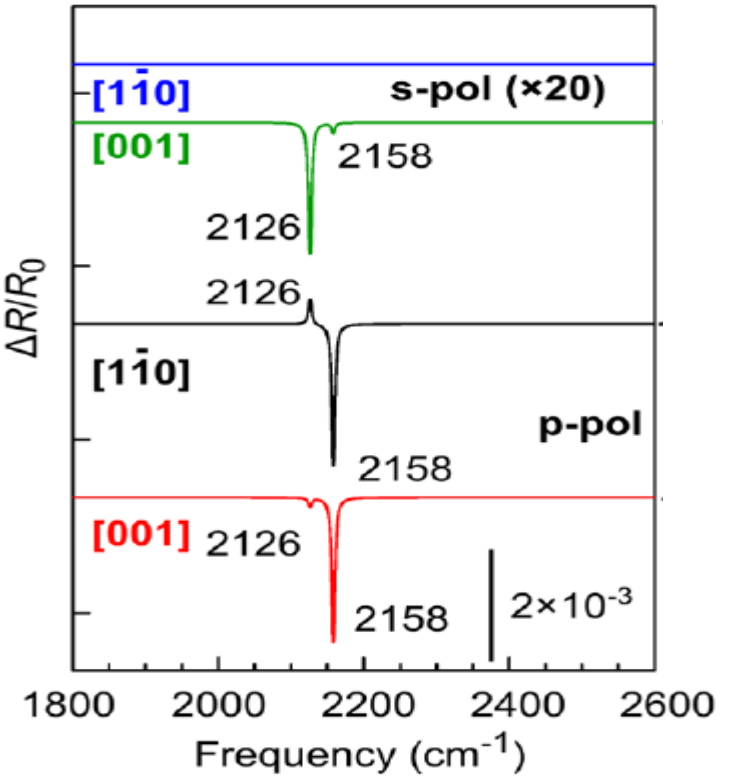

Shuanglin Hu, Z Wang, A Mattsson, L Österlund, and K Hermansson, J. Phys. Chem. C **2015**, 119, 5403.

1.5 monolager CO on TiO_2(110) – studied by IRRAS*

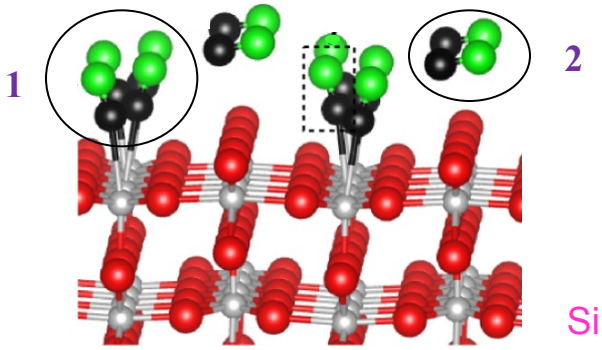

Experimental IRRAS spectra
USA 2012

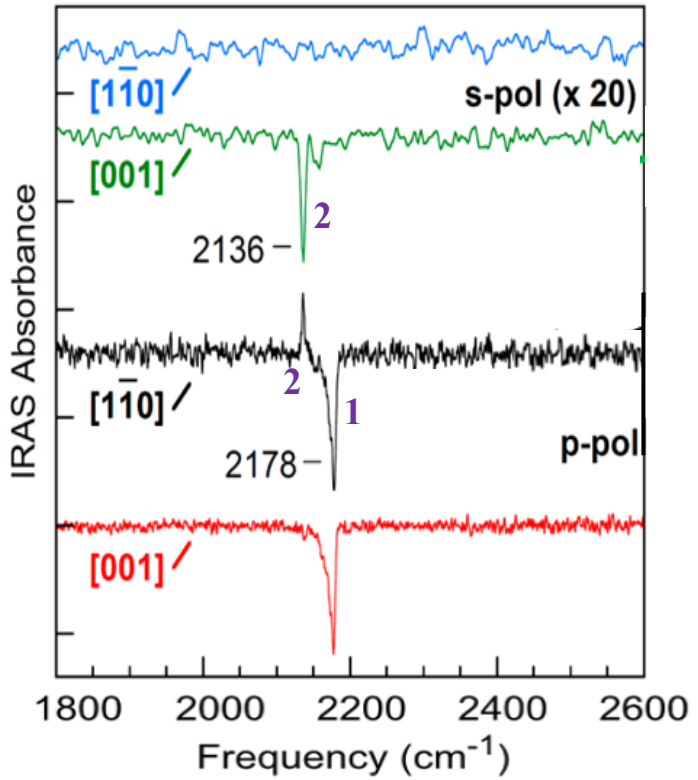

Nikolay G. Petrik and Greg A. Kimmel
J. Phys. Chem. Lett. **2012**, 3, 3425.

Simulated IRRAS spectra
Sweden 2015

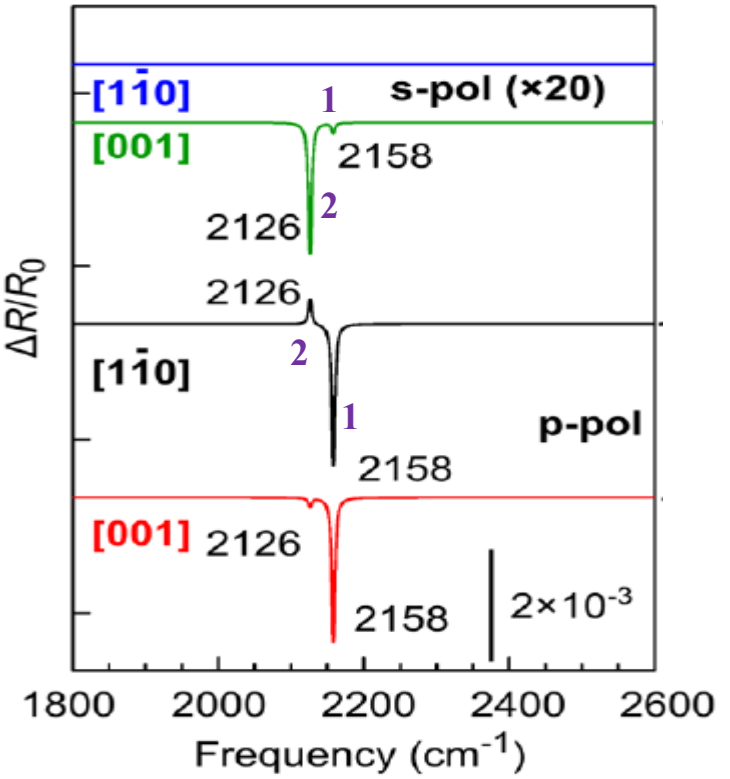

Sh. Hu, Z Wang, A Mattsson, L Österlund, and
K Hermansson, J. Phys. Chem. C **2015**, 119, 5403.

Result: Calculated vs. experimental anharmonic OH frequencies

G. Kebede et al. J. Chem. Theory Comput. 15, 584−594 (2019)

Calc.ν_{anh} *vs.* Expt.ν_{anh}

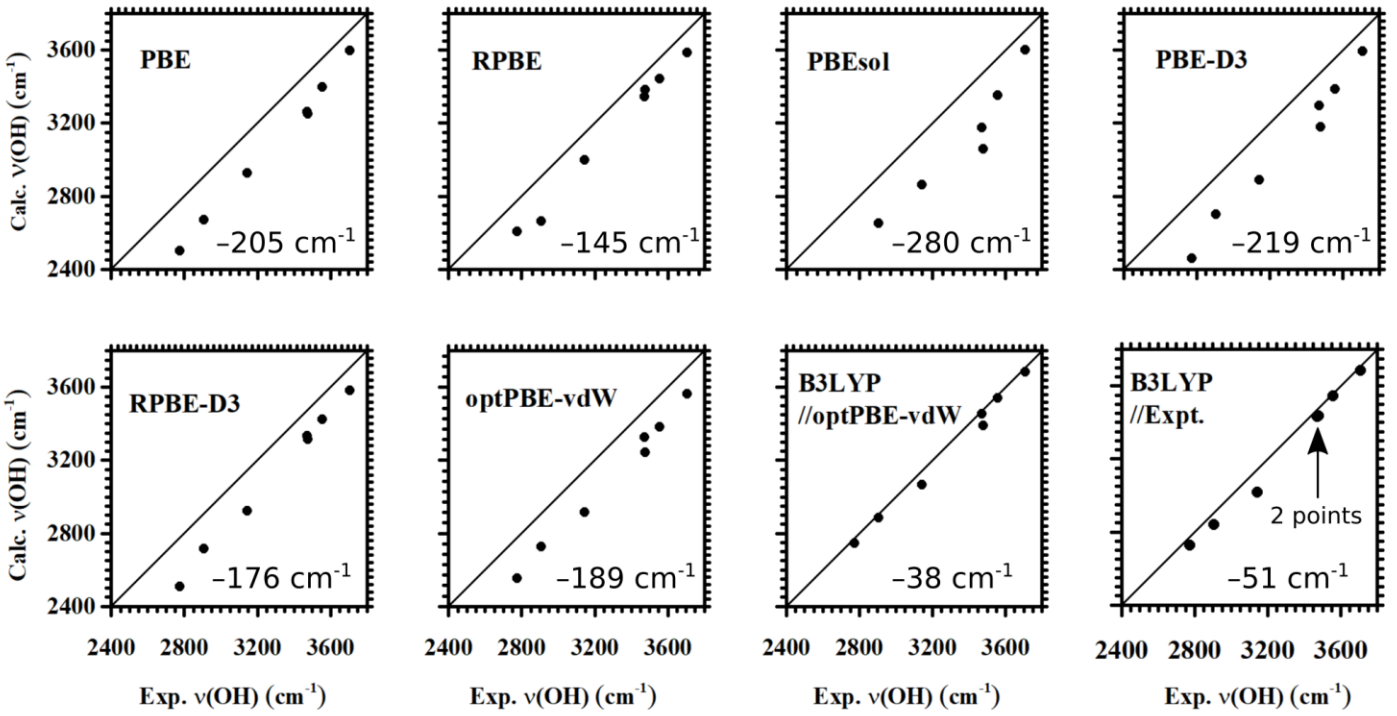

Calc. $\Delta\nu_{anh}$ *vs.* Expt. $\Delta\nu_{anh}$

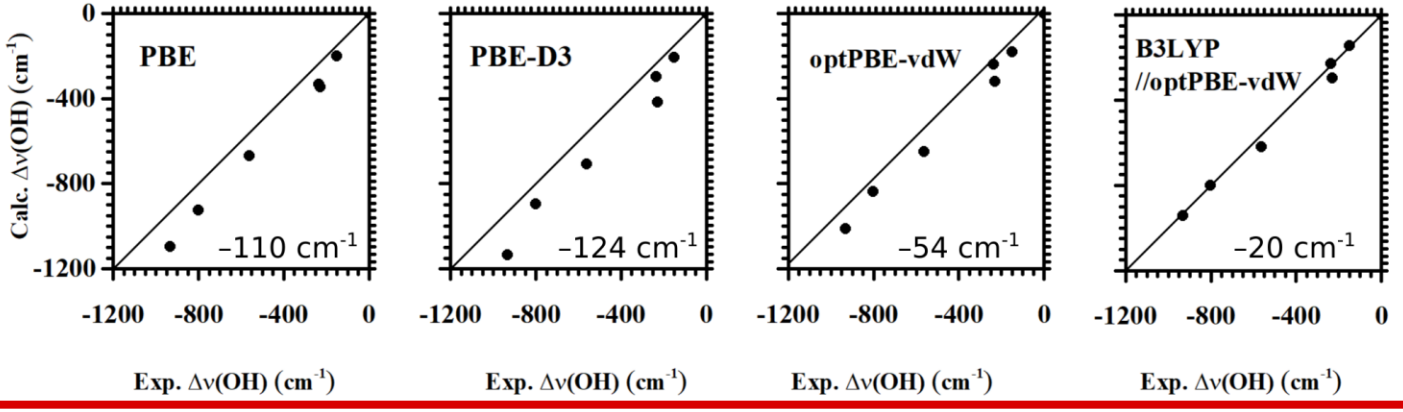

optPBE-vdWs =>

ν(OH) vibrational frequency calculations: method

P.D. Mitev, A.Eriksson, J-F Boily, K. Hermansson, *PCCP 17, 10520--10531 (2015)*

1. MD simulations
2. Select snapshots, do PES scans using . . .
3. Solve vibrational 1-dimensional Schrödinger equation using a DVR discrete-variable basis set representation) approach.
   Note: 1-dim is NOT an approximation.
4. Calculate anharmonic vibrational frequencies

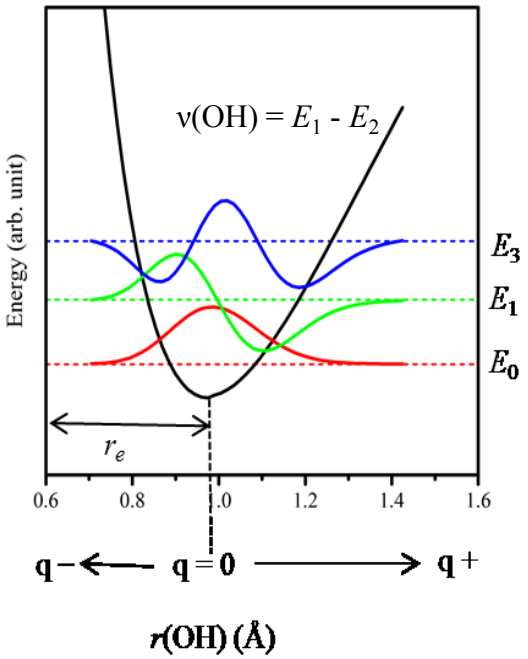

TABLE I. Distances from the ZnO surface defining the different regions and corresponding numbers of frequencies used in the analysis. The frequencies considered in the respective regions are determined by the positions of the hydrogen atoms of the OH bonds.

Region	Distance from surface (Å)	No. of frequencies
I	0–4	29 531
II	4–8	1 931
III	8–12	1 914
Bulk-like	>20	2 064

555 water molecules in the cell

Region	Distance from surface (Å)	No. of frequencies
I	0–4	29 531
II	4–8	1 931
III	8–12	1 914
Bulk-like	>20	2 064

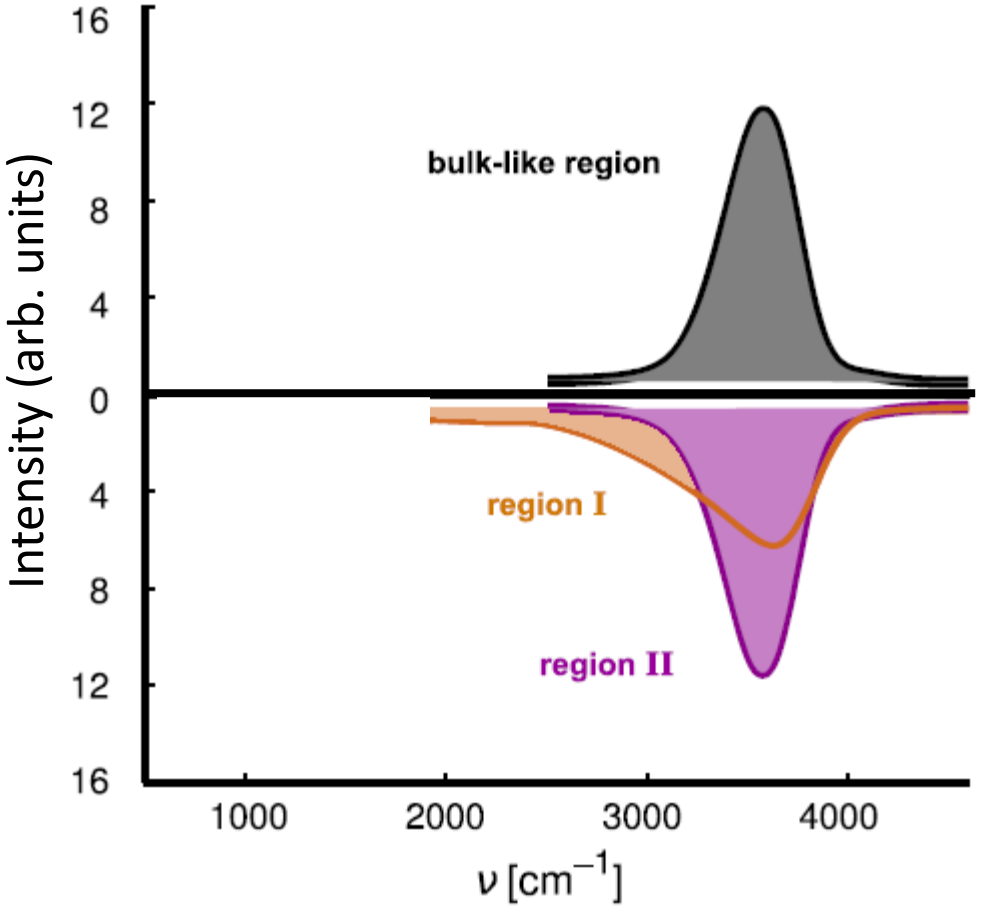

Experiment vs calculation

Experiment
[Wöll et al., Angew. Chem. 131, 2 (2019)
Water on ZnO(1 0 -1 0)
IRRAS p-pol

Our calculations
Quaranta et al. (2018)
Water on ZnO(1 0 -1 0)
From velocity autocorr. fcn

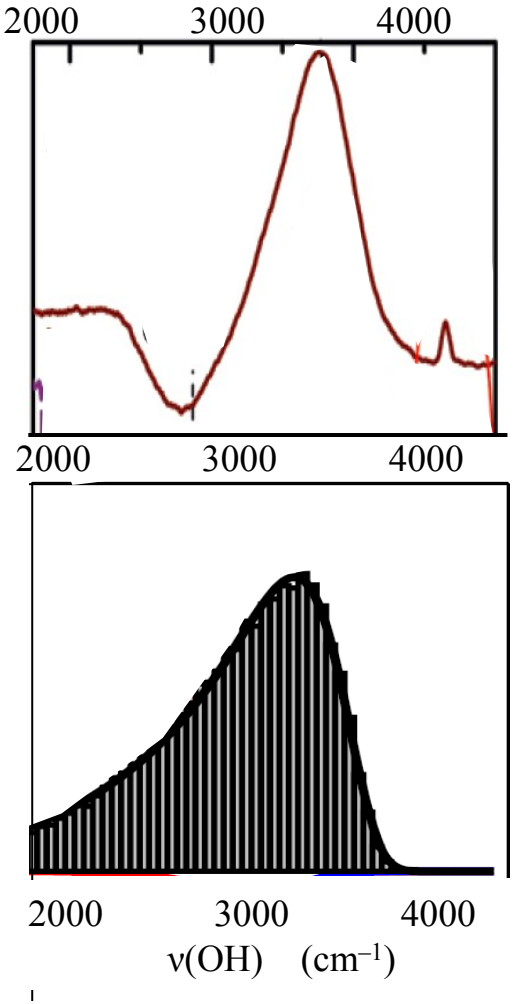

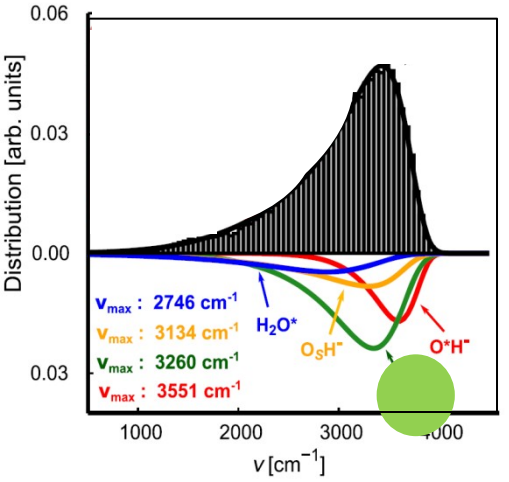

Connect to phonons local modes!!!
yesterday lattice calc for thermal conductivity calc phonon, transferm ebergy, scattering.
hethermal con in semicond is weakly anharmonic semiconductors
sattering i= anhamonic + isotrupic
SiC
Beyond this model
Scatterig and Green's functions due o bounded defects (vacancy, subst, internatitial, antisite)
broken transk symm, elastic phonon
Accelerated workflows of compressed sensing and IFCs solve the underdetermined linear regr scgeme by ...
Zhou (2014), and P Erhardt

A differentialble NN FF for Ionic Liquid
Montes Campos 2022 62 J of chem inform abd modelling

Bichelmaier Carrete PRB 107 the ket is Automatic differentiation
IJQC 123 e27895 (2023) They calc dyn matrix directly they do not need the force constants They avoid a lot of DFT calc

Computational spectroscopy → identification/assignment of experimental peaks

Correlations

(*involving for example spectroscopic quantities*)

= scientific relations (models)

→ validation & prediction & insight

from Henan

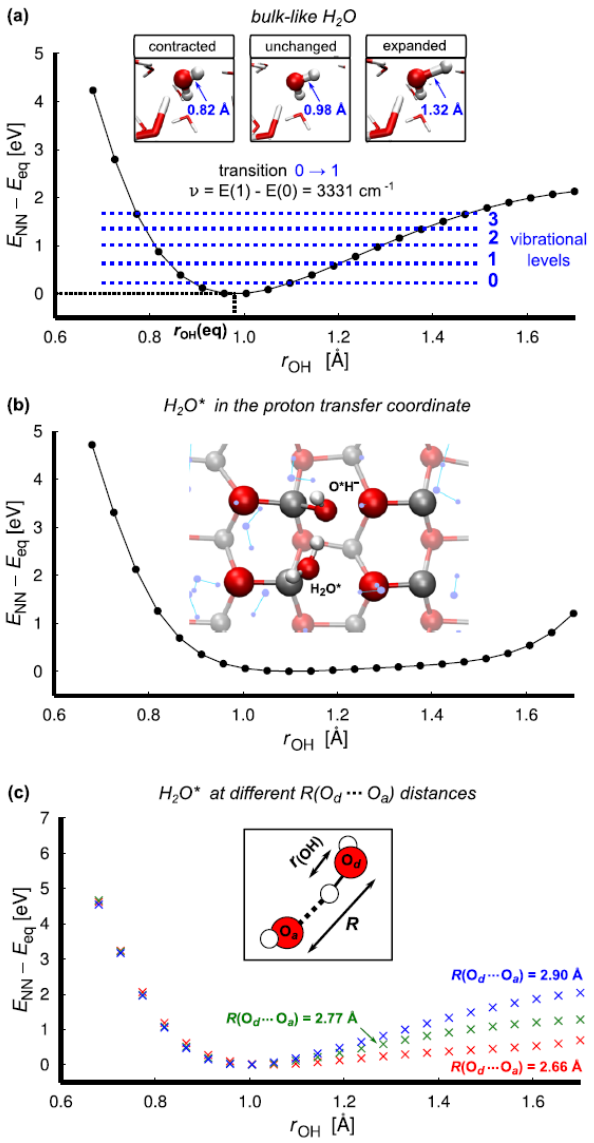
(a)
bulk-like H_2O
contracted
unchanged
expanded
0.82 Å
0.98 Å
1.32 Å
transition 0 → 1
ν = E(1) - E(0) = 3331 cm^{-1}
3
2
1
0
vibrational levels
$E_{NN} - E_{eq}$ [eV]
r_{OH}(eq)
r_{OH} [Å]
(b)
H_2O^* in the proton transfer coordinate
O*H$^-$
H_2O^*
$E_{NN} - E_{eq}$ [eV]
r_{OH} [Å]
(c)
H_2O^* at different $R(O_d \cdots O_a)$ distances
r(OH)
O_d
O_a
R
$R(O_d \cdots O_a)$ = 2.90 Å
$R(O_d \cdots O_a)$ = 2.77 Å
$R(O_d \cdots O_a)$ = 2.66 Å
$E_{NN} - E_{eq}$ [eV]
r_{OH} [Å]

Now: DFTMD simulations of H_2O / CeO_2 interfaces

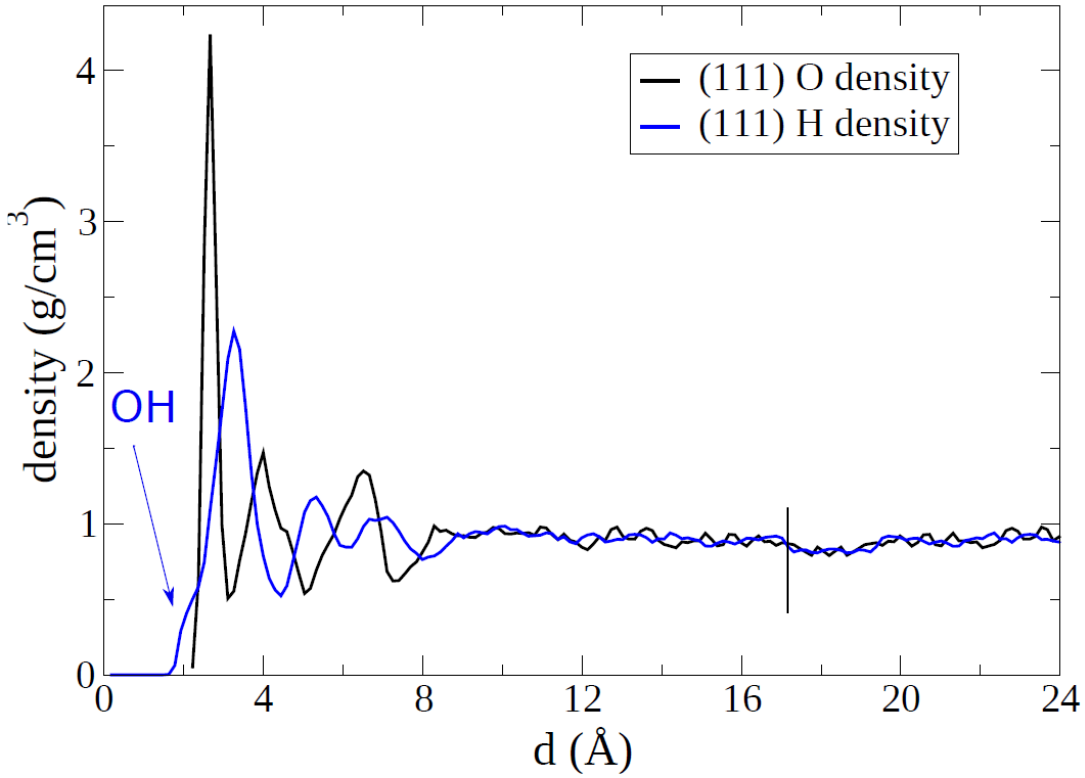

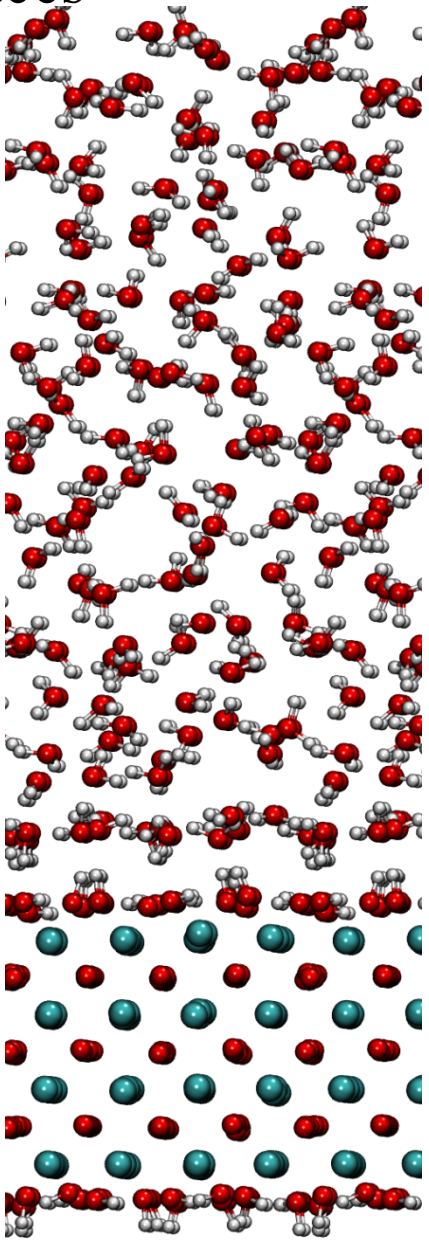

Lorenzo Agosta et al.

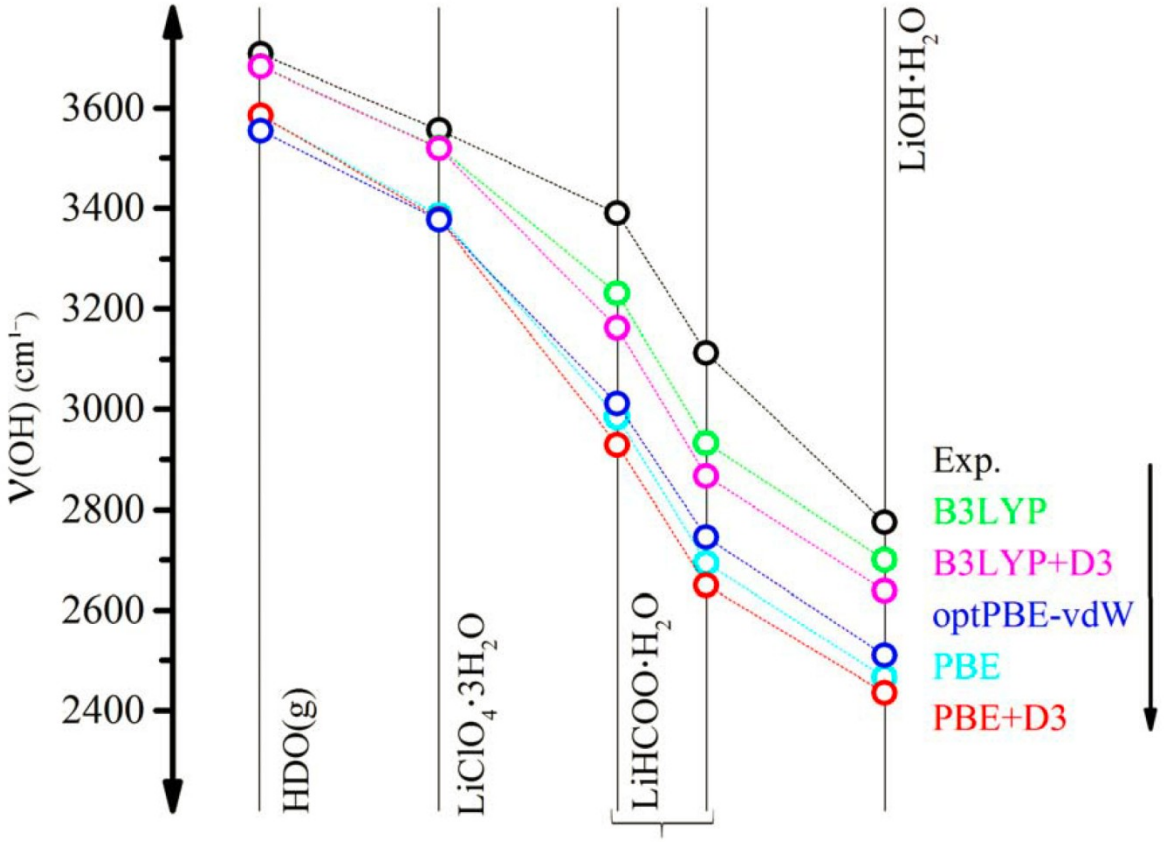

Från paper version Hydrates_methods_GK_12Dec17.pdfi GK's cryst. hydrates directory.

So: good agreement with experiment. But why is $\Delta\nu_{gas\text{-}to\text{-}solid}$(OH) upshifted ?

We placed a water and an OH^- ion in a uniform electric field
(ab initio calculations)

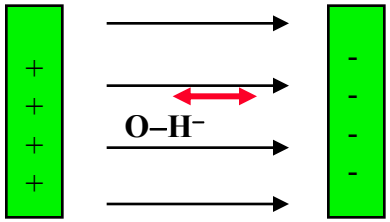

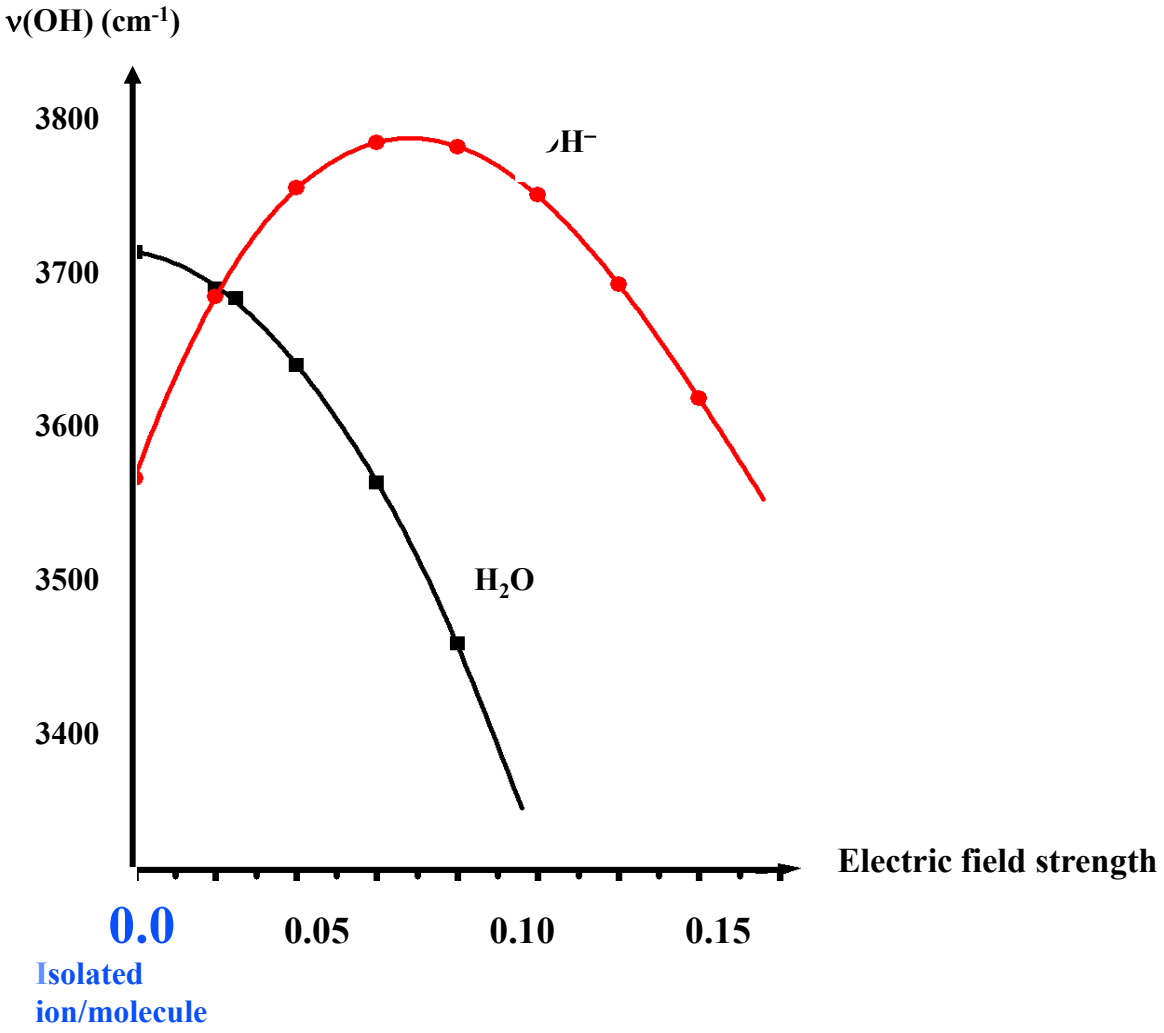

It seems that electrostatics can explain the major trends.

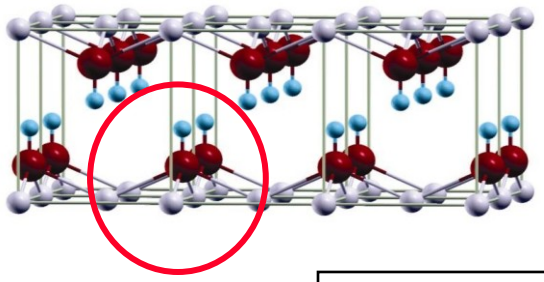

2-D vibrational calculations for the LiOH crystal: at the periodic DFT (GGA) level

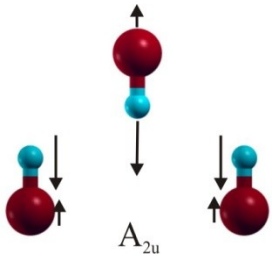

	IR-active mode ν(OH-)	Δν(OH-)
DFT: 1-D mode-following, harmonic	3802	+100
DFT: 1-D mode-following, anharmonic	3918	+422
DFT: Coupled oscillators (2-D), anharmonic	3615	+119
Experiment (Phillips&Busing, 1957, Adams&Haines, 1991)	*3677*	*+121*

(The results are equally good for the Raman-active mode.)

	Isotope-isolated mode ν(OH-)	Δν(OH-)
DFT: 1-D mode-following, harmonic	3787	+85
DFT: 1-D mode-following, anharmonic	3598	+102
Experiment (Buchanan et al. , 1962)	*3674*	*+118*

G. Gajewski, P. Mitev and K. Hermansson, J. Chem. Phys. Aug. 12 2008.

RMSE assessment - pairs of descriptors

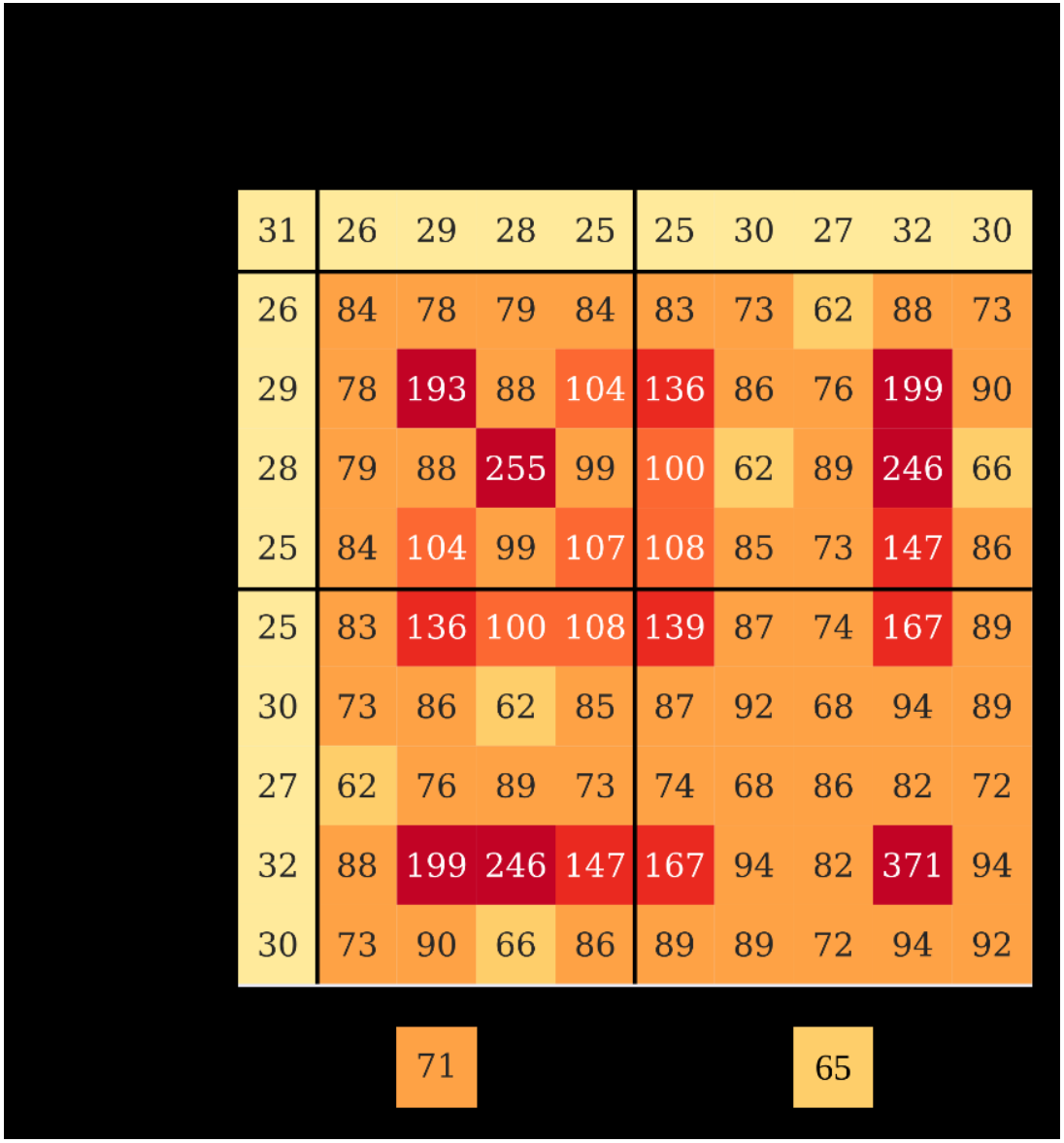

31	26	29	28	25	25	30	27	32	30
26	84	78	79	84	83	73	62	88	73
29	78	193	88	104	136	86	76	199	90
28	79	88	255	99	100	62	89	246	66
25	84	104	99	107	108	85	73	147	86
25	83	136	100	108	139	87	74	167	89
30	73	86	62	85	87	92	68	94	89
27	62	76	89	73	74	68	86	82	72
32	88	199	246	147	167	94	82	371	94
30	73	90	66	86	89	89	72	94	92

71

65

Another view of multiscale modelling

Larger particles in the equations

No patrticles, but continuum Conservation equations

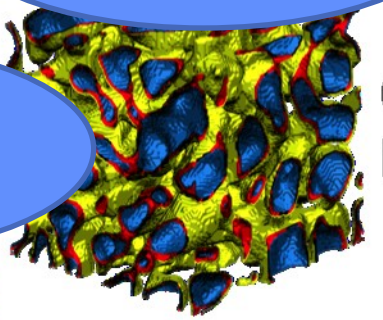

Continuous Model

$$\frac{\partial \rho}{\partial t} + \nabla \cdot \mathbf{j} = 0$$

Particle= "mesoscale" Diverse (e.g. Langevin equation)

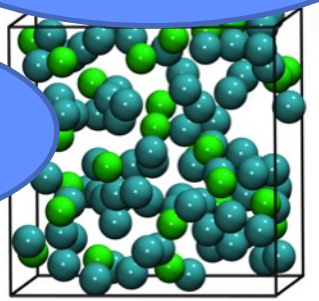

Coarse Graining Methods

$$\langle \eta_i(t)\, \eta_j(t') \rangle = 2\lambda k_B T \delta_{i,j} \delta(t - t'),$$

Particle =Atoms Newton equation

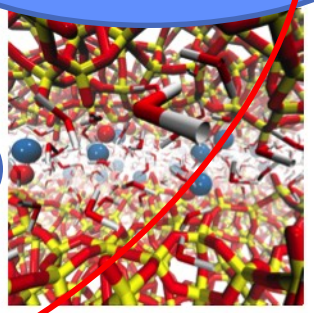

Molecular Dynamics Simulations

$$\frac{dV}{dr} = -m\frac{d^2 r}{dt^2}$$

Particle=Electron Schrödinger equation

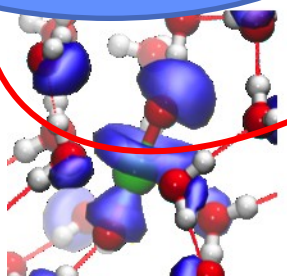

Ab initio calculations

$$i\hbar\frac{\partial}{\partial t}\Psi(\mathbf{r},t) = \left[\frac{-\hbar^2}{2\mu}\nabla^2 + V(\mathbf{r},t)\right]\Psi(\mathbf{r},t)$$

Just some water/CeO_2(111) data

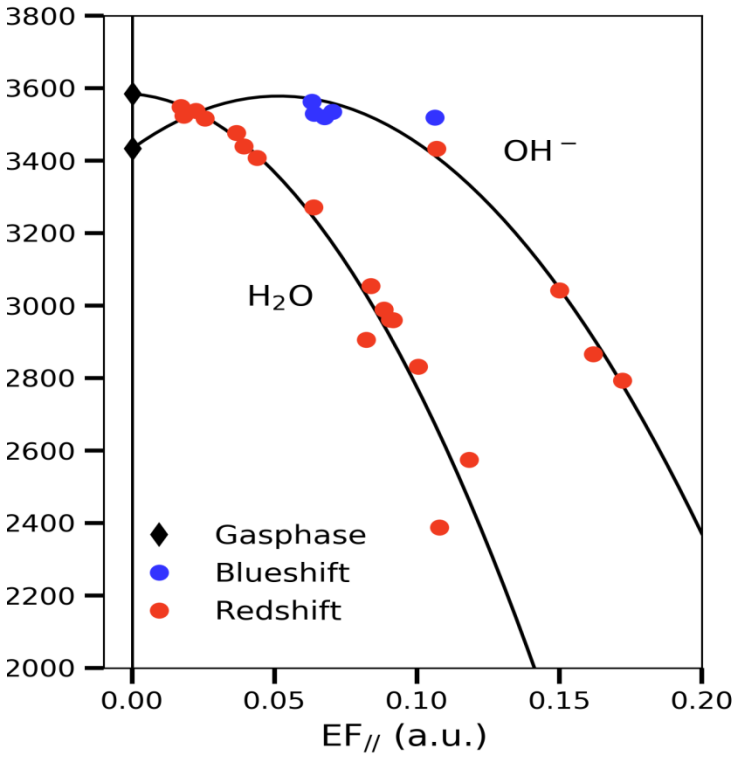

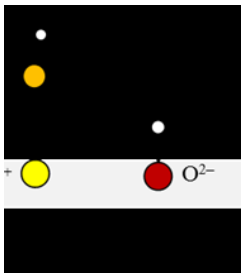

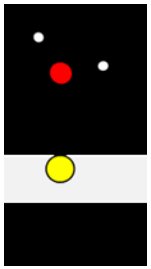

The EF probed at H is a good descriptor also for ceria!

Result: Calculated vs. experimental neutron diffraction R(O⋯O) distances

G. Kebede et al. J. Chem. Theory Comput. 15, 584−594 (2019)

MRE,
MARE

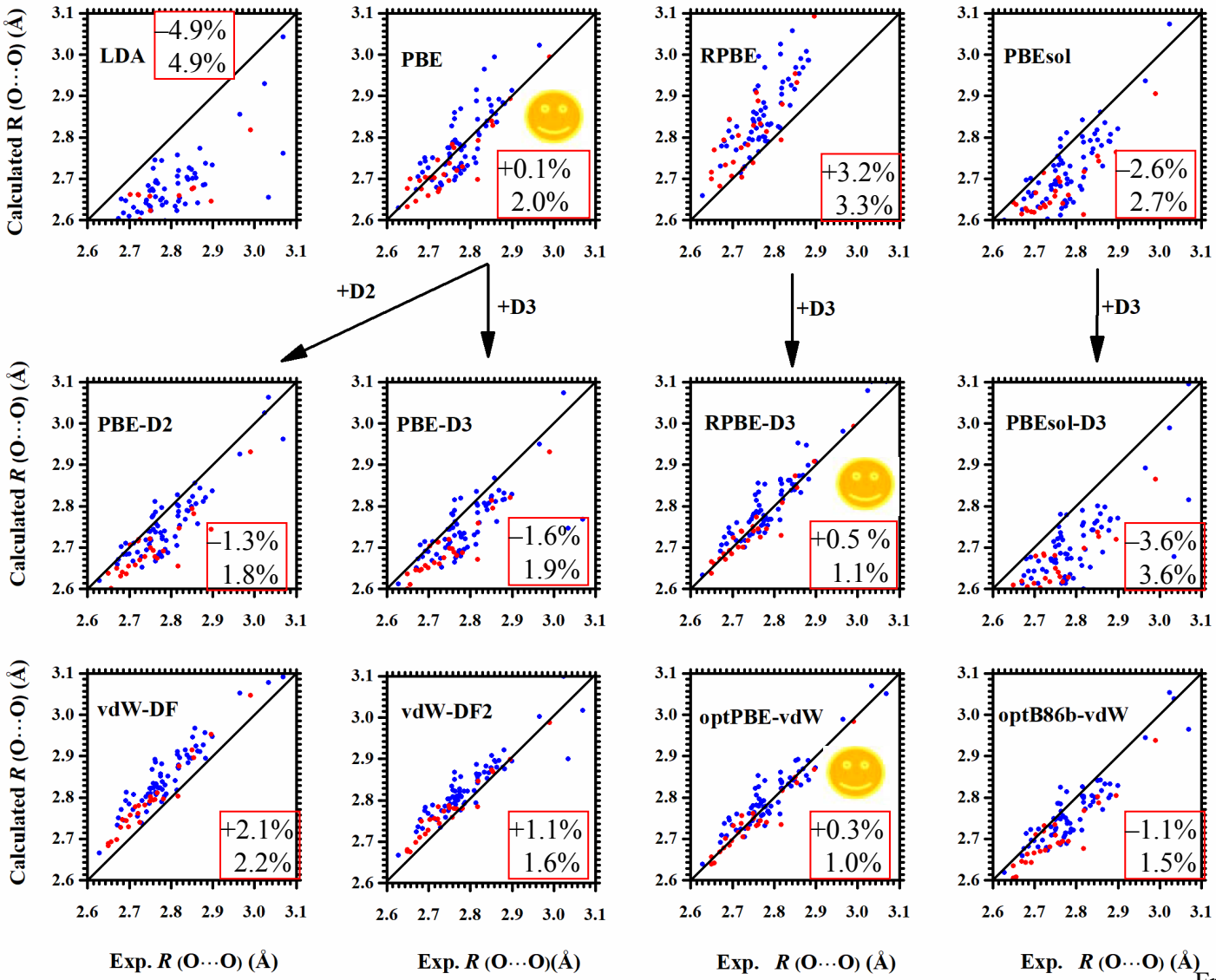

Frequencies =>

Correlation curves

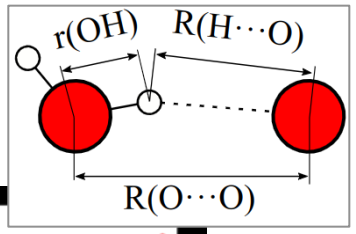

INTERNAL

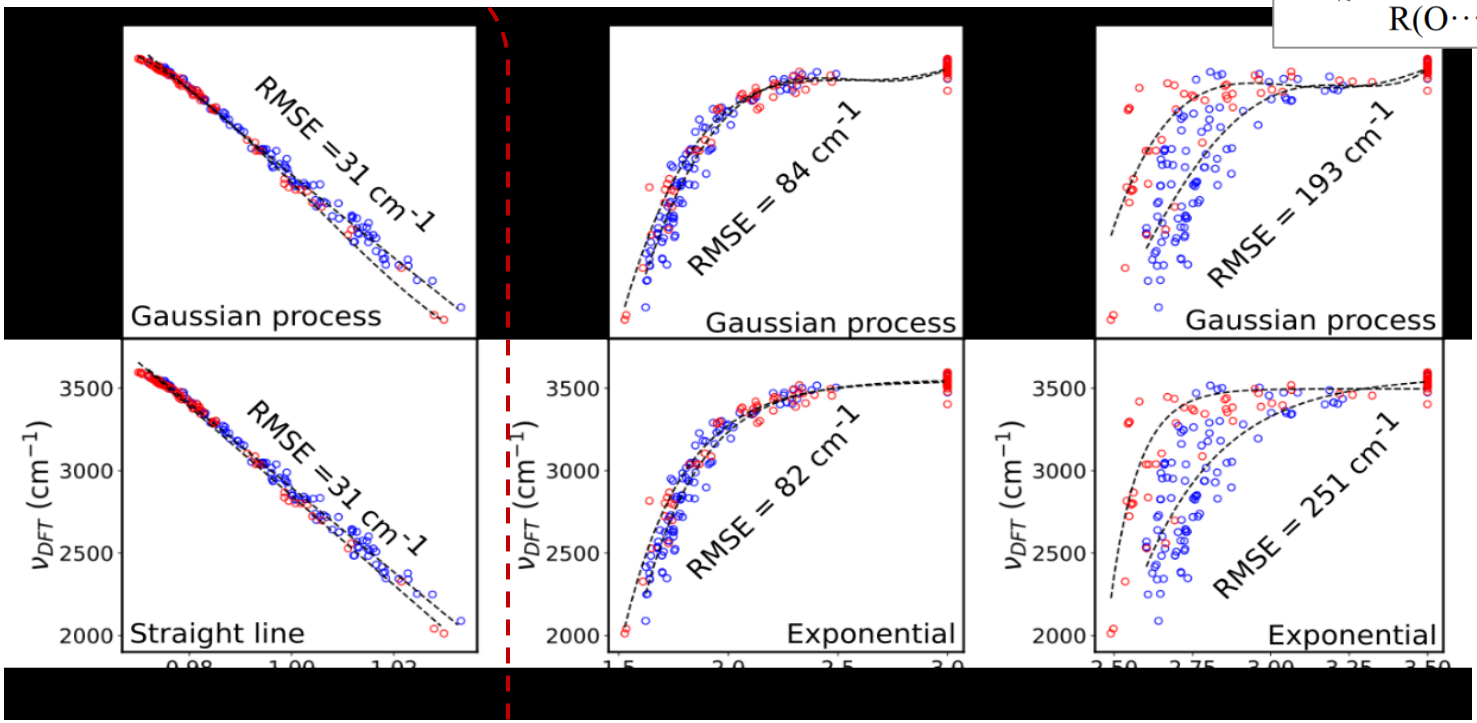

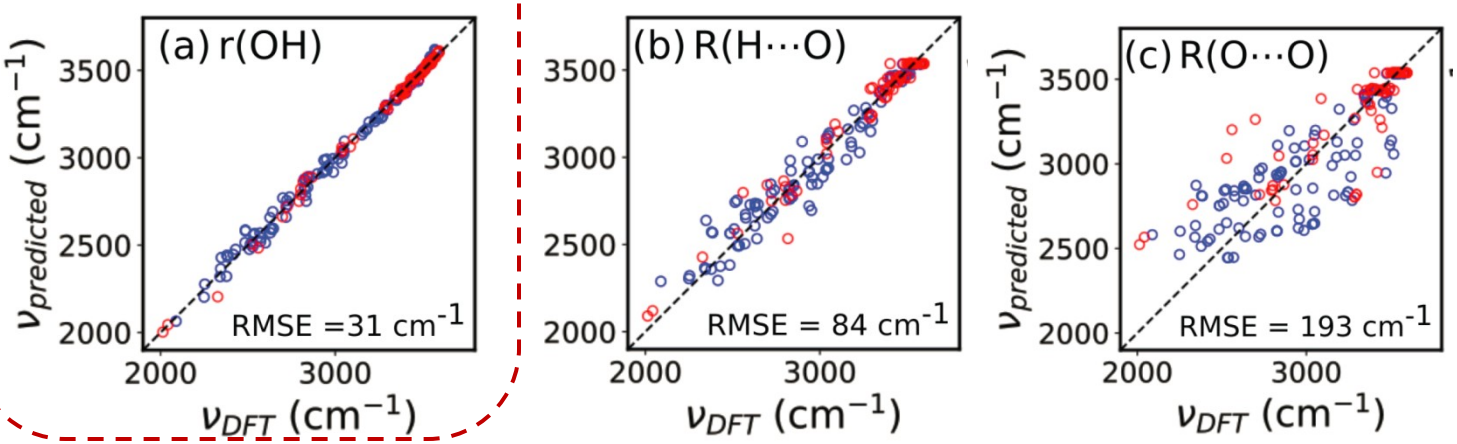

Correlation curves

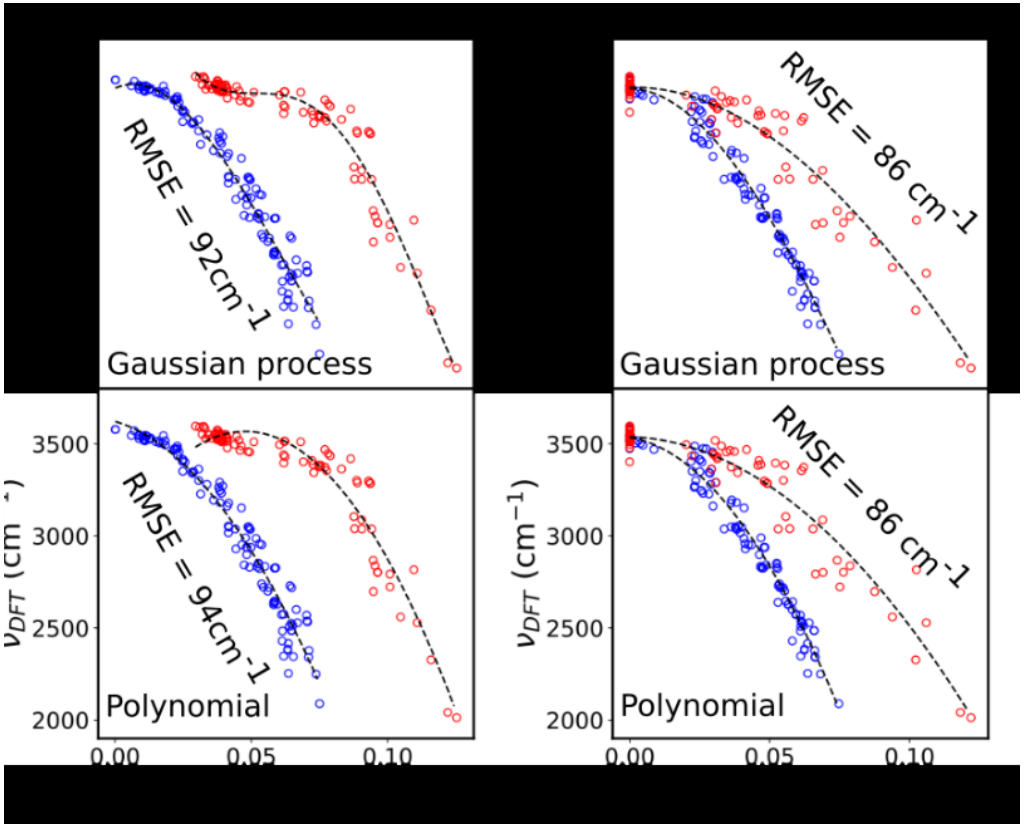

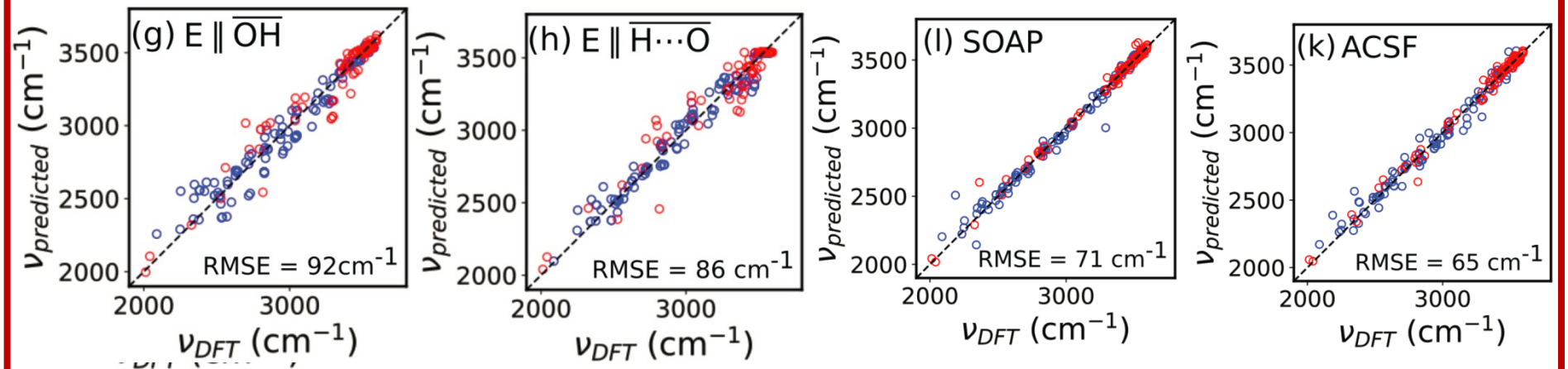

RMSE assessment - pairs of descriptors

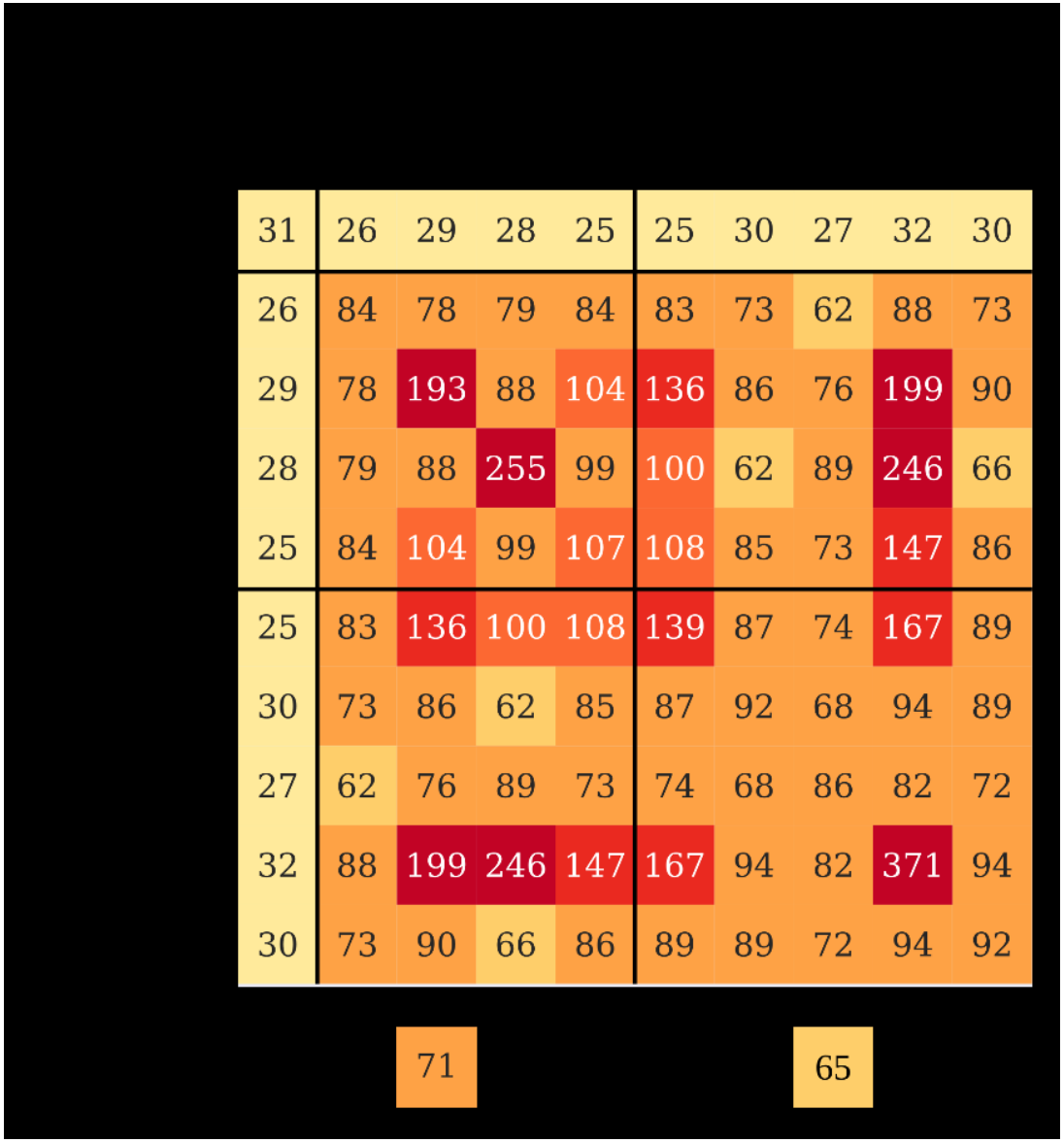

31	26	29	28	25	25	30	27	32	30
26	84	78	79	84	83	73	62	88	73
29	78	193	88	104	136	86	76	199	90
28	79	88	255	99	100	62	89	246	66
25	84	104	99	107	108	85	73	147	86
25	83	136	100	108	139	87	74	167	89
30	73	86	62	85	87	92	68	94	89
27	62	76	89	73	74	68	86	82	72
32	88	199	246	147	167	94	82	371	94
30	73	90	66	86	89	89	72	94	92

71

65

RMSE assessment (only H_2O)

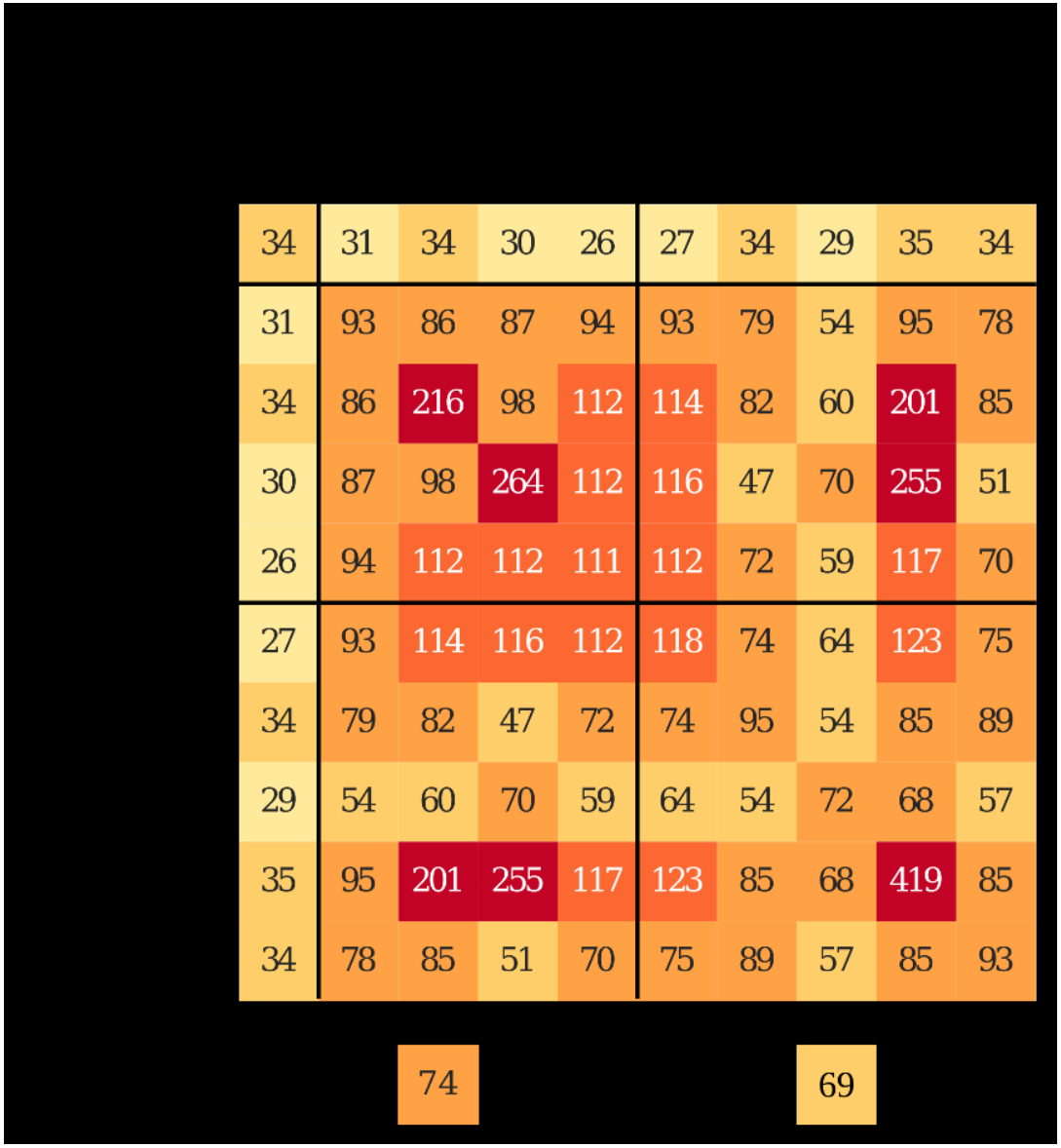

RMSE assessment (only OH^-)

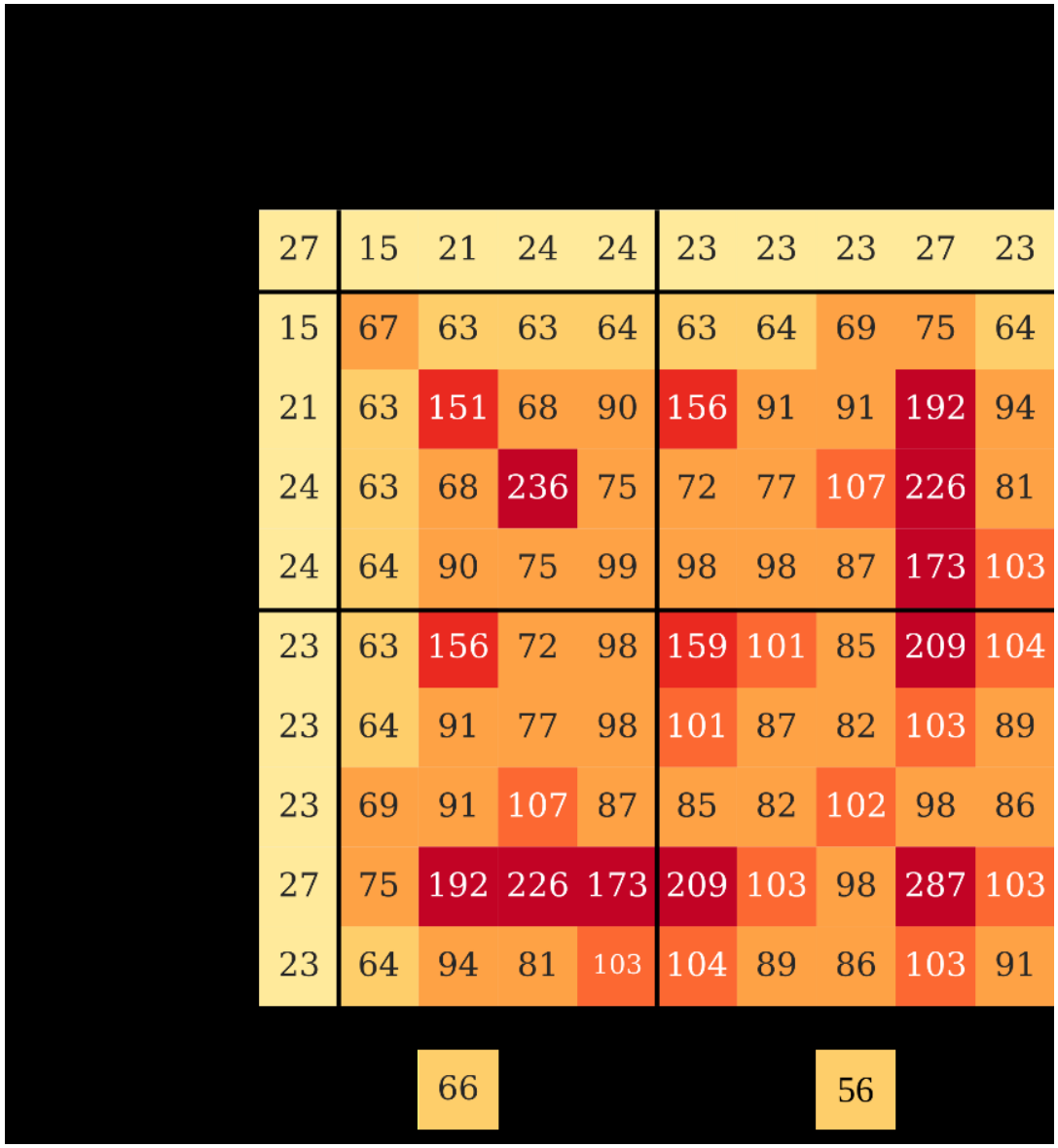

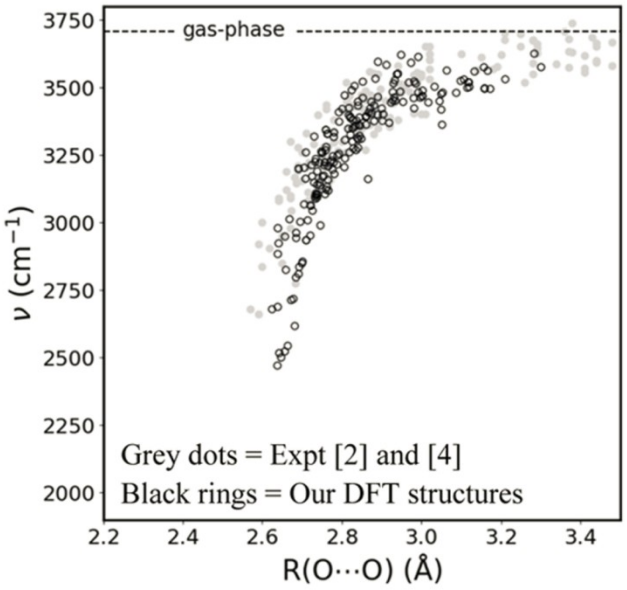
gas-phase
ν (cm⁻¹)
R(O···O) (Å)
Grey dots = Expt [2] and [4]
Black rings = Our DFT structures

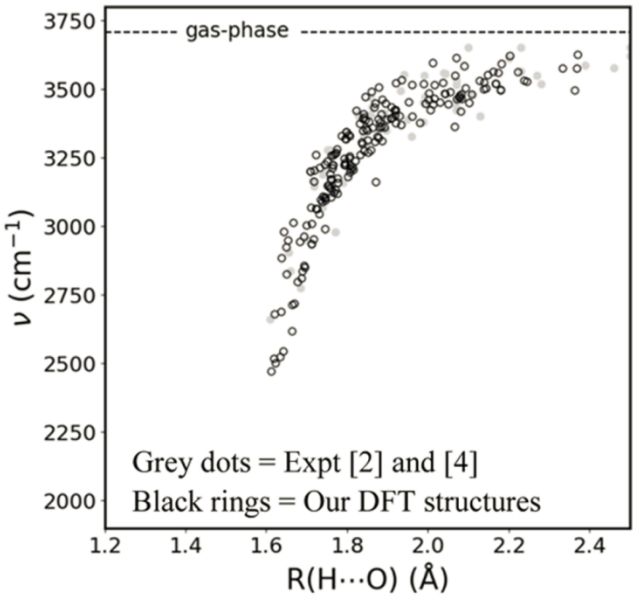
gas-phase
ν (cm⁻¹)
R(H···O) (Å)
Grey dots = Expt [2] and [4]
Black rings = Our DFT structures

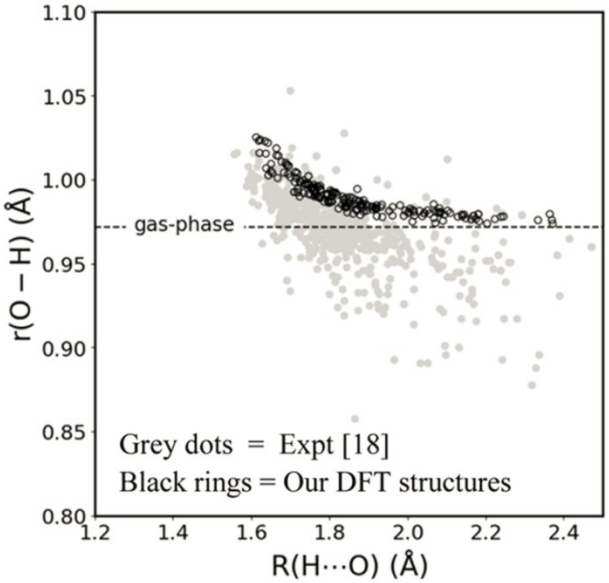
gas-phase
r(O – H) (Å)
R(H···O) (Å)
Grey dots = Expt [18]
Black rings = Our DFT structures

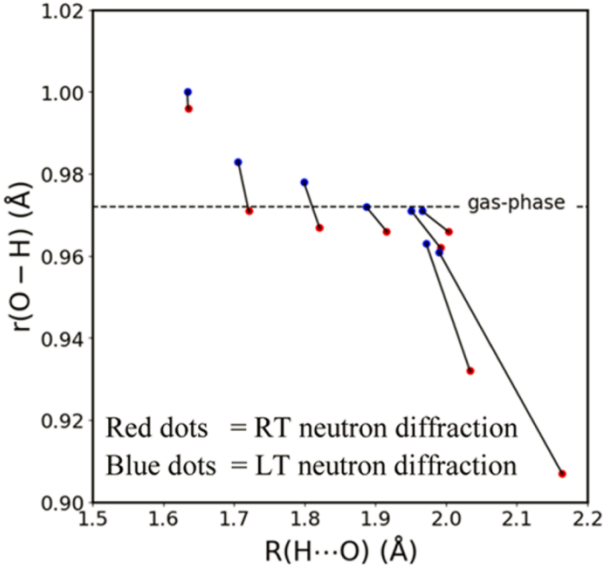
gas-phase
r(O – H) (Å)
R(H···O) (Å)
Red dots = RT neutron diffraction
Blue dots = LT neutron diffraction

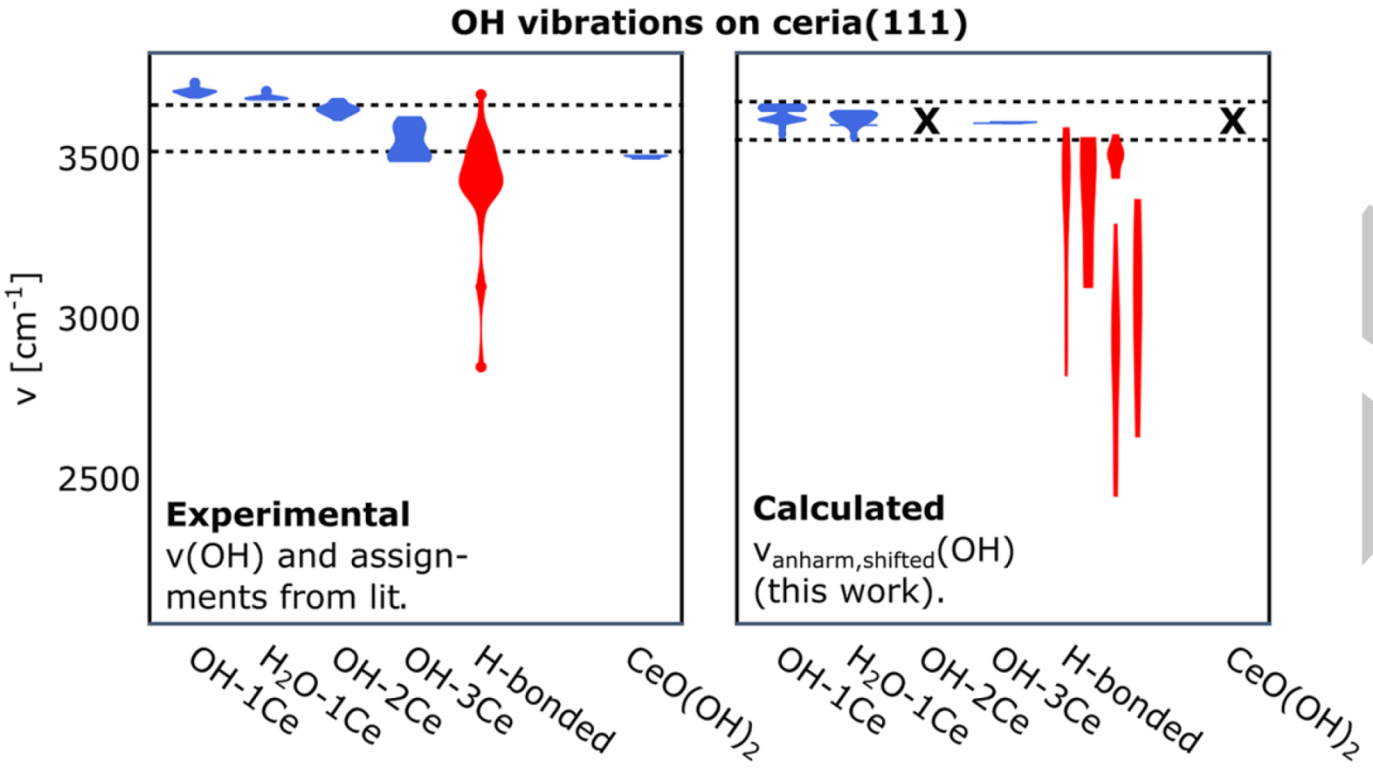
OH vibrations on ceria(111)
v [cm-1]
3500
3000
2500
Experimental
v(OH) and assign-
ments from lit.
Calculated
vanharm,shifted(OH)
(this work).
X
X
OH-1Ce
H2O-1Ce
OH-2Ce
OH-3Ce
H-bonded
CeO(OH)2
OH-1Ce
H2O-1Ce
OH-2Ce
OH-3Ce
H-bonded
CeO(OH)2

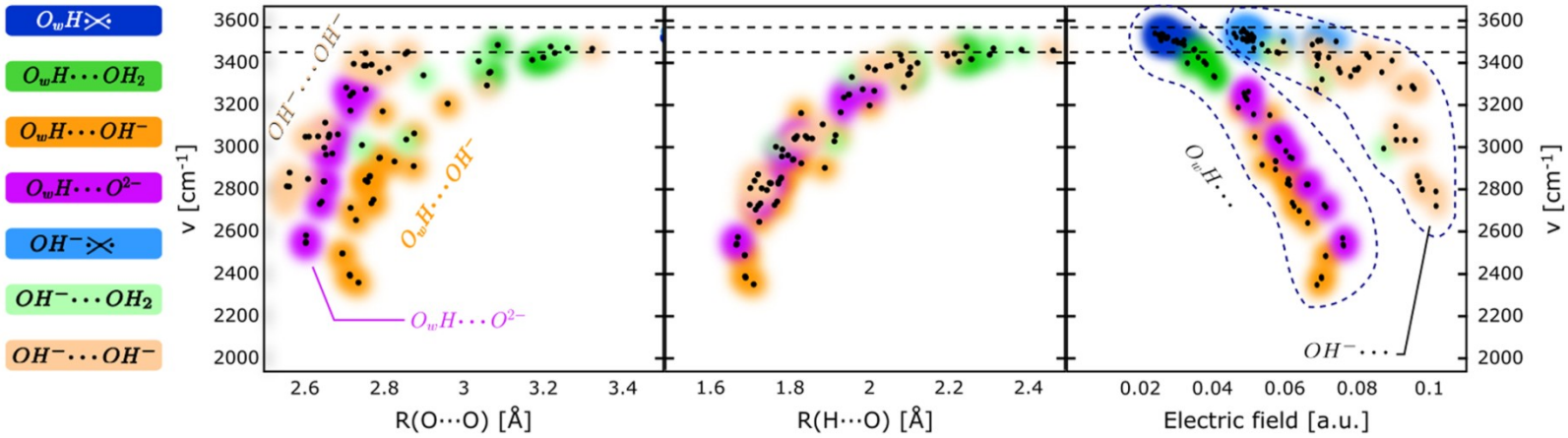
$O_wH\times$
$O_wH\cdots OH_2$
$O_wH\cdots OH^-$
$O_wH\cdots O^{2-}$
$OH^-\times$
$OH^-\cdots OH_2$
$OH^-\cdots OH^-$
ν [cm^{-1}]
3600
3400
3200
3000
2800
2600
2400
2200
2000
$OH^-\cdots OH^-$
$O_wH\cdots OH^-$
$O_wH\cdots O^{2-}$
2.6
2.8
3
3.2
3.4
R(O⋯O) [Å]
1.6
1.8
2
2.2
2.4
R(H⋯O) [Å]
$O_wH\cdots$
$OH^-\cdots$
0.02
0.04
0.06
0.08
0.1
Electric field [a.u.]

Modelling can mean different things. Typically one of the following:

(A) **Computer simulations** that generate data and phenomena based on scientific/engineering **EQUATIONS** and materials relations.

(B) Statistical **data-driven modelling** (≈ machine-learning≈ "AI") that generates models based entirely on **DATA.**

(C) Mixes thereof, i.e. (A) + (B)

In data-driven modelling (**B**), **domain knowledge** enters via the selection of variables (features, descriptors) and via constraints. If very many features are used, most **insight is lost**, but the **prediction capability** may be large.

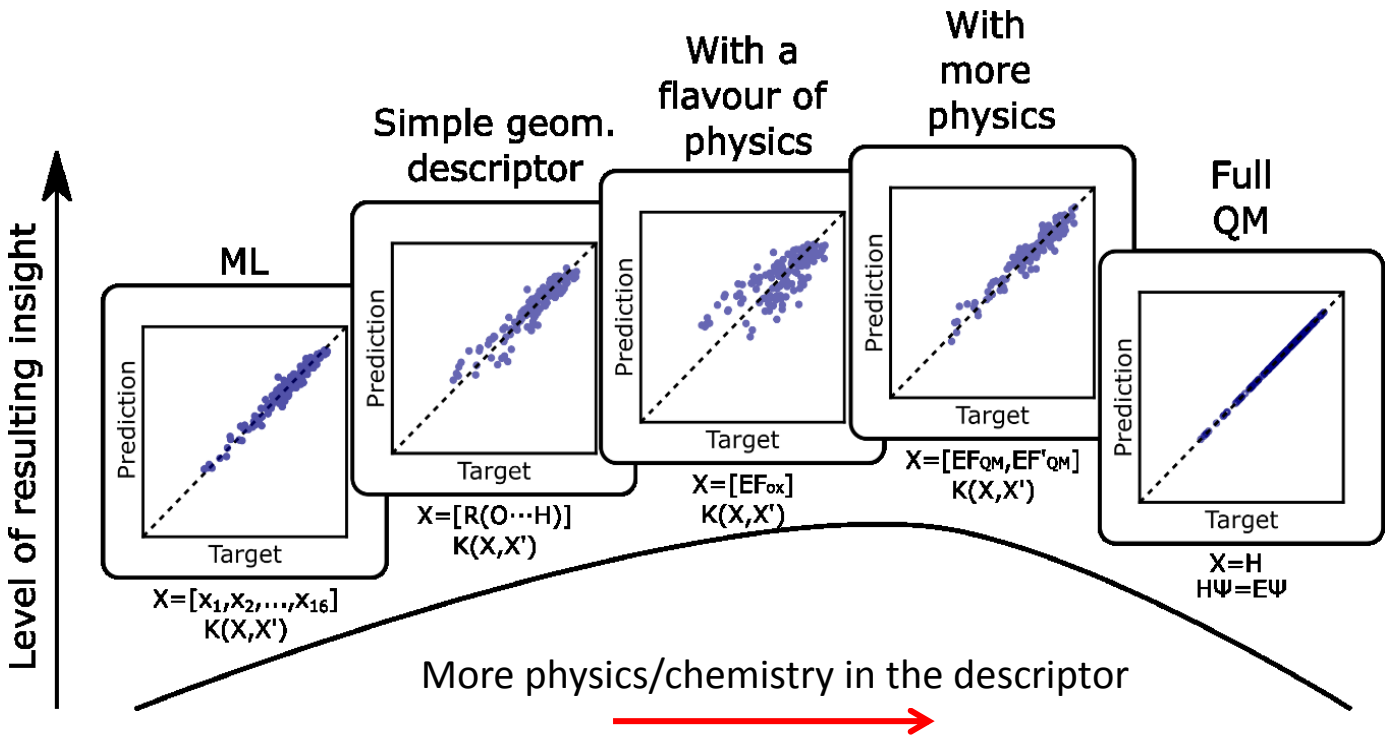

Simulated filled-state STM images for defects on $CeO_2(111)$

J. Kullgren, M. J. Wolf, C.W. M. Castleton, P. Mitev, W. J. Briels, and K. Hermansson
PRL 112, 156102 (2014)